INVESTIGATION OF LIGAND SIZE ON TARGETED PLGA NANOPARTICLES FOR HER2 BREAST CANCER: TRASTUZUMAB AND ITS ScFv ANTI-HER2 ANTIBODY

A Thesis Submitted to

the College of Graduate and Postdoctoral Studies

in Partial Fulfillment of the Requirements

for the Degree of Master of Science

in the College of Pharmacy and Nutrition

University of Saskatchewan

Saskatoon, Saskatchewan

By

Ayat Hesham Zagzoog

PERMISSION TO USE

In presenting this thesis in partial fulfillment of the requirements for a postgraduate degree from the University of Saskatchewan, I agree that the Libraries of this University may make it freely available for inspection. I further agree that permission for copying this thesis in any manner, in whole or in part, for scholarly purposes may be granted by the professor who supervised my thesis work or, in their absence, by the Head of the Department or the Dean of the College in which my thesis work was done. It is understood that any copying, publication or use of this thesis or parts thereof for financial gain shall not be allowed without my written permission. It is also understood that due recognition shall be given to me and to the University of Saskatchewan in any scholarly use which may be made of any material in my thesis. Requests for permission to copy or make any other use of material in this thesis in whole or in part should be addressed to:

Dean of the College of Pharmacy and Nutrition

University of Saskatchewan

Saskatoon, Saskatchewan S7N 4L3

Canada

OR

Dean College of Graduate and Postdoctoral Studies

University of Saskatchewan

116 Thorvaldson Building, 110 Science Place

Saskatoon, Saskatchewan S7N 5C9

Canada

ABSTRACT

This research focuses on assessing the effect of various formulation parameters on targeting human epidermal growth factor receptor-2 (HER2) specifically in breast cancer. Poly (D, L-lactide-co-glycolide) (PLGA) polymer, which is approved by FDA, was used to form nanoparticles (NPs) encapsulating docetaxel (DOC) as chemotherapy. HER2 antibody moieties, either whole IgG (TrAb) or single chain fragment variable (ScFv), were decorated on the PLGA NPs surface and evaluated in terms of their ability to target HER2 breast cancer cells. We observed the effects of these NPs against different cell lines (MCF-7 and SK-BR-3). Thus, ligand modified structurally concealed PLGA NPs could be a promising delivery tool for targeting HER2 breast tumor *in vitro* that improves the release of chemotherapy while reducing the systemic side effects.

A solvent evaporation procedure was adjusted to form NP formulations using both ester and carboxylic acid terminated PLGA. Incorporation of ligands (TrAb or ScFv) was conducted through chemical covalent conjugation processes by using different cross-linkers bis(sulfo-succinimidyl) (BS3) or N-hydroxysuccinimide esters (NHS) and 1-ethyl-3-(-3-dimethylaminopropyl) carbodiimide hydrochloride (EDC). The size, zeta potential, polydispersity index, which were determined for the physicochemical characterizations. The physicochemical characterizations of formulations were executed to assess the effects of different ligands *in vitro* for drug targeting. Also, Fourier Transform Infrared (FTIR) was used to conform the covalent bond insertion between the linkers and ligands (TrAb or ScFv). DOC loading was quantified by a fully validated mass spectrometry method and antibody (Ab)

quantification was performed by using the bicinchoninic acid (BCA) assay. Moreover, *in vitro* drug release profile was assessed. *In vitro* cellular targeting was examined by measuring the level of HER2 expression through Fluorescence-activated cell sorting (FACS) in two cell lines as well as western blot analysis. Cytotoxicity assay was performed in SK-BR-3 cell line for all the formulations.

Modified PLGA NPs showed a mean diameter particle size below 400 nm with approximately neutral zeta potential; for example, ScFv-DOC-Ester PLGA NPs formulation size was 312 ± 8.769 nm, and their zeta potential was 0.024 ± 0.075 mV. The average size of the acidic PLGA TrAb-DOC NPs was 382.5 ± 21.5 nm, and their zeta potential was 0.045 ± 0.037 mV. DOC encapsulation efficiency reached up to 65% to 85% depending on the type of the NPs formulations, and the amount of anti-HER2 attachment efficiency exceeded 40%. The cellular targeting of nanoparticles was studied using two cell lines MCF-7 (low HER2 expression) and SK-BR-3 (high HER2 expression), and different levels of HER2 expression were evaluated. The significant reduction in the level of HER2 expression was observed for all modified NPs formulations in HER2 overexpressed SK-BR-3 cells.

Overall, *in vitro* targeting further demonstrated that modified NPs accumulated DOC in tumor cell line more efficiently than conventional medication. The TrAb conjugated to DOC modified NPs formulations were able to increase the HER2 targeting for DOC compared to ScFv modified NPs. In SK-BR-3 cells, the cytotoxicity of modified NPs was more potent than the conventional DOC due to the targeting, and

slow release of DOC from the modified NPs. This system has the potential of improving the targeting and the release of chemotherapeutic drugs into the tumor cells while reducing the side effects caused by affecting healthy tissues.

Our data demonstrated that the high affinity for anti-HER2 modified PLGA NPs formulations to efficiently and explicitly target DOC to the HER2 overexpressing cancer cells can be exploited as a potential strategy for chemotherapeutic drug delivery system for HER2 overexpressing breast cancers. Thus, ligand modified structurally concealed PLGA NPs could be a promising delivery tool for targeting HER2 breast tumor *in vivo* that improves the release of chemotherapy while reducing the systemic side effects.

ACKNOWLEDGMENTS

Before all, thanks to Allah for lighting my way and giving me

the power and strength to finish my work.

This piece of work is a testimony to the hard work and the endless amount of effort that I have put into this work. It would not have been possible without the love and support of all my family, friends, and colleagues. First, I would like to express my love and gratitude to my mother, Iman Hafez, who has always been my anchor and life mentor. Because of her, I present this work to you. Also, I would like to express my sincere appreciation to my supervisor, Dr. Azita Haddadi, who supported me all the way. I also express my thanks to my advisory committee members, Dr. Adil Nazarali and Dr. Franco Vizeacoumar, and committee chair, Dr. Jane Alcorn, for their advice. I acknowledge the time and consideration of Dr. David Blackburn for chairing my defense committee.

I am also grateful to Dr. Mehran Yarahmadi, who taught me several technical skills. Special appreciation and thanks for Ms. Deborah Michel, as she always was there to help and advise me whenever needed. My wholehearted gratitude to my friends: Mays Al-Dulaymi, Mona Hamada, Waleed Saeid, and Omar Abouhasan thank you for supporting me all the way, pushing me harder to break barriers to achieve my dreams.

Finally, for my brothers and sisters, Hattan, Shadi and Bassel Zagzoog, Asmaa and Shimaa Ezzat and Mohamed Yusuf, they were always supporting me physically and emotionally.

DEDICATION

For the memory of my Father Hesham Gameel Zagzoog whose soul always surrounds me with his love, and my mother Iman Hafez whom I owe every success in my life. Thank you for supporting me in every step of my life.

TABLE OF CONTENTS

LIST OF TABLES

LIST OF FIGURES

LIST OF ABBREVIATIONS

Ab…….. Antibody

ADCC…… Antibody-Dependent Cellular Cytotoxicity

ANOVA……. Analysis of Variance

BCA……... Bicinchoninic Acid Assay

BS3…… Bis(Sulfosuccinimidyl)

^{o}C……... Degree Celsius

DLS…… Dynamic Light Scattering

DOC……... Docetaxel

EDC……1-ethyl-3- (3-dimethylaminopropyl

EGF…… Epidermal Growth Factor

ER…….. Estrogen Receptor

EPR…… Enhanced Penetration and Retention effect

ERK……... Extracellular Signal-Regulated Kinases

FACS……. Fluorescence-Activated Cell Sorting

FBS…… Fatal Bovine Serum

FD…….. Freeze-Drying

FDA…… Food and Drug Administration

FITC…….. Fluorescein Isothiocyanate

FTIR…….. Fourier Transform Infrared Spectroscopy

EE…….. Encapsulation Efficiency

HER2…… Human Epidermal Growth Factor Receptor 2

IC_{50}…….. 50% Inhibitory Concentration

IgG…….. Immunoglobulin G

IR……. Infrared

kDa……... Kilo Dalton

LHRHR…… Luteinizing Hormone Releasing Hormone Receptor

MAPK……. Mitogen-Activated Protein Kinases

MFI……. Median Fluorescence Intensity

mg/ml…….. Milligram per Milliliter

mg……... Milligram

ml…… Milliliters

μg/ml…….. Micrograms per Milliliter

μg……. Micrograms

MRM……... Multiple Reaction Monitoring

nm……..... Nanometers

NHS…….. N-Hydroxysuccinimide Esters

NPs…… Nanoparticles

O/W……... Oil in Water Emulsion

PBS…… Phosphate Buffer

PDI……. Polydispersity Index

PEG…… Polyethylene Glycol

PF%..... Parent Fluorescence Percentage

PI3K……... Phosphatidylinositol-4,5-Bisphosphate 3-Kinase

PLGA……. Poly (lactic-co-glycolic acid)

PR…….. Progesterone Receptor

PVA……... Poly (vinyl alcohol)

Rpm……... Revolutions Per Minute

ScFv…….. Single Chain Fragment Variable

SD……. Standard Deviation

SEM…….. Emission Electron Microscopy

TEM…….. Transmission electron microscopy analysis

TrAb…….. Trastuzumab

ZP…….. Zeta Potential

1. INTRODUCTION

Various types of cancer overexpress a number of proteins called *tumor antigens*. One of which is human epidermal growth factor receptor-2 (HER2) that is present in 25–30% of breast cancer types in women (Antonio C. Wolff, Mitchell Dowsett, Edith A. Perez, & Marc van de Vijver, 2007). The HER2 antigen is one of the most useful biomarkers in early stages of diagnosis. In addition, HER2 antigen can be useful in targeted therapies (Choi et al., 2015).

Classical chemotherapeutic agents used in treating cancer show many limitations and severe side effects due to lack of selectivity. This lack of selectivity means that chemotherapy works on both cancer cells as well as healthy cells (Kamaly, Xiao, Valencia, Radovic-Moreno, & Farokhzad, 2012). Recently, many research studies have been focusing on using nanotechnology to overcome chemotherapeutic limitations. For instance, enhancing the selectivity of cancerous cells using targeting ligands on nanoparticles would improve drug efficacies in cancerous cells and minimize the effect on healthy cells.

Recently, the humanized monoclonal antibody such as trastuzumab (Herceptin®) is approved by the FDA for treating HER2 overexpressed breast cancer patients. Trastuzumab could selectively target cancer cells that overexpress HER2 receptors. However, using trastuzumab as monotherapy showed low response as well as low survival rate. Therefore, the combination of trastuzumab with the first-line chemotherapy clinically has indicated significant synergistic effect in latest years (B. Sun, Ranganathan, & Feng, 2008).

One of the most effective chemotherapeutic drugs for treating HER2 breast cancer is docetaxel as one of the most effective chemotherapy, but patients typically suffer from severe adverse effects (such as leukopenia, thrombocytopenia, and alopecia, etc.) (Fauzee et al., 2012). Therefore, combining both trastuzumab and docetaxel in nano-delivery systems for targeting HER2-positive breast cancer could be a promising approach. Application of a targeted drug delivery system against a specific tumor antigen would enhance the concentration of docetaxel in the defective cells, leading to improved therapeutic effect and reduce side effects. The modified drug delivery system could ultimately minimize the systemic exposure of the chemotherapeutic agent (Nobs, Buchegger, Gurny, & Allemann, 2004).

This research will propose the formulation of the PLGA (Poly (D, L-lactide-co-glycolide) NPs that encapsulate the chemotherapeutic agent (docetaxel); and ultimately conjugate with either monoclonal Ab (trastuzumab, which binds to HER2) or ScFv (Single-Chain Fragment Variable) IgG anti-HER2 on the surface of NPs. The rationale behind this research is to improve the potential for targeting and releasing docetaxel to cancerous cells overexpressing the HER2 receptor, subsequently leading to enhancing the therapeutic effect and minimizing the adverse effects of the chemotherapeutic agents.

2. LITERATURE REVIEW

2.1. Breast Cancer Overview

Cancer is considered the second cause of death worldwide after Cardiovascular diseases. Lung, breast, colorectal, prostate, and stomach are the most frequent areas of tumor growth and spread (Ferlay et al., 2015). Breast cancer is the most common type of cancer affecting women worldwide leading to a higher rate of mortality among females and is the second most common recurrent type of cancer (Jemal et al., 2011; Torre et al., 2015). Over 10 million cases of cancer are diagnosed each year globally (Misra, Acharya, & Sahoo, 2010). According to the Canadian Cancer Society's Steering Committee on Cancer Statistics, the occurrence of breast cancer is estimated to be approximately 130.1 cases per 100,000 women, and 90% of deaths related to cancer cases are due to metastatic growth ("Canadian Cancer Statistics ", 2017)

Genetic damage or alteration causes cancerous diseases that lead to abnormal proliferation and activities. Cancerous cells start competing for more nutrients to keep up with the rapid proliferation and uncontrollable cell division (Brannon-Peppas & Blanchette, 2004). The second most common type of cancer leading to death are the breast tumors (McGuire, 2016; Tarver, 2012). Breast cancer is classified into four subtypes according to biomarker and gene expression profiles:

(1) *Luminal A*: affects around 50–60% of breast cancer patients. This subtype express an estrogen receptor (ER). The expression of progesterone receptor (PR) could be positive or negative, and a low level of Ki67 protein with no expression of HER2. *Luminal A* subtypes commonly metastasize in bone.

(2) *Luminal B*: incidence is almost 10–20%. ER-positive, high level of Ki67, and HER2-negative are the frequent pattern of biomarker expression; however, in a few cases this subtype can be HER2 positive and ER negative, which is a very aggressive type of breast tumor with a high rate of proliferation. This subtype commonly metastasizes in bone.

(3) *Basal-like or triple-negative* cancer has a high expression of proliferation genes, but with the absence of HER2, ER, and PR receptors. This subtype is usually identified in African American women and commonly metastasizes to lung and nervous system tissues (Barnato & Gradishar, 2015).

(4) *HER2 breast cancer* encompasses around 25-30% of the cancer cases (Scheuer et al., 2009). HER2 amplification means that patients get proliferation in chromosome 17(17q12), causing a greater production of the proto-oncogene leading to expression of more HER2 receptors on the cell surface. Also, HER2 is a receptor of tyrosine kinase (ErbB2). Therefore, more epidermal growth factor (EGF) will bind to the cells and cause enhanced proliferation. In addition to HER2 cancer, 40% of the patients get a P53 mutation. HER2 tumors have a higher rate of local recurrence and commonly metastasize in the brain, liver, and lungs. In the past, HER2 tumors have had a poor prognosis and survival rate; however, after producing a targeted medication for HER2 (trastuzumab), there has been an improvement in survival rates for early-stage diagnosis (Barnato & Gradishar, 2015; Tai, Mahato, & Cheng, 2010).

2.2. Breast Cancer Treatment

Conventional treatment of cancer includes surgery alongside radiotherapy for localized primary or secondary tumors. However, such treatments are ineffective for metastatic cancer (Toraya-Brown et al., 2013). Additionally, chemotherapeutic agents are considered the most efficient way to treat cancer, but they have high adverse effects due to their lack of specificity, which destroys healthy cells along with cancer cells (Hamdy, Haddadi, Hung, & Lavasanifar, 2011). Common side effects of chemotherapy include nausea, vomiting, alopecia, and neutropenia (Figure 1). Chemotherapy is also limited due to poor stability and physiochemical properties. The most common drawback of anticancer drugs is poor bioavailability due to their high molecular weight and multiple drug resistance (Shapira, Livney, Broxterman, & Assaraf, 2011). Specific targeted drug delivery can overcome the limitations of chemotherapeutic agents. Therefore, many researchers are focusing on nanotechnology to carry cytotoxic drugs to the specific target tumor site (Gillet & Gottesman, 2010; C.-M. J. H. a. L. Zhang, 2009).

Today hundreds of chemotherapeutic agents are available for cancer treatment, and cancer patients generally take a combination of two or three chemotherapeutic agents. One of the most primary chemotherapeutic agent that has been used for treating breast cancer is 5-Fluorouracil (antimetabolites), which works on inhibiting the cell cycle by preventing the chromosomes to cope (Longley, Harkin, & Johnston, 2003). Another class of chemotherapeutic agents is antitumor antibiotic (doxorubicin and daunorubicin) which is widely used for breast cancer. Doxorubicin is main mechanism depends on altering the DNA to prevent the multiplication of cancerous cell (Keizer,

Pinedo, Schuurhuis, & Joenje, 1990). Finally, the mitotic inhibitor chemotherapeutic agents which is paclitaxel and docetaxel. Paclitaxel (Taxol ®), was a chemotherapeutic agent, that was isolated from the bark of *Taxus brevifolia* in 1990, and docetaxel (Taxotere ®), which is a semisynthetic analogue to paclitaxel was first used in 1995. The two taxanes are used commonly for breast cancer patients as one of the first line chemotherapy (Tsai, 2001).

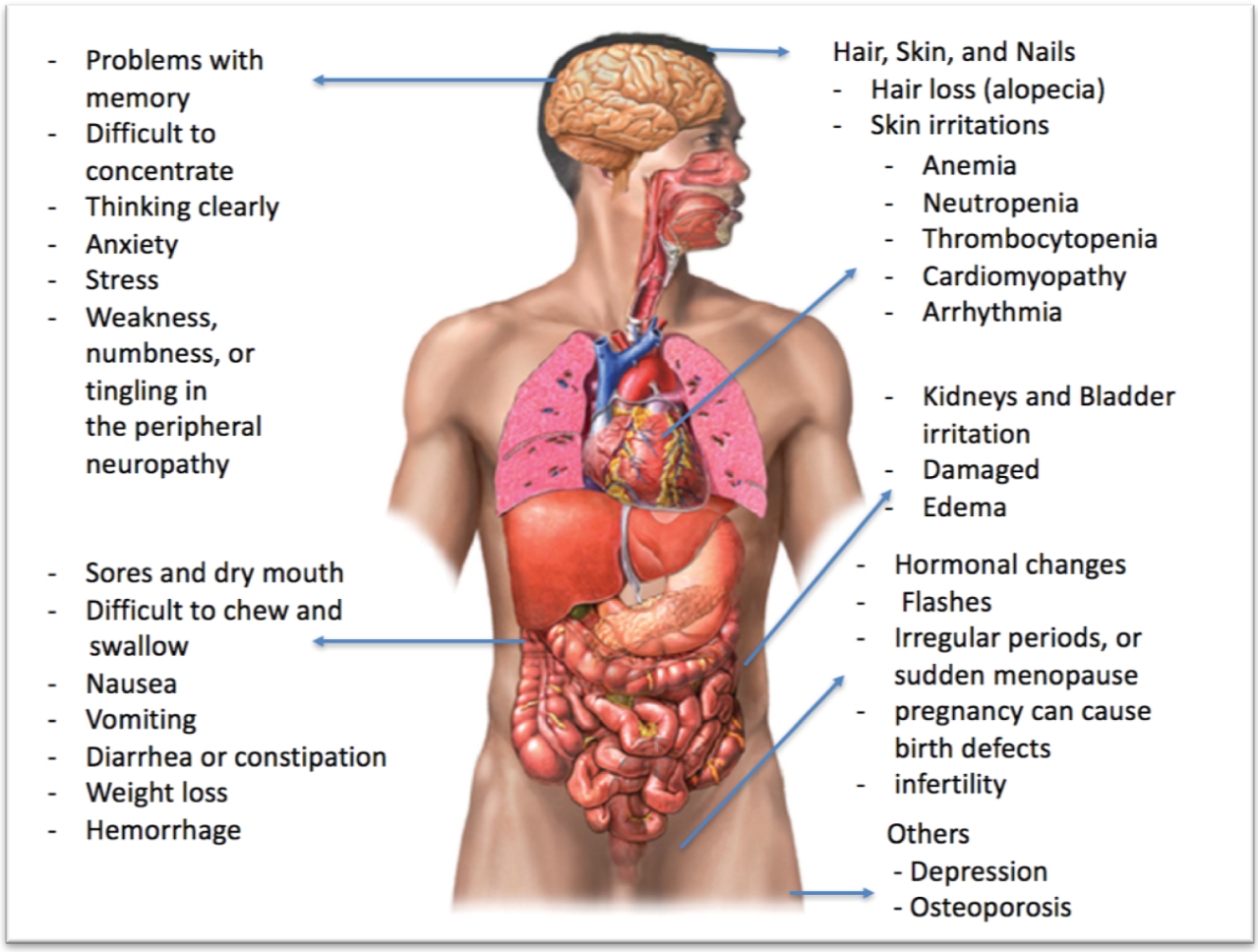

Figure 1. A summary of the main side effects of chemotherapy on different organs in the body.

2.2.1. Docetaxel

Docetaxel (DOC) is a microtubule inhibitor anticancer agent extensively used to treat breast cancer (Figure 2). It functions in the G2/M phase of the cell cycle by binding to β-tubulin to inhibit depolymerization of the microtubules. The microtubule is one of the most important structures in the cytoplasm of a eukaryotic cell, as it acts intra-cellularly as a cytoskeleton and is essential for movement within the cell; for example, moving the chromosomes during cell mitosis. Docetaxel suspends cells in metaphase due to the desegregation of the chromosome which leads to cell death (Fumoleau, Seidman, Trudeau, Chevallier, & Ten Bokkel Huinink, 1997; Youm, Yang, Murowchick, & Youan, 2011).

From a pharmacokinetic perspective, DOC has a high volume of distribution due to high binding affinity with tissues. However, it does not cross the blood-brain barrier as it is a substrate for efflux transporters. Docetaxel is metabolized mainly by liver cytochrome P450. As with other chemotherapeutic agents, DOC has many side effects, including nausea, diarrhea, hair loss, weakness, infection, peripheral neuropathy, and fluid retention (Byrne, Betancourt, & Brannon-Peppas, 2008).

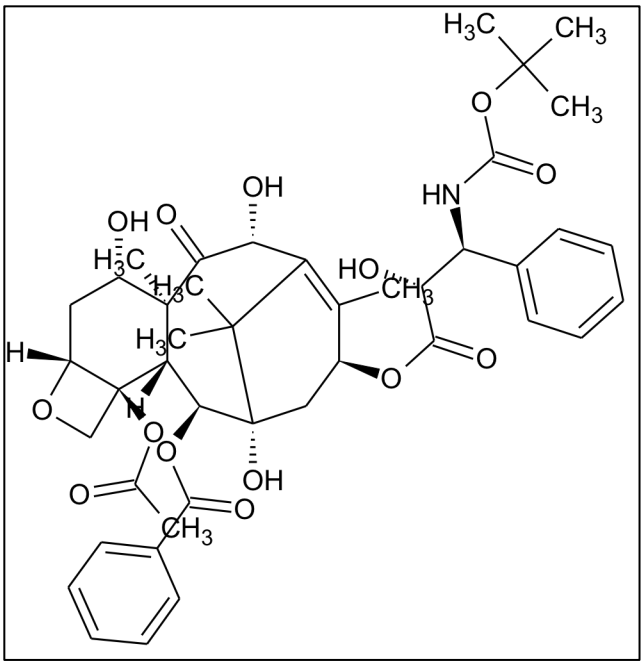

Figure 2. Docetaxel's chemical structure (molecular weight 807.879 g/mol).

2.3.Active Targeting

The ideal approach to deliver cytotoxic drugs to tumor cells with minimal effect on healthy cells is by active targeting, which could minimize the systemic side effects and enhance the therapeutic outcome. Aptamers, antigen-antibody interaction, and ligand receptors are examples of molecules specific for different targeting moieties on the cells that are able to recognize and actively target the tumor cells (Nishioka & Yoshino, 2001). For instance, Farokhzad et al., produced PLGA-PEG nanoparticles that encapsulated docetaxel and conjugated with A10 2-flouoropyrimidine RNA aptamers to target prostate cancer (prostate-specific membrane antgine). *In vitro,* there was a significant cellular toxicity and full tumor reduction *in vivo* (Farokhzad et al., 2006). Another example, is using transferrin as a target ligand to target PLGA NPs to

pancreatic cancer cell (Frasco, Almeida, Santos-Silva, Pereira Mdo, & Coelho, 2015). In HER2 breast tumors, HER2 receptors would be overexpressed 100 times more on the surface of tumor cells than normal cells. This could also occur in some types of lung and prostate cancers (Salomon, 1995). The human body treats drug delivery formulations as a foreign agent, so it could be removed by the liver and spleen from circulation via the reticuloendothelial system (Davis, Chen, & Shin, 2008; Grislain, 1983).

Producing targeted NPs formulation requires ligands attached on the surface to bind them with the tumor cell. There are different cross-linking agents used to conjugate the ligand to NPs (Koopaei et al., 2011). Firstly, bis-sulfosuccinimidyl suberate (BS3) is a homobifunctional spacer that has been used as a cross-linker to develop covalent amide bond between Ab and NPs (Thamake, Raut, Ranjan, Gryczynski, & Vishwanatha, 2011). The mechanism of action is in one step without any modification; it forms a covalent amide bond between a carboxylic group of BS3 and Lysine of Ab by releasing a sulpho-NHS group at the end of both sides of the spacer. This conjugation can be carried out at physiological pH which decreases the chances of degradation of the targeting moiety including the Ab. However, undesirable polymerization or self-conjugation of Ab can be occurred (Brufsky, 2010).

The second group of cross-linker agents is NHS (N-Hydroxysuccinimide Esters)/EDC (1-ethyl-3- (3-dimethylaminopropyl), which is a heterobifunctional cross-linker containing an amine-reactive succinimidyl ester (NHS) at one end and a sulfhydryl-reactive group at the other end. It is a commonly used strategy to crosslink the carboxylic acid group on the nanoparticle surface and the amine group of the ligand

(carbodiimide chemistry) to form an amide linkage. This is a two-step conjugation, which would minimize antibody-to-antibody linkages. NHS esters are reactive groups formed by carbodiimide-activation of carboxylate molecules.

Polymeric NPs have specific ligands that can carry docetaxel to tumor cells without affecting other cells. Also, many studies have shown that a combination of DOC with other medications (trastuzumab) improves the prognosis of administration and reduces side effects.

2.4. HER2 Receptor

Human epidermal growth factor receptor (HER) has four (homologous) subtypes: HER1, HER2, HER3, and HER4. HER2 is also known as receptor tyrosine-protein kinase (erbB-2, CD340, Proto-oncogene Neu, ERBB2). Normally, HER2 has low expression in the healthy adult human body. It exists as either a heterodimer or homodimer; therefore, it has two extracellular domains as well as intracellular, but HER2 is the only one in this family that does not have an identifiable ligand for the extracellular domain (Mitri, Constantine, & O'Regan, 2012). Moreover, HER2 has an N-terminal cysteine in the extracellular domain, a single α-helix trans-membrane lipophilic, and an intracellular tyrosine kinase in the cytoplasm (Tai et al., 2010). The binding of epidermal growth factor (EGF) to HER2 receptors will auto-phosphorylation the receptor. Then, auto-phosphorylated HER2 will activate the phosphorylation residues intracellular and regulate cellular processes: *a.* MAPK/ ERK pathway (mitogen-activated protein kinase [MAPK] extracellular signal-regulated kinase [ERK]), and *b.* phosphoinositide 3-kinase (PI3K) pathway (Citri & Yarden,

2006; Koutras1 & Evans2, 2008). The pathway outputs promote cells to move on in the cell cycle from the interphase to the G1 phase by increasing the affinity of the RNA-polymerase to the promoter to initiate gene transcription (Figure 3) (Scheuer et al., 2009). As a result, amplification of the HER2 receptor will lead to uncontrollable cell proliferation. The distinctive antigen (HER2) exposed on the cells' surface makes it ideal for antibodies to target without affecting other cells (Arruebo, Valladares, & González-Fernández, 2009). Similar monoclonal antibodies work against particular antigens (trastuzumab), so they have minimum side effects. Therefore, it has been an active area of pharmaceutical development for researchers (Arruebo et al., 2009).

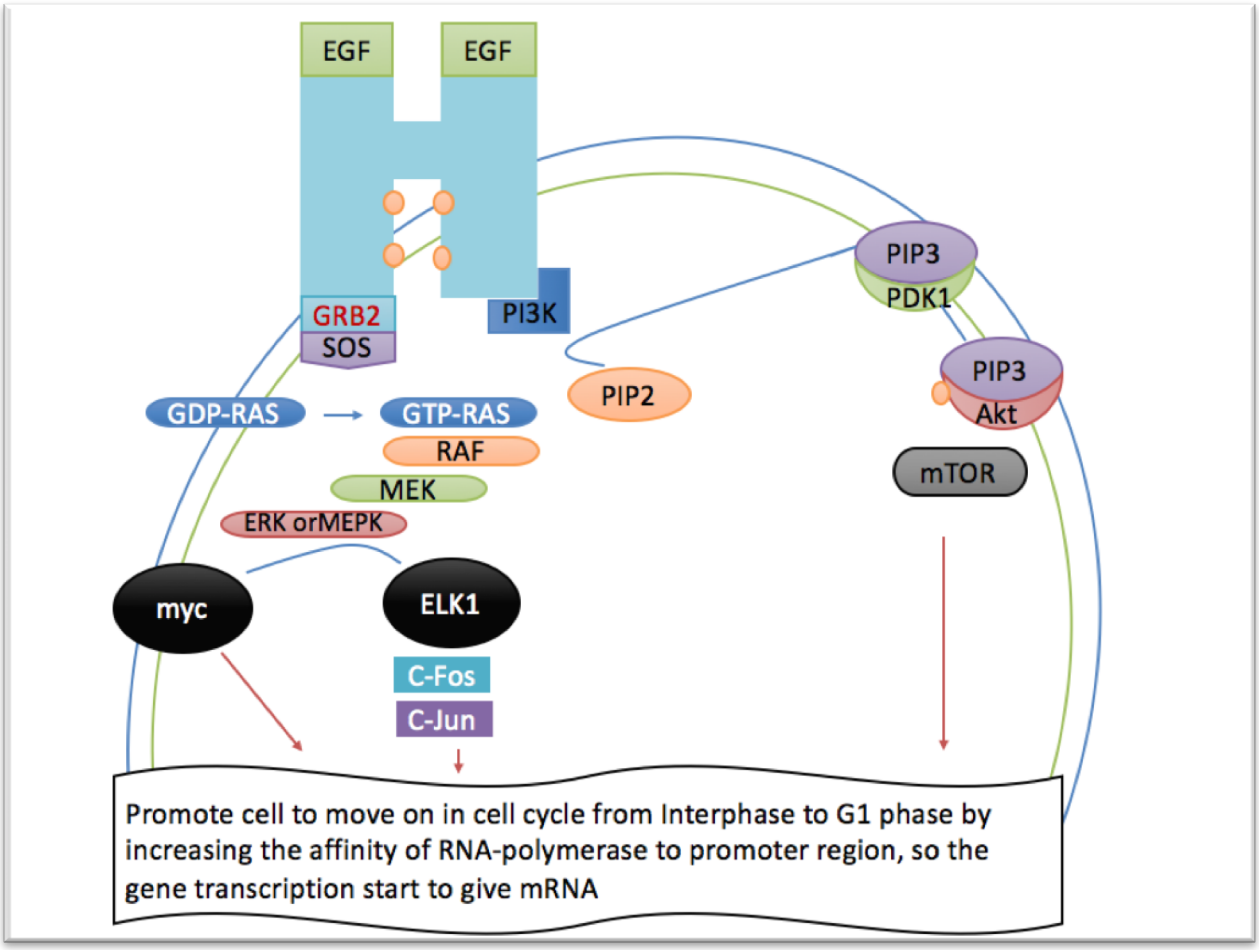

Figure 3. Human epidermal growth factor receptor-2 intracellular activation signaling pathway.

2.4.1. Trastuzumab

Trastuzumab (brand name Herceptin® from Genentech) is an IgG1 humanized monoclonal Ab that has been approved mainly for treating HER2 breast cancer as well as other HER2 tumors such as gastric cancer. The average molecular weight of trastuzumab is 150 kDa, and the route of administration is via intravenous infusion. Trastuzumab's effectiveness in improving the survival rate as monotherapy is found to be around 30% for HER2 breast cancer (Bang, Van Cutsem, Feyereislova, & Investigators, 2010; Smith et al., 2007; Vogel et al., 2002). Therefore, the standard

treatment has been recommended as a combination of trastuzumab with other chemotherapy medications such as capecitabine, 5-fluorouracil, and cisplatin for metastatic gastric cancer (Bang, Van Cutsem, Feyereislova, Chung, et al., 2010). In HER2 breast cancer, most of the studies suggest combining trastuzumab with paclitaxel, docetaxel, or aromatase inhibitors for post-menopausal women (Boekhout, Beijnen, & Schellens, 2011). The combination of trastuzumab plus chemotherapy (Taxanes mainly) has demonstrated disease-free and overall survival advantages for patients in early stages of HER2 breast cancer. Table 1 provides a summary of the chemotherapy agents (DOC) used in combination with trastuzumab in phase III clinical trials (adapted from Komen, 2015). Furthermore, Genentech received approval from the FDA on April of 2013 to use a combination of trastuzumab and Taxane as an adjuvant therapy for patients with HER2 cancer due to the positive outcome. Although the combination reduces dysfunction of left ventricular ejection velocity, which is the primary toxicity for trastuzumab, in most cases this ventricular dysfunction is found to be reversible (Boekhout et al., 2011). Also, some patients develop resistance from trastuzumab (K. X. Zhang et al., 2011).

Table 1. Summary of different chemotherapy agents used in combination with trastuzumab in phase III clinical trials (adapted from Komen, 2015).

Drug Combination†	Overall Response Percentage	Overall Survival Percentage After One Year
Trastuzumab with chemotherapy (docetaxel)	69%	62%*
Trastuzumab with chemotherapy (docetaxel)	59%	88%
Trastuzumab with chemotherapy (docetaxel)	73%	89%
Trastuzumab with chemotherapy (docetaxel and carboplatin)	73%	91%
Trastuzumab with chemotherapy (docetaxel)	70%	N/A

N/A = Not available
* Estimated survival at 15 months of follow-up.
† Each represents a different set of the larger study.

Trastuzumab (F_{ab} region) acts by binding to the C-terminal at the extracellular domain of the HER2 receptor, and the mechanism of action is not yet fully understood. (see Figure 4) However, trastuzumab Ab blocks HER2 dimerization (homodimerization with itself and heterodimerization with other HERs) that deactivates the intracellular signaling pathways (MAPK/ERK and PI3K) (Spector & Blackwell, 2009). Also, trastuzumab stimulate the immune system by producing antibody-dependent cellular cytotoxicity (ADCC) against HER2 tumor cells which decompose the cells. In addition, cell apoptosis will happen due to the increase in p27 level because of the suppression of the G1 phase of the cell cycle (Scheuer et al., 2009). Figure 4 illustrates the trastuzumab mechanism.

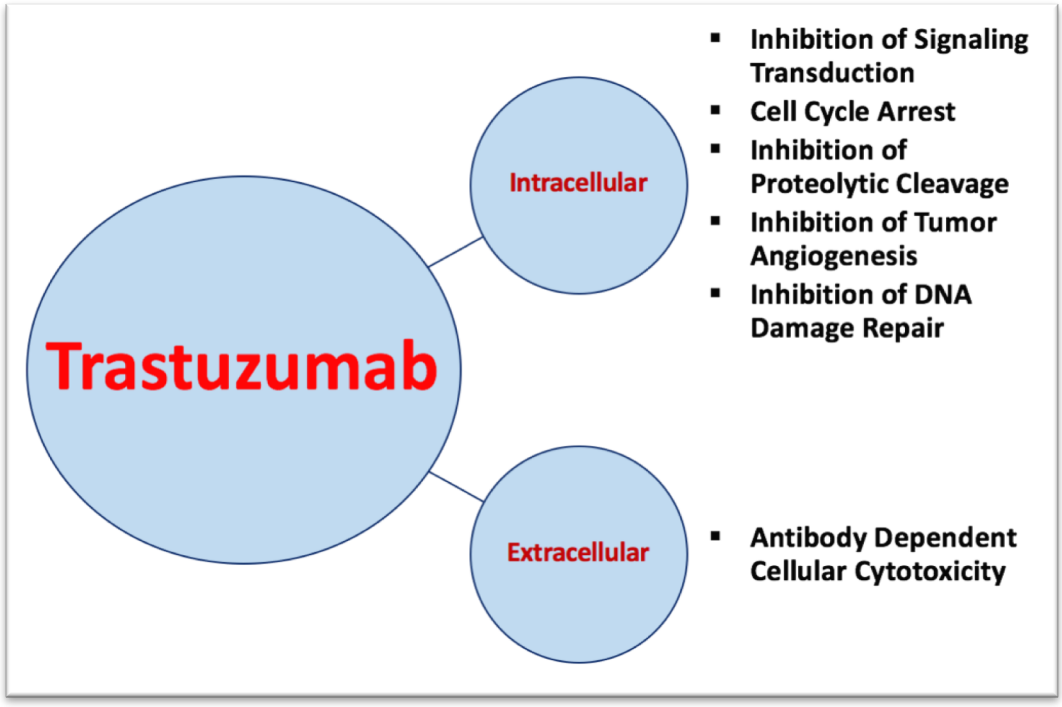

Figure 4. Trastuzumab intracellular and extracellular mechanism of action

Many studies have suggested the benefits of using trastuzumab as a targeted ligand, for instance, loading paclitaxel in poly(lactic-co-glycolic acid) or polyethylene glycol (Ma et al., 2015). Table 2 shows how trastuzumab has been used as a surface decorating ligand in different nano-systems to target HER2 cancer.

Table 2. Different polymeric NPs used to target HER2 cancer cells.

Formulation	Diameter (nm)	Synthesis Method	Ligand Coupling Method	Loaded Drug	Cell	Pathology/Target	Reference
Polylactide (PLA)	237± 43	Salting out	Thiolated, anti-HER2 and anti-CD20 mAb	Paclitaxel 7.8±0.8% (w/w)	SKOV-3, *in vivo*	Ovarian cancer therapy	(Cirstoiu-Hapca et al., 2010)
Poly(DL-lactide-co-glycolide) (PLGA) montmorillonite	312± 8.2	Solvent extraction/ evaporation	Trastuzumab	Paclitaxel 51.6 ± 2.7% (w/w)	SK-BR-3, Caco-2	Breast cancer therapy	(B. Sun et al., 2008)
Human Albumin Serum (HAS) protein based nanoparticles	411±2.3	Desolvation	40% thiolating anti-HER2 14.92±1.34 (μg/mg)	Doxorubicin 51.39±1.29 (μg/mg)	SK-BR-3, MCF-7	Targeted cancer therapy	(Anhorn, Wagner, Kreuter, Langer, & von Briesen, 2008)
	395±1.7		100% thiolating anti-HER2 16.09±3.71 (μg/mg)	57.90±0.44 (μg/mg)			
Polyamidoamine PEG (Poly ethylene glycol)	35.8±11	-	Thiolated Trastuzumab	Paclitaxel	MCF-7, BT474, *in vivo*	Targeted breast cancer	(Ma et al., 2015)

2.4.2. Fragment Antibody

Some studies have used fragment Ab (ScFv, Single-Chain Fragment Variable) to target medications instead of the whole Ab. ScFv consists only the antigen-binding unit of the immunoglobulin. This may overcome some challenges of monoclonal antibodies especially regarding its large size; in addition, it enhances the rate of tumor uptake as well as the specification of targeting (Ahmad et al., 2012). Table 3 summarizes the application of fragment Ab to target the formulations for imaging and treatment purposes. For example, Kanazaki et al. (2015) lab used ScFv anti-HER2 to target iron oxide NPs for tumor imaging.

Table 3. Different studies using fragment Ab for targeting drug delivery systems.

Conjugate to	**Ab Fragment**	**Targeting**	**Reference**
Yttrium-90-labeled CHX-A	ScFv C6.5K-A diabody	Radio immunotherapy against HER2	(Adams, 2004)
Iron Oxide NPs	Anti-HER2 ScFv	Photoacoustic tumor imaging	(Kanazaki et al., 2015)
Gallium-68	Anti-HER2 ScFv	Evaluate HER2 state by positron emission tomography (PET) imaging	(Ueda et al., 2015)

2.4.3. Nanoparticles

Nanotechnology is considered a novel technique in the pharmaceutical field for treatment and disease diagnosis, especially in oncotherapy. There are different structures and compositions of nanoparticles, which produce various types of nanosystems, such as liposomes, gold nanoparticles, and polymeric nanoparticles, etc. Different types of nanosystems are used in imaging such as magnetic iron oxide NPs to target the luteinizing hormone-releasing hormone (LHRHR) tumor receptor and in targeting different medications to different organs. (Yingna Ha, Linhua Zhang, Dunwan Zhu, & Song, 2014), and thiolated trastuzumab in human serum albumin NPs to target HER2 breast cancer cells (Steinhauser, Spankuch, Strebhardt, & Langer, 2006).

Nanoparticles could target and deliver therapeutic agents with minimal side effects; and can exhibit superior pharmacokinetic properties and therapeutic outcomes over the conventional forms of the treatments. Also, nanoparticles have the ability to overcome drug resistance in some cases because of the differences in physiochemical characteristics such as the large surfaces, which enhance the nanoparticles ability to bind, adsorb, or carry therapeutic agents (De Jong & Borm, 2008; Valladares, & González-Fernández, 2009). In addition, change in nanoparticle surface charge helps to avoid endosome and lysosome degradation so that therapeutic agents can be delivered to the cell cytoplasm. Nanoparticles require biodegradable materials for transporting and releasing the therapeutic agents in the affected organs. Moreover, selecting the place of release to achieve the high level of drug administration can be passive by depending on the enhanced permeability and retention effect (EPR) in cancer site. On

the other hand, conjugating nanoparticles with the ligands, such as antibodies, aptamers, and peptides, will target the tumor organ actively. Different ligands can be conjugated on the surface of nanoparticles to bind to a specific receptor that is overexpressed on cancer cells. This would decrease the toxicity effect in normal cells and improve the selectivity for tumor cells while defeating them (De Jong & Borm, 2008). Huang et al. (2014) have also used protamine to target and overcome drug resistance to doxorubicin-loaded PLGA NPs to treat breast tumors. Consequently, nanomedicine could be justified as an optimal approach to deliver chemotherapeutic agents due to the improvements in its pharmacological properties and cytotoxic effects.

However, targeting nanoparticles *in vivo* has been challenging because the majority of NP formulations will be taken up through phagocytosis. Adding polyethylene glycol (PEG) on the surface can enhance the half-life and prevent phagocytosis. Besides, NP size is a critical issue; small particle size (10-30 nm) will be eliminated by renal excretion, and larger size (>400 nm) will be engulfed by macrophages (Joanna Rejman, 2004).

2.4.3.1. PLGA Nanoparticles

Poly (lactic-co-glycolic acid), or PLGA, is the only synthetic biodegradable polymer that has been approved by the Food and Drug Administration (FDA). It is composed of lactic and glycolic acids, and it is degraded via a bulk erosion mechanism. The degradation rate depends on its crystalline-amorphous structure, hydrophilicity, and molecular weight; therefore, a higher proportion of glycolic acid increases hydrophilicity and degradation (see Figure 5) (Hamdy et al., 2011). Also, PLGA can

have different terminal groups such as free carboxylic acid (COOH), which can result in acidity or an esterified terminal. The terminal group can impact the therapeutic agent encapsulation efficiency, degradation, and stability of the formulation (Jahan & Haddadi, 2015). PLGA nanoparticles have been used in many drug delivery systems due to enhanced pharmacodynamic and pharmacokinetic profiles of therapeutic agents. There are many methods to prepare PLGA NPs, such as emulsification solvent evaporation, precipitation, polymerization, self-assembly, and salting out. The goal of NP application and the type of therapeutic agents are the main criteria for choosing the appropriate method of preparation (Makadia & Siegel, 2011; J. J. Wang et al., 2011).

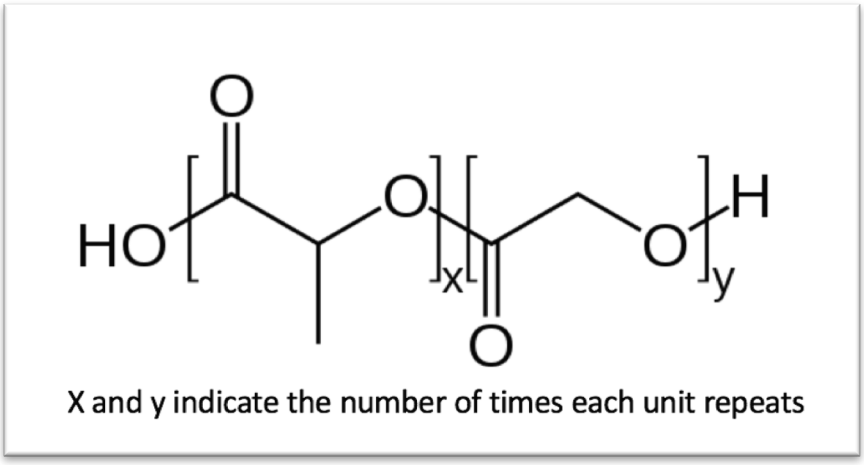

Figure 5. The chemical structure of PLGA.

Targeting NPs can be divided into two subtypes: first passive targeting which depends on the enhancement of the permeability retention effect. Second, active targeting by conjugating the nanoparticles with a ligand or Ab that will bind to a

particular receptor. Conjugating nanoparticles with peptides, nucleotide aptamers, or antibodies enhance particle recognition and accumulation in tumor areas (De Jong & Borm, 2008; Valladares, & González-Fernández, 2009). In HER2 breast cancer, using a monoclonal Ab such as trastuzumab enhances the targeting properties. An Ab fragment can also be used that will maintain its specificity and improve its ability to penetrate different types of tissues. Table 4 shows examples of various studies that have used different ligands or a fragment of Ab to target NPs. It has been reported that the penetration into a solid tumor takes about 54 hours for an entire IgG, whereas a F_{ab} fragment takes only 16 hours (Arruebo et al., 2009).

There are many factors to be considered preparing nanoparticles, such as the release and incorporation of therapeutic agents, biocompatibility, formulation stability, distribution, functionality, targeting, and adverse effects. One of the biggest challenges of modified NPs is losing the functional activity of the therapeutic agents and ligands when it encapsulated in NPs. Also, many of the materials used in preparing NPs has a toxicity effect.

One of the most significant problems of nanoparticle preparation is reticuloendothelial phagocytosis system which recognizes the NPs by the liver and spleen (for large NPs) (De Jong & Borm, 2008). Therefore, NPs size is critical to prevent the NPs clearance until it reaches the defected organ because the kidney will filter small particles. Also, surface charge (ZP) of NPs affect the cellular uptake. Neutral ZP particle will have longer blood circulation with better ability to target cells. Whereas, the extreme positive or negative ZP will have high phagocytosis rate.

Table 4. Different types of nanosystems used to target different organs.

Target Delivery System	Delivering Agent	Purpose of Study	Output	Linker	Ligand	Reference
Superparamagnetic iron oxide coated with fibronectin extra domain B-specific aptides	-	Targeting magnetic resonance imaging for cancer	Enhance the selectivity for tumor cell both *in vitro* and *in vivo.*	Prior to attached aptide, the superparam agnetic iron oxide stabilized by oleic acid	Anti-fibronectin extra domain B aptide	(Park et al., 2012)
Polymeric PLGA nanoparticle with low-molecular- weight protamine (C24-LMWP)	Doxorubicin	Enhanced intracellular and intranuclear delivery to overcome drug-resistant breast cancer	Improved penetration intracellular, intranuclear, and intratumoral.	Alkyl-chained to LMWP	Protamine	(H. Wang et al., 2014)
Colloidal systems of human serum albumin nanoparticles	-	Direct targeting of HER2 breast tumor cells	Efficient uptake for trastuzumab by which reduce the side effects.	NHS	Thiolated trastuzumab	(Steinhauser et al., 2006)
Nanoparticles of methoxy polyethylene glycol-polylactic- co-glycolic acid-polylysine (mPEG-PLGA-PLL)	Cisplatin	Targeting ovarian carcinoma (SKOV3) cells	*In vitro*, increasing cell apoptosis. Enhanced antitumor efficiency for SKOV3 cancer-bearing mice without causing toxicity.	NHS/EDC	Epidermal growth factor (EGF)	(Y. Wang et al., 2013)

Target Delivery System	Delivering Agent	Purpose of Study	Output	Linker	Ligand	Reference
Selenium nanoparticles	Doxorubicin	Enhanced cellular uptake and efficacy of anticancer drug	Enhance drug selectivity cytotoxicity for cancer cells *in vitro*. *In vivo* showed synergistic efficacy with low side effects.	EDC/ chitosan	Tansferrin	(Y. Huang et al., 2013)
Poly ($_{D, L}$-lactide-co-glyco-lide/hyaluronic acid block copolymers	Docetaxel	Selectivity for breast cancer overexpressed with CD44	Enhanced tumor targeting by improving the antitumor efficacy and reduced systemic toxicity.	NHS/EDC		(J. Huang et al., 2014)
Nanoparticles of poly (ethylene glycol)-b-poly (D, L-lactide)	siRNA and cyclin-dependent kinase 1	Target triple-negative breast cancer that overexpresses c-Myc	Inhibit tumor growth *in vitro*. No toxicity or immunogenicity effect for the formulation *in vivo*.	-	-	(Liu et al., 2014)
Copolymer of poly (ethylene glycol) with poly (d,l-lactide)	Decitabine and doxorubicin	Overcoming drug resistance by cancer stem cells and improve the response for chemotherapy	Combination of decitabine NP and doxorubicin NP is more efficient.	-	-	(Li et al., 2015)

Target Delivery System	Delivering Agent	Purpose of Study	Output	Linker	Ligand	Reference
Nanoparticle of poly (lactic co-glycolic acid)	Plasmid DNA	Improve tumor targeting and gene therapy	Enhance targeting the cancer cells. Enhanced NP uptake and gene therapy efficacy.	-	Didodecyl dimethyla mmonium bromide	(Sharma, Peetla, Adjei, & Labhasetwar , 2013)
Poly (L-g-glutamyl glutamine) (PGG)	Docetaxel	Target chemotherapy to breast cancer cells that overexpress folate	Improve anticancer efficacy and reduce systemic toxicity.	EDC/NHS, and ethylenedi-amine, ethyl acetate, dichloromet hane (DCM)	Folate	(Tavassolian et al., 2014)
Gold nanoparticles,	Doxorubicin	Targeting doxorubicin to breast cancer	Enhanced targeting to cancer cells	Etyltrimethy lammonium (CTAB)	Folic acid-PEG-Thiol	(Banu et al., 2015)
Folic acid-PEG, dual amino acid-modified chitosan complexed	DNA	Target cancer cells and enhance anti-tumor efficacy	Enhance efficacy of the delivery system	EDC/NHS	Folic acid	(Gaspar et al., 2015)
Cobalt oxide-coated nanoparticles with phosphonomethyl minodiacetic acid (PMIDA)	Doxorubicin	Anti-cancer activity, introduces better efficacy and lower toxicity for treatment	Targeted cancer cells. Enhanced anticancer activity. Reduced side effects. Positive result *in vitro* only. And *in vivo* under investigation.	-	-	(Chattopadh yay et al., 2012)

Target Delivery System	Delivering Agent	Purpose of Study	Output	Linker	Ligand	Reference
Gelation process to thiolated chitosan (N-acetyl cysteine-chitosan) and (N-acetyl penicillamine-chitosan)	Doxorubicin and antisense oligonucleotide	Target epidermal growth factor receptor in T47D cell line	Highly targeted EGFR. Research in future experiments *in vivo*.	EDAC	Thiolated chitosans	(Talaei, Azizi, Dinarvand, & Atyabi, 2011)
Magnetic iron oxide nanoparticles	Gonadorelin mitoxantrone	Image and target treatment for cancer cells	Targeted tumor cells overexpressing LHRH receptor. Inhibited tumor growth.	PEG2000-DSPE	Gonadorlin	(Yingna Ha et al., 2014)
Dual aptamer-modified silica nanoparticles coated with PEG		Diagnostic complexes, for two types of breast cancer cells: -The mucin 1 (MUC1) and - Human epidermal growth factor receptor 2 (HER2)	Highly sensitive and selective. However, it is needed to overcome: instability of nucleic acids in the blood, the short half-life of silica in circulation and the degradation of the fluorescence.	Avidin	Biotin-HER2 aptamer and MUC1 aptamer	(Jo, Her, & Ban, 2015)

3. PURPOSE OF PROJECT

3.1. Purpose

The study aims to formulate ideal PLGA NPs that can encapsulate docetaxel and allow its surface to be decorated with trastuzumab or fragment ScFv IgG anti-HER2 to target HER2 expressing breast cancer cells *in vitro*.

3.2. Rationale

The rationale of my research is to develop a targeted therapy using nanoparticles that if successful can overcome the adverse effects of conventional chemotherapy for cancer patients involving administration of nonspecific treatment with a broad-spectrum approach. Various chemotherapy treatments have poor characteristics, such as a short half-life, instability and systemic toxicities. Nanotechnology research focuses on overcoming these challenges by targeting drug delivery systems to enhance the therapeutic efficacy for anticancer drugs as well as the early detection of tumors by imaging. This study takes advantage of polymeric NPs to formulate the ideal NPs that will target and deliver the drug (docetaxel) to HER2 breast cancer.

3.3. Hypothesis

The hypothesis is that the modification of the surface of PLGA NPs carrying docetaxel by a monoclonal Ab (trastuzumab) or fragment ScFv IgG anti-HER2 will preferentially target the HER2 receptor on the membrane of tumor cells and improve the targeted delivery of the chemotherapeutic agent.

3.4. Objective

Docetaxel as a chemotherapeutic agent can be carried by polymeric PLGA nanoparticles modified with trastuzumab (monoclonal Ab) or fragment ScFv IgG anti-HER2 to target mainly breast cancer cells that overexpress HER2 receptors. This will lead to target the drug delivery systems which would avoid the systemic distribution (toxicity) of chemotherapy to the body. In this regard, the following specific objectives have been considered:

1. To develop PLGA polymeric NPs loaded with docetaxel and decorated with a humanized monoclonal Ab (trastuzumab) or fragment ScFv IgG anti-HER2 on the NPs' surface by using two different cross-linking agents BS3 (suberic acid bis [3-sulfo-N-hydroxysuccinimide ester] sodium salt) and NHS/EDC (N-hydroxysuccinimide)/(1-ethyl-3-[3 dimethylaminopropyl]-carbodiimide)
2. To study the physicochemical characterization of modified nanoparticles in terms of:
    a) Size, zeta potential, polydispersity index, and surface imaging
    b) Quantification of docetaxel loading and encapsulation efficiency
    c) Quantification of Ab attachment on PLGA NPs that encapsulated docetaxel
    d) *In vitro* docetaxel release for modified PLGA nanoparticles
3. To evaluate cell viability and IC_{50} in SK-BR-3 cell line
4. To investigate the *in vitro* tumor cell targeting by evaluation of HER2 receptor expression in MCF-7 (moderately expressed HER 2 receptor) and SK-BR-3 (overexpressed HER2) by flow cytometry and western blot

4. MATERIALS & METHODS

4.1. Materials

Both ester- and COOH-terminated PLGA were purchased from Birmingham Polymers, (LA, USA) and the inherent viscosity of both polymers was 0.15-0.25 dl/g. Docetaxel was purchased from LC Laboratories. Trastuzumab (Herceptin ®) was from Genentech. Anti-HER2 fragment (ScFv) was purchased from Creative Biolabs. Polyvinyl alcohol (PVA), bis(sulfo-succinimidyl) suberate (BS3), 0.25% Trypsin-EDTA solution and Fetal Bovine Serum were purchased from Sigma-Aldrich Co., (St Louis, USA). Other reagents used were N-hydroxysuccinimide esters (sulfo-NHS), 1-ethyl-3-(-3-dimethylaminopropyl) carbodiimide hydrochloride (EDC), bicinchoninic acid (BCA) protein assay kit, and dialysis cassettes 3.5 k MWCO (66330) from Thermo Fisher Scientific (Waltham, USA). All cell lines (MCF-7, and SK-BR-3) were from American Type Culture Collection (ATCC) (Manassas, USA). Solvents like chloroform and ethyl acetate were of analytical grade. Also, MTS assay kit (CellTiter 96 AQueous One Solution Cell Proliferation Assay) was purchased from Promega. Finally, the Purified Mouse Anti-Human ErbB2 was secured from Biosciences and the Goat Anti-mouse IgG was obtained from BioRad.

4.2. Preparation of NPs

Two techniques of NPs preparation were carried out to prepare modified drug delivery NPs as well as variable parameters were considered in NPs preparation (Table 5).

Table 5. Variable parameters considered in NPs drug delivery systems.

Polymer PLGA	• Carboxylic acid- (COOH) terminal • Ester-terminal
Organic solvent	• Chloroform • Ethyl acetate
Cross-linkers	• NHS-EDC • BS3
PVA	• 2.2%
Cryoprotectant	• Sucrose

4.2.1. Solvent Evaporation Method

The solvent evaporation technique was used for preparing an oil-in-water (o/w) emulsion to encapsulate docetaxel in PLGA NPs. The oil phase was composed of an organic solvent (chloroform or ethyl acetate depending on the PLGA terminal), 3% w/v docetaxel, and 6.5 % w/v of PLGA. Then 2.2% w/v PVA (polyvinyl alcohol) was added as a water phase followed by sonication. Subsequently, the emulsion was left to allow evaporation of the organic solvent (see Figure 6). The NP formulation was washed to remove the residual PVA. Then the NPs were freeze-dried (FD) and stored at -20° C.

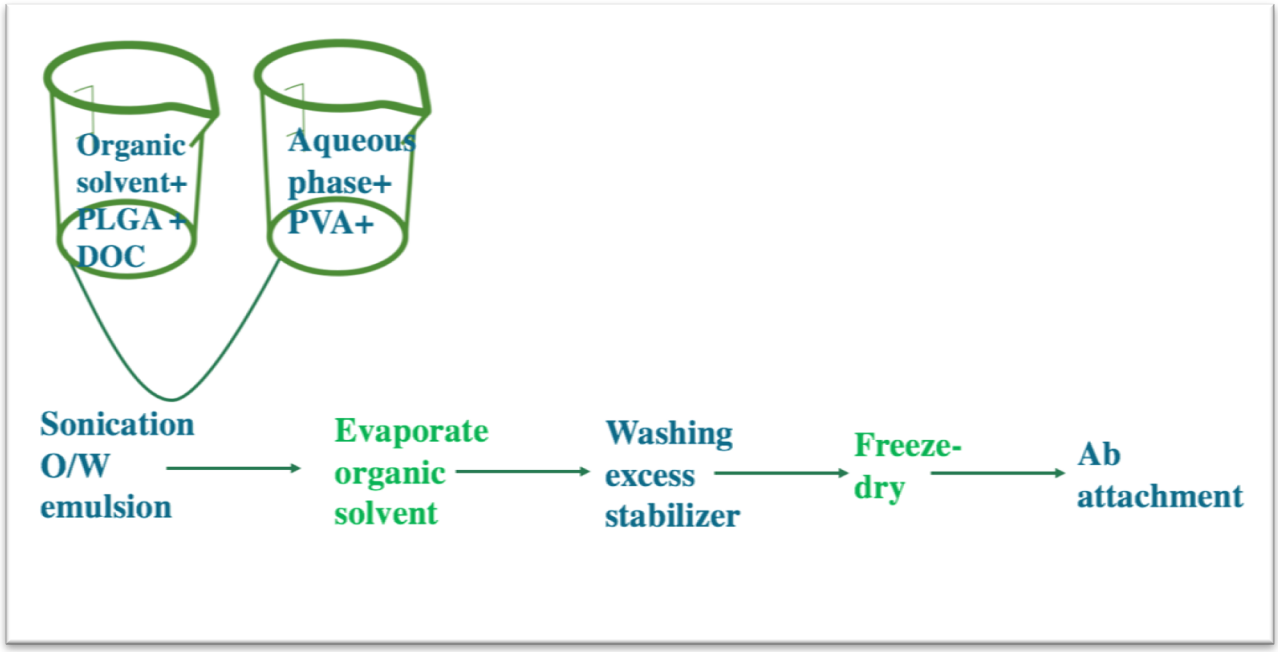

Figure 6. The scheme shows the solvent evaporation technique for NPs preparation.

4.2.2. Precipitation Method

The NanoAssemblr Benchtop (Vancouver, Canada) machine was used to mix the organic and water phases; the flow rate ratio was selected to be 1:1 according to the instrument manual. Different concentrations of PLGA (5%, 6.5%, and 10% w/v) and docetaxel (3%, 5%, and 10% w/v) were used and dissolved in acetone as the oil phase, and 2% of PVA was utilized as the aqueous phase.

4.2.3. Trastuzumab and Fragment ScFv IgG Conjugation

A covalent amide bond was created to attach trastuzumab and the fragment ScFv IgG to PLGA-DOC NPs by BS3 (suberic acid bis [3-sulfo-N-

hydroxysuccinimide ester] sodium salt) or NHS (N-Hydroxysuccinimide esters) /EDC (1-ethyl-3- [3-dimethylaminopropyl] carbodiimide hydrochloride) as linkers.

4.2.3.1. Trastuzumab extraction from Herceptin

PBS buffer (pH 7.4) was used to dissolve Herceptin in a 2:1 ratio, followed by centrifugation (Allegra^{TM} 25R, Beckman Coulter) in filtration tube, for 10 minutes at 4^{o}C and 4,100 rpm. After that, the concentration body will be reverted to the filtration tube and centrifuged again at 3,000 rpm for 5 minutes. At the final process, the concentrated filtrate will be collected, which will contain the trastuzumab without other excipients.

4.2.3.2. Using BS3

BS3 at 0.05 % w/v was dissolved in PVA 2.2% w/v while preparing NPs to carry docetaxel. Ester-terminated PLGA-DOC-BS3 in PBS (pH =7.4) was added to trastuzumab or ScFv IgG and stirred at room temperature for 1 hour followed by washing steps. The NPs were freeze-dried and stored at -20° C for future studies.

4.2.3.3. Using NHS/EDC

NHS/EDC was dissolved in PBS (pH = 5), and then DOC-COOH PLGA NPs was added followed by addition of trastuzumab or ScFv IgG. The mixture was stirred at room temperature for 1 hour followed by centrifugation and freeze-drying for 24 hours.

4.3. Physical Characteristics

4.3.1. Size Analysis, Surface Charge and Polydispersity Index

The Malvern Zetasizer Nano series (Montreal, Canada) was used to measure NP size, zeta potential (ZP), and the polydispersity index (PDI) for the NP formulations before and after freeze-drying as well as after trastuzumab and ScFv IgG attachment. Different NP formulations were suspended in deionized water and measurements were conducted at 25^{o} ±1 C. Also, the yield of NPs recovery was measured by the following equation:

$$\text{Yield (\%)} = \frac{\text{Weight of obtained NPs}}{\text{Initial weight of polymer, drug, and other ingredients}} \text{ X } 100$$

4.3.2. Surface Morphology

4.3.2.1. Transmission electron microscopy analysis

NPs morphology for all formulations was assessed via Transmission electron microscopy analysis (TEM). TEM micrographs were obtained on a Hitachi HT7700 from Hitachi, Ltd (Kyoto, Japan) which had high contrast and high resolution. The freeze-dried samples were suspended in water and then one drop of this suspension was placed into a small mold of the carbon-coated copper grid. The samples were stained with a negative stain of the specimen with 0.5% phosphotungstic acid. To evaporate the solvent, the samples were incubated for 5–10 min at room temperature (25 ± 2° C).

4.3.2.2. Scanning electron microscopy analysis

NPs morphology for all formulations was examined by Field Emission Electron Microscopy (SEM). It was seen under the SU8010 microscope from Hitachi High-Technologies (Kyoto, Japan). The dried NPs were sprinkled onto a stub covered with an adhesive conductive carbon tab, then sputter coated with a 5-nm layer of chromium or 10 nm of gold by using Sputter Coater Q150T ES from Quorum. The NPs were imaged at 5 to 50 kV accelerating voltage.

4.4. Identification of the Covalent Bond Between Linker and Ab

A Bruker IFS 66v/S Fourier Transform Spectrometer (Bio-Rad-Win-IR, Saskatchewan Structural Sciences Centre) was used in the mid-IR range (infrared). All samples were mixed with spectroscopic-grade potassium bromide (KBr) and mold to prepare the pellets. The spectrum range was 4,000–400 cm^{-1} in the absorbance mode. This test identifies the covalent bond between Ab and the linker (BS3 and NHS/EDC) by a Fourier Transform Infrared (FTIR) spectroscopy.

4.5. Docetaxel Loading Quantification

The mass spectrometer was used to quantify the loading quantity of docetaxel in the NPs' formulations. A fully validated quantitation procedure was performed on the equivalent docetaxel and internal standard (paclitaxel) MRM graphs using Analyst software version 1.6. The samples had to be extracted prior to reading them in mass. The method of extraction was established in our laboratory (Rafiei, Michel, & Haddadi, 2015).

To prepare the standard, we used plain PLGA NPs and added different concentrations of docetaxel in methanol. 100 μg/ml of docetaxel was prepared as stock solution. We then prepared serial dilutions (500, 1000, 2000, 4000, 8000, 16,000, 32,000, and 64,000 ηg/ml) as standard samples with adding 10 μl of an internal standard (paclitaxel). In Eppendorf tubes, we added 1 ml of each concentration and evaporated the methanol. We added 1 mg of plain PLGA NPs in each tube. The mixture was vortexed for one minute after we added 1 ml of acetone. The samples were sonicated in a water bath for 30 minutes and then centrifuged for 20 minutes at 8,000 rpm. The supernatant was separated in a new tube to evaporate the acetone, and the pellet was resuspended in 1 ml of acetone by vortex-mixing, bath sonication, and centrifugation. Sequentially, we transferred the supernatant into the previous tube and evaporated the acetone. Finally, we added 500 μl of methanol to dissolve the residue by vortex.

For preparing of the PLGA-DOC NPs extraction, we followed the same steps, except we did not add docetaxel from stock. Also, preparing the quality control is needed in the dilutions of (2500, 30000, 50000 ηg/ml). The amount of docetaxel loaded in the NPs was quantified in a supernatant via a mass spectrometry method. Finally, we calculated drug loading and encapsulation efficiency (EE) using the following equation:

$$\text{Docetaxel loading } \left(\frac{\text{w}}{\text{w}}\right) = \frac{\text{Amount of loaded docetaxel (µg)}}{\text{Amount of polymer (mg)}}$$

$$\text{Encapsulation efficiency (\%)} = \frac{\text{Amount of loaded Docetaxel (mg)}}{\text{Initial amount of drug used (mg)}} \text{ X } 100$$

4.6. Loading Quantification for Trastuzumab and Fragment ScFv IgG

The amount of trastuzumab or ScFv IgG anti-HER2 attached to PLGA-DOC NPs was determined by using the bicinchoninic acid assay kit (Pierce™ Microplate BCA Protein Assay Kit, Thermo, Fisher) through indirect calculation by subtraction of the unbound Ab present in the collected supernatant during washing steps from the original amount. We performed the BCA protein assay by following the kit's instructions. In this case, the supernatant of unmodified NPs (without the Ab attachment) was used as a standard blank. Also, the amount of Ab attached to NPs surface after FD was measured as a direct way by conducting the BCA assay on FD modified NPs formulations after Ab attachment. The absorbance of the samples was measured at 562 nm in the BioTek Microplate Reader using Gen5 data analysis software. The attachment efficiency was calculated as such:

$$\text{Trastuzumab attached (per mg of NPs)} \left(\frac{\text{w}}{\text{w}}\right) = \frac{\text{Amount of TrAb attached (µg)}}{\text{Amount of NPs (mg)}}$$

$$\text{Attachment efficiency (\%)} = \frac{\text{Amount of TrAb per mg of NPs (µg)}}{\text{Initial amount of TrAb used per mg of NPs (µg)}} \text{ X } 100$$

4.7. Evaluating *in Vitro* Release Pattern of Docetaxel from Modified NPs

In vitro drug release of DOC was performed on ester-PLGA-DOC-BS3-TrAb FD NPs for 120 hours in phosphate buffered saline (PBS) at different pH values (pH 7.4 and 5.0). Thirty mg of NPs were suspended in PBS and then added into dialysis

cassette (Slide-A-Lyzer Dialysis Cassette; MWCO 3,500 Da from Thermo scientific). The dialysis cassette was submerged in PBS that was placed in the incubator shaker (5000I/R Shaker-platform promo) at 37°C with an agitation speed of 100 rpm. At the following time intervals (0, 1, 2, 4, 6, 8, 12, 24, 48, 72, 96, 120 hours) 4 ml of the bulk media was taken out and replaced by equal volume of fresh media to prevent drug saturation. The samples were tested to identify the concentration of DOC released by mass spectrometer as described above. The following formulae calculated the cumulative percentage of drug released from NPs:

$$\text{Loading efficiency} = \frac{\text{Residual drug in the nanoparticle}}{\text{Initial feeding amount of drug}} \times 100$$

4.8. Cell Culture

SK-BR-3 and MCF-7 are human breast cancer cell lines. MCF-7 is considered a cell line with low expression of HER2, but SK-BR-3 overexpresses HER2. These cells were cultured in 75 cm^2 flasks and incubated at a temperature of 37°C and a humidified atmosphere containing 5% CO_2 (Carbon dioxide). MCF-7 cell lines were grown in Dulbecco's Modified Eagle Medium (DMEM Sigma) while McCoy's 5A Medium was used for SK-BR-3 cell line. The media contained 10% fetal bovine serum (FBS) and 1% penicillin (100 IU/ml)-streptomycin (100 µg/ml) solution, as dictated by the American Type Culture Collection (ATCC) guidelines. Also, a 0.25% trypsin-EDTA solution was used to harvest cells.

4.9. Cytotoxicity Assay *in Vitro*

MTS (3-(4,5-dimethylthiazol-2-yl)-5-(3-carboxymethoxyphenyl)-2-(4-sulfophenyl)-2H-tetrazolium, inner salt) cell viability assay was performed on SK-BR-3 cell line that was plated into 96 well plates at a cell density of 15,000 per well and left for 24 hours to allow the attachment of the cells. Subsequently, the growth medium was removed and different formulations were added at various concentrations (0, 1, 2.5, 5, 10, 100, 1000, 10,000 ng/ml) and incubated for 48 hours. After that, the MTS was added to each well of the plate. The absorbance was measured at 490 nm using a microplate reader (BioTek Microplate Reader) using Gen5 data analysis software. The IC_{50} values were calculated by the formula of logarithmic curves, and cell viability percentage was calculated using the following equation:

$$\text{Cell viability \%} = \frac{\text{intensity of cell incubated with the samples – Blank control}}{\text{intensity of untreated cell incubated media – Blank control}} \times 100$$

4.10. Measuring HER2 Expression

4.10.1. Flow Cytometry Analysis

1.5 x 10^5 cells of each cell line (MCF-7 and SK-BR-3) were plated in each well of 6-well plates with the medium and incubated for 24 hours. After that, cells were treated with the same concentration of DOC (as a standard) attached to Ab PLGA-DOC NPs. The plate was incubated for 48 hours. Then a 0.25% trypsin-EDTA solution was used to harvest adherent cells from the plate. After centrifugation, the cells were washed twice with ice cold PBS. FITC conjugated with Anti-HER-2/neu (Neu 24.7) FITC (from Biosciences) was used to stain the HER2 receptor on the cells. After

incubation, unbound Ab was washed with ice cold FACS buffer twice prior to flow cytometry analysis.

4.10.2. Western Blot Analysis

Protein was isolated from SK-BR-3 cell line after NP treatment by lysis with sample buffer and then to ensure an equal amount was loaded on the gel, proteins concentration was assayed using the BCA protein assay kit. For different types of NPs formulations, HER2 expression was measured by 8% polyacrylamide gel which were loaded with 15 μl of sample. After electrophoresis gels were transferred to a nitrocellulose membrane and non-specific binding was primarily blocked with 5% skim milk solution that has Purified Mouse Anti-Human ErbB2 Ab from BD Biosciences, at + 4°C overnight on a rocking platform. After incubating the primary Ab, the membrane washed two times with PBS containing 0.05 % Tween20. Goat Anti-Mouse IgG was used to react with the proteins at room temperature for an hour. After the washing step, the protein bands were visualized using ChemiDoc XRS; Bio-Rad Laboratories, Hercules, CA). Immunoblotting with GAPDH was used as a protein-loading control. The quantifications were performed by a digital image J system and Quantity One software.

4.11. Statistical Analysis

Data were analyzed by descriptive statistics calculating the mean and standard deviation (mean $\pm$ SD) for continuous variables. Analysis of variance (ANOVA) with multiple comparison (Tukey's and Pairwise Comparison) tests were performed to

demonstrate statistical difference at an α level of 0.05 using the software SPSS.

5. RESULTS

- ✓ ***First objective:*** **To develop PLGA polymeric NPs loaded with docetaxel and decorated with a humanized monoclonal antibody (trastuzumab) or fragment ScFv IgG anti-HER2 on the NPs' surface by using two different cross-linking agents BS3 (suberic acid bis [3-sulfo-N-hydroxysuccinimide ester] sodium salt) and NHS/EDC (N-hydroxysuccinimide)/(1-ethyl-3-[3 dimethylaminopropyl]-carbodiimide)**

5.1. NP Yield Percentage

5.1.1. Solvent Evaporation Preparation Technique

To prepare NPs, the first o/w emulsion must be prepared first, and the organic solvent must be evaporated. When ethyl acetate was used as the organic solvent in the case of ester-terminated PLGA, it provided a reasonable NPs yield, as shown in Tables 6 and 7. However, the yield was lower when ethyl acetate was used with COOH terminated PLGA.

5.1.1.1. Plain PLGA NPs yield percentage

Table 6 summarizes the results for the yield of plain PLGA NPs formulations using both ester- and COOH-terminated PLGA with different organic solvent. Ethyl acetate was used first based on its safety as determined by the FDA. However, COOH PLGA polymer was used to prepare NPs with ethyl acetate which showed a low yield percentage (around 20 to 25%). Whilst, chloroform provided a better yield percentage up to 33% for a formulation with 1.7 mg/ml sucrose.

Table 6. Percentage of yield for plain NPs formulations using ester- and acidic-terminal of PLGA (n=5).

NPs Formulation	Yield (%) Average ± SD
Plain PLGA ester in ethyl acetate	20.34 ± 4.59
Plain PLGA ester -1 mg/ml sucrose in ethyl acetate	22.62 ± 1.65
Plain PLGA ester-1.7 mg/ml sucrose in ethyl acetate	25.245 ± 1.45
Plain PLGA COOH-1 mg/ml sucrose in ethyl acetate	15.22 ± 2.36
Plain PLGA COOH- 1 mg/ml sucrose in chloroform	26.59 ± 12.14
Plain PLGA COOH-1.7 mg/ml sucrose in chloroform	33.2 ± 3.99

5.1.1.2. Yield percentage of ester PLGA NPs loaded with docetaxel

Table 7 shows the yield percentages for DOC-NPs formulations using the ester-terminal of PLGA as well as different amounts of cryoprotectant (sucrose) in nanosuspension formulation. To improve the yield of dispersed NPs, the cryoprotectant sucrose, which acts to decrease aggregation and stress during the NPs formulation, was added in increasing concentrations. NPs yield did not change with increasing sucrose concentration (table 7). Adding 1 mg/ml of sucrose to PLGA ester-DOC-BS3 gave 55.63 ± 2.02 yield percentage. Simultaneously, increasing the quantity of sucrose (up to 8.3 mg/ml) did not show a significant difference in the yield percentage (51.99 ± 14.79).

Table 7. Data of yield percentage for ester-terminal PLGA encapsulating DOC (n=5).

NPs Formulation	Yield (%) Average ± SD
PLGA ester-DOC	46.88 ± 4.37
PLGA ester-DOC-BS3	54.19 ± 4.96
PLGA ester-DOC-BS3-1 mg/ml sucrose	55.63 ± 2.02
PLGA ester-DOC-BS3-1.7 mg/ml sucrose	54.93 ± 4.27
PLGA ester-DOC-BS3-3.3 mg/ml sucrose	51.42 ± 13.18
PLGA ester-DOC-BS3-5 mg/ml sucrose	46.27 ± 13.03
PLGA ester-DOC-BS3-6.7 mg/ml sucrose	52.93 ± 15.93
PLGA ester-DOC-BS3-8.3 mg/ml sucrose	51.99 ± 14.79

5.1.1.3. Yield percentage of COOH PLGA NPs loaded with docetaxel

The yield percentage that resulted from using different solvents (ethyl acetate and chloroform), as well as different quantities of cryoprotectant is shown in Table 8. The yield percentage for COOH PLGA NPs is larger than that of ester PLGA (around 65%, and 45% respectively), which means COOH PLGA has higher recovery rate. With respect to ester PLGA NPs, the quantity of cryoprotectant did not cause any significant change in the yield percentages of the formulations. For example, having 1 mg/ml of sucrose in PLGA COOH-DOC NPs showed about 60% yield; whereas, the same yield percentage showed when the sucrose concentration increased to 3 mg/ml and higher. Furthermore, loaded COOH PLGA NPs confirmed that chloroform provided a higher yield percentage than ethyl acetate.

Table 8. Results of yield percentage using COOH PLGA terminal (n=5).

NPs Formulation	Yield (%) Average ± SD
PLGA COOH-DOC-1 mg/ml sucrose in ethyl acetate	16.12 ± 2.49
PLGA COOH-DOC-1 mg/ml sucrose in chloroform	60.37 ± 1.36
PLGA COOH-DOC-1.7 mg/ml sucrose in chloroform	69.52 ± 2.61
PLGA COOH-DOC-3 mg/ml sucrose in chloroform	63.97 ± 7.12
PLGA COOH-DOC-5 mg/ml sucrose in chloroform	58.56 ± 11.43
PLGA COOH-DOC-6.7 mg/ml sucrose in chloroform	55.06 ± 12.45
PLGA COOH-DOC-8.3 mg/ml sucrose in chloroform	62.91 ± 4.68
PLGA COOH-DOC-10 mg/ml sucrose in chloroform	62.2 ± 7.04

5.1.2. Precipitation Preparation Technique

The NanoAssemblr machine prepared NPs formulations by molecular self-assembly mixing in a millisecond time period. There are many criteria for controlling particle size, such as flow rate, polymer composition, and the ratio between oil and water phases. Different concentrations were used to reach small particles; however, some of the formulations were lost during Freeze-dry (FD), and it did not turn from the solid phase to powder (instead of becoming liquid, NA).

5.1.2.1. Yield percentage of ester-loaded PLGA NPs

Different amount (5%, 6.5%, and 10% w/v) of ester PLGA were dissolved in acetone as well as a different quantity of docetaxel (3%, 5%, and 10% w/v). Several ratio percentage were used to find the optimal concentration for forming NPs. Adding 5% PLGA ester with to 3% DOC gave 42% yield percent; when the DOC quantity

increased to 10% the result was with a higher yield percentage (63%). However, when the quantity of PLGA ester increased, no significant increase in the yield percentage was noted. With 5% of PLGA ester and 3% of DOC the yield percentage was 42% contrary to the yield percentage which was 35% for 10% PLGA ester and 3% DOC NPs. The use of COOH PLGA gave a high yield percentage compared with that of ester PLGA. Similar to ester-PLGA NPs increasing the quantity of DOC (3%, 5%, and 10%) did not show any significant increase in the yield percentage of COOH-PLGA-DOC (60.06%, 47.8%, and 57.77%, respectively) (Table 9).

Table 9. Yield percentage for PLGA ester and COOH formulations encapsulating docetaxel (n=1).

NPs Formulation	Yield (%)	NPs Formulation	Yield (%)
PLGA ester 5% mg/ml-DOC 3%	42.3	PLGA COOH 5% mg/ml-DOC 3%	60.06
PLGA ester 5% mg/ml-DOC 5%	NA	PLGA COOH 5% mg/ml-DOC 5%	47.8
PLGA ester 5% mg/ml-DOC 10%	63.4	PLGA COOH 5% mg/ml-DOC 10%	57.77
PLGA ester 6.5% mg/ml-DOC 3%	NA	PLGA COOH 6.5% mg/ml-DOC 3%	33.24
PLGA ester 6.5% mg/ml-DOC 5%	NA	PLGA COOH 6.5% mg/ml-DOC 5%	92.24
PLGA ester 6.5% mg/ml-DOC 10%	31.05	PLGA COOH 6.5%mg/ml-DOC 10%	88
PLGA ester 10%mg/ml-DOC 3%	35.36	PLGA COOH 10% mg/ml-DOC 3%	NA
PLGA ester 10% mg/ml-DOC 5%	37.27	PLGA COOH 10% mg/ml-DOC 5%	48.6
PLGA ester 10% mg/ml-DOC 10%	NA	PLGA COOH 10% mg/ml-DOC 10%	NA

5.2. Identification of Covalent Bond by FTIR

The peak around 1750 cm^{-1} wavelength is one of the characteristics of carbonyl bond C=O presence of PLGA. The presence of the covalent conjugation between both ester- and acidic-terminal PLGA NPs and target ligand (whole IgG and ScFv anti-HER2) can be confirmed by detecting the amide bond. Usually, amide bond appears around 1640 cm^{-1} wavelength. The differences in the wavelength intensity for unmodified and modified ester NPs, accordingly the presence of the amide bond was confirmed around 1650 cm^{-1} (Figure 7). Figure 8 represents the same concept of COOH-terminated NPs.

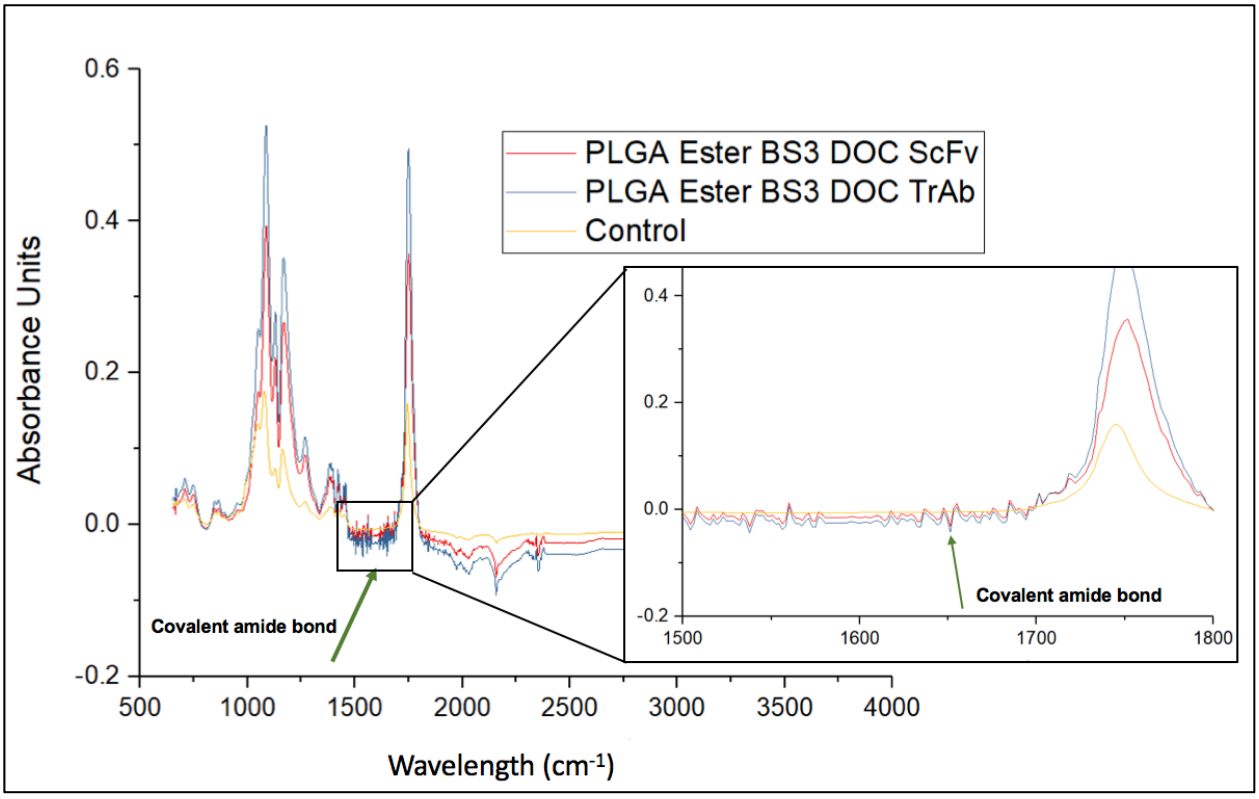

Figure 7. The FTIR derivative spectra of ester-terminated PLGA NPs: PLGA ester-DOC (yellow), PLGA ester-DOC-TrAb (blue), and PLGA ester-DOC-ScFv (red). Data is represented in absorbance units versus wavelength (cm^{-1}).

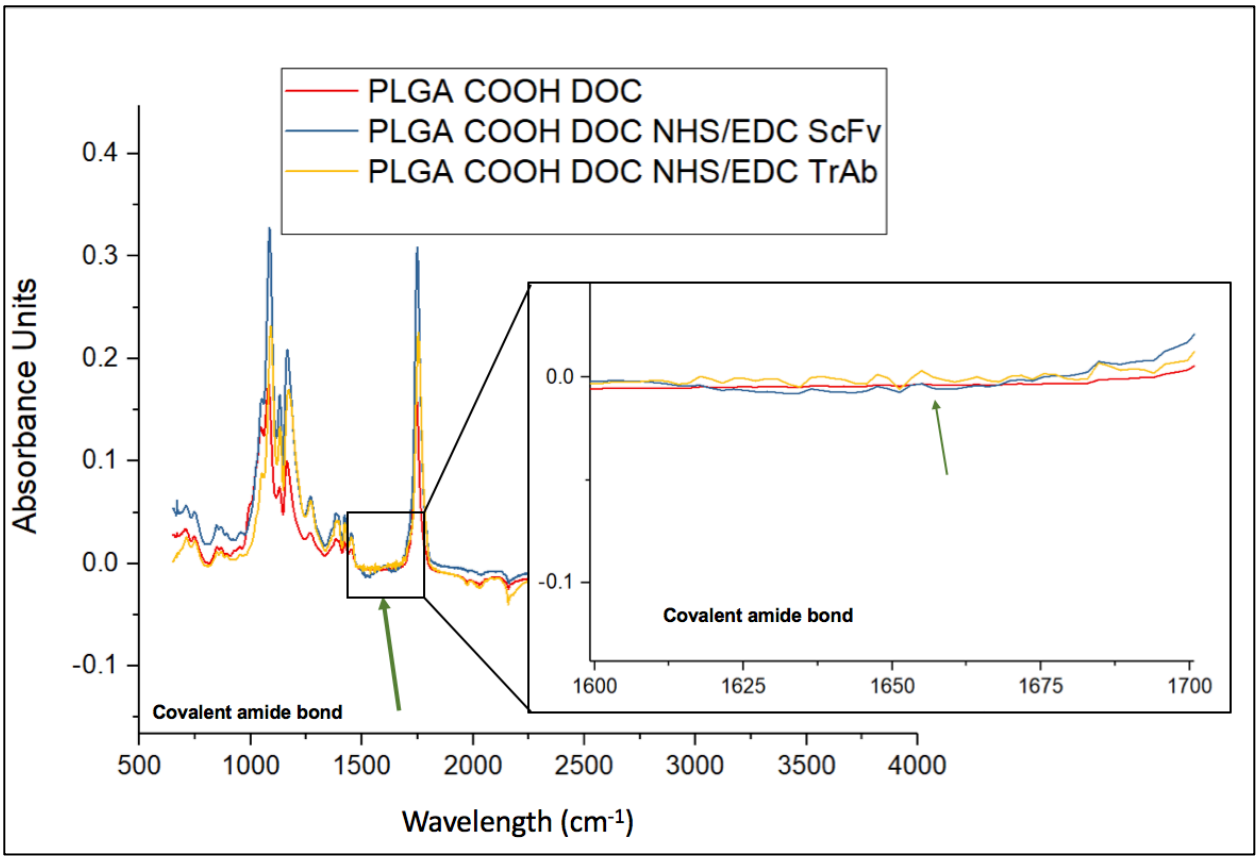

Figure 8. The FTIR derivative spectra of acidic terminated PLGA NPs. PLGA COOH-DOC (red), PLGA COOH-DOC-TrAb (yellow), and PLGA COOH-DOC-ScFv (blue). Data is represented in absorbance units versus wavelength (cm^{-1}).

- ✓ ***Second Objective:*** **To study physicochemical characterization of modified nanoparticles in terms of:**
  - **a)** Size, zeta potential, polydispersity index and surface imaging
  - **b)** Quantification of docetaxel loading and encapsulation efficiency
  - **c)** Quantification of Ab attachment in PLGA NPs that encapsulated docetaxel
  - **d)** *In vitro* docetaxel release for modified PLGA nanoparticles

5.3. Physical Characterization

5.3.1. Size Analysis, Surface Charge and Polydispersity Index

Size, PDI and ZP are critical parameters to consider prior to starting *in vitro* and *in vivo* experiments because it affects NPs uptake fundamentally. These measurements were taken before and after FD as well as after Ab attachment.

5.3.1.1. Solvent evaporation technique

5.3.1.1.1. Size, ZP, and PDI for ester-terminal PLGA NPs

Different quantity of sucrose was used to determine its effect on NPs size, ZP and PDI before and after FD (Table 10). The average size of plain NPs without BS3 is 150.9 ± 1.786 nm before FD, which is larger than plain NPs containing BS3 (141.34 ± 1.2 nm prior FD). Importantly, the data showed that increasing the quantity of cryoprotectant (1.7mg/ml) led to smaller NPs size after FD (257.2 ± 15.77 nm) and reduced the negative charge on NPs surface to - 4.7 ± 0.447 ZP. Using only 1 mg/ml of sucrose gave particle sizes above 500 nm in diameter, which would affect the uptake of the NPs.

Table 10. Size, PDI, and ZP before and after freeze-drying with different amounts of cryoprotectant (n=5).

NPs Formulation	Mean Size ± SD		Mean PDI ± SD		Mean ZP ± SD	
	Before FD	After FD	Before FD	After FD	Before FD	After FD
Plain PLGA ester	150.9 ± 1.79	1059 ± 42.04	0.127 ± 0.01	0.85 ± 0.01	-7.96 ± 0.21	-14.7 ± 3.6
Plain PLGA ester-BS3	141.3 ± 1.2	905 ± 56.18	0.127 ± 0.01	0.709 ± 0.04	-5.4 ± 0.18	-10.7 ± 1.86
PLGA ester-DOC-BS3-1 mg/ml sucrose	135.5 ± 0.21	504.5 ± 117.6	0.143 ± 0.14	0.505 ± 0.11	-12.2 ± 0.28	-6.99 ± 1.39
PLGA ester-DOC-BS3-1.7 mg/ml sucrose	139.2 ± 0.47	257.2 ± 15.77	0.112 ± 0.01	0.311 ± 0.05	-9.82 ± 0.29	-4.7 ± 0.45

5.3.1.1.2. Size, ZP, and PDI for COOH-terminal PLGA NPs

Similar to ester-PLGA NPs different quantity of sucrose as well as organic solvent (ethyl acetate and chloroform) were used to identify its effect on COOH-PLGA NPs loaded with DOC (Table 12). The average size of DOC NPs is 329.8 ± 9.39 nm after FD, which showed that increasing the amount of cryoprotectant helps to reduce the aggregation during FD process. Another observation is that the use of ethyl acetate created smaller sizes but produced lower yield percentage in the case of acidic PLGA NPs. For instance, the size for PLGA COOH-DOC-1 mg/ml sucrose was around 133.8 ± 1.52 nm before FD when the ethyl acetate was used as organic solvent; where, the using of chloroform gave larger size (228.2 ± 3.61 before FD). In addition, using 1.7

mg/ml of sucrose gave a size of 329.8 ± 9.39 nm for COOH PLGA encapsulated DOC, in contrast with COOH PLGA-DOC with 1 mg/ml of sucrose (854.6 ± 22.93 after FD).

Table 11. Acid-terminal PLGA using different quantities of cryoprotectant (n=5).

NPs Formulation	Mean Size ± SD		Mean PDI ± SD		Mean ZP ± SD	
	Before FD	After FD	Before FD	After FD	Before FD	After FD
Plain PLGA COOH-1mg/ml sucrose in ethyl acetate	112.7 ± 3.62	718.9 ± 38.97	0.234 ± 0.12	0.733 ± 0.02	-18.9 ± 0.37	-17.1 ± 1.02
Plain PLGA COOH-1mg/ml sucrose in chloroform	246.7 ± 5.17	2271 ± 267.3	0.289 ± 0.02	1 ± 0	-11.3 ± 0.32	0.00611 ± 0.06
PLGA COOH-DOC-1mg/ml sucrose in ethyl acetate	133.8 ± 1.52	232.4 ± 13.55	0.259 ± 0.02	0.588 ± 0.04	-22.8 ± 0.57	-17.1 ± 0.64
PLGA COOH-DOC-1mg/ml sucrose in chloroform	228.2 ± 3.61	854.6 ± 22.93	0.24 ± 0.01	0.301 ± 0.01	-12.5 ± 0.39	-22.7 ± 0.61
PLGA COOH-DOC-1.7 mg/ml sucrose in chloroform	230.7 ± 8.93	329.8 ± 9.39	0.298 ± 0.02	0.314 ± 0.03	-12.7 ± 0.56	-17.1 ± 1.02

5.3.1.1.3. Size, ZP, and PDI for ester and COOH PLGA NPs-encapsulated DOC and modified with anti-HER2

Both TrAb and fragment Ab were attached to the surface of different NPs formulations. Therefore, it is necessary to measure the size, ZP, and PDI after the attachment. The size of both ester and acidic NPs-encapsulated DOC did not show

significant differences between the whole Ab and ScFv anti-HER2 when attached to the surface (Table 12). For all formulations, the average size was less than 400 nm. Ab attachment increased the surface charge to reach neutral.

Table 12. Physiochemical characteristics of trastuzumab and ScFv IgG anti-HER2 considering both linkers (BS3 and NHS/EDC; n=5).

NPs Formulation	Mean Size ± SD After FD	Mean PDI ± SD After FD	Mean ZP ± SD After FD
PLGA ester-DOC-BS3-1.7mg/ml sucrose-300 μg TrAb	379.3 ± 3.04	0.34 ± 0.01	-0.14 ± 0.27
PLGA ester-DOC-BS3-1.7mg/ml sucrose-300 μg ScFv	312 ± 8.77	0.35 ± 0.03	0.02 ± 0.07
PLGA COOH-DOC-NHS/EDC-1.7mg/ml sucrose-300 μg TrAb	382.5 ± 21.5	0.38 ± 0.02	0.05 ± 0.04
PLGA COOH-DOC-NHS/EDC-1.7mg/ml sucrose-300 μg ScFv	367.2 ± 8.46	0.33 ± 0.04	0.28 ± 0.10

5.3.1.2. Precipitation technique

5.3.1.2.1. Ester-terminal PLGA NPs

The precipitation technique yielded very large NPs with an average size greater than 2,000 nm. This large size affects the physiochemical properties of NPs formulations, which would prevent cell uptake and immediately be cleared from the

body. All the formulations had high polydispersity index, which indicates there was no uniformity in the size of NPs (Table 13).

Table 13. Size, PDI, and ZP ester-terminal PLGA encapsulating docetaxel before FD (n=1).

NPs Formulation	Mean Size ± SD Before FD	Mean PDI ± SD Before FD	Mean ZP ± SD Before FD
PLGA ester 50 mg/ml-DOC 3 mg/ml	2980 ± 207.3	1	7.55 ± 0.36
PLGA ester 50 mg/ml-DOC 5 mg/ml	2078 ± 201	0.97 ± 0.05	4.17 ± 0.34
PLGA ester 50 mg/ml-DOC 10 mg/ml	2268 ± 148.5	0.97 ± 0.02	1.11 ± 0.27
PLGA ester 65 mg/ml-DOC 3 mg/ml	1066 ± 68.6	0.64 ± 0.09	-0.01 ± 0.07
PLGA ester 65 mg/ml-DOC 5 mg/ml	2030 ± 75.8	0.99 ± 0.02	-4.44 ± 0.34
PLGA ester 65 mg/ml-DOC 10 mg/ml	2931 ± 31.8	1	-7.68 ± 0.55
PLGA ester 100 mg/ml-DOC 3 mg/ml	2038 ± 107.5	0.99 ± 0.2	-4.29 ± 0.23
PLGA ester 100 mg/ml-DOC 5 mg/ml	2656 ± 206.4	1	-8.05 ± 0.60
PLGA ester 100 mg/ml-DOC 10 mg/ml	2058 ± 358.1	0.98 ± 0.04	0.60 ± 0.04

5.3.1.2.2. COOH terminal PLGA NPs

Increasing the quantity of COOH PLGA polymer reduced the mean of NPs size to be about 1,500 nm and decreased PDI to approximately 0.768 ± 0.05. Regardless of this slight improvement, all formulations were very large in size and un-uniform, which affects the physical properties of formulations. (Table 14)

Table 14. Physical characteristics of COOH PLGA-carried docetaxel prior FD (n=1).

NPs Formulation	Mean Size ± SD Before FD	Mean PDI ± SD Before FD	Mean ZP ± SD Before FD
PLGA COOH 50 mg/ml-DOC 3 mg/ml	3664 ± 635.6	1	-3.21 ± 0.46
PLGA COOH 50 mg/ml-DOC 5 mg/ml	2443 ± 299.5	1	-4.76 ± 0.45
PLGA COOH 50 mg/ml-DOC 10 mg/ml	4405 ± 430.7	0.767 ± 0.24	-0.29 ± 0.15
PLGA COOH 65 mg/ml-DOC 3 mg/ml	1944 ± 230.4	0.998 ± 0.09	-5 ± 0.43
PLGA COOH 65 mg/ml-DOC 5 mg/ml	1587 ± 422.2	0.939 ± 0.09	0.02 ± 0.07
PLGA COOH 65 mg/ml-DOC 10 mg/ml	1430 ± 176.5	0.837 ± 0.08	-5.1 ± 0.28
PLGA COOH 100 mg/ml-DOC 3 mg/ml	1413 ± 167.4	0.756 ± 0.08	-0.671 ± 0.15
PLGA COOH 100 mg/ml-DOC 5 mg/ml	1704 ± 156.3	0.768 ± 0.05	0.4 ± 0.07

As a result of the above data, we found that the ideal way to prepare polymeric NPs was solvent evaporation technique, which gave the highest yield as well as the best physical characteristics in terms of size, surface charge (ZP), and polydispersity index (PDI). Following are the final formulations used for further analysis based on the positive possibility of targeting HER2 breast cancer raptors: PLGA ester-DOC-BS3-1.7mg/ml sucrose-300 μg TrAb, PLGA ester-DOC-BS3-1.7mg/ml sucrose-300 μg ScFv, PLGA COOH-DOC-NHS/EDC-1.7mg/ml sucrose-300 μg TrAb, and PLGA COOH-DOC-NHS/EDC-1.7 mg/ml sucrose-300 μg ScFv.

5.3.2. Surface morphology

5.3.2.1. TEM

The NPs formulations were visualized by TEM to analyze their morphological characteristics, such as size, shape, and PDI. NPs had quasi-spherical geometry with uniformity in the dispersion (Figure 9). The images also confirmed that the conjugation of anti-HER2 may occur without affecting the morphology of the NPs. The diameter of NPs was larger in the measurement by Zetasizer (a Malvern instrument) compared to the TEM measurement because TEM provides the results of a dry state of NPs formulations, whereas Zetasizer collects results from the NPs in hydrated form. Also, TEM can show the image of a single particle, whereas Zetasizer provides an estimate of size average, which favors the larger NPs distributions. In addition, Zetasizer measures size by determining the dynamic light scattering (DLS), which is a different form of analysis.

Figure 9. Surface morphology of both ester and acidic PLGA-encapsulated docetaxel and conjugated by either trastuzumab (TrAb) as a whole IgG antibody or single-chain variable fragment (ScFv).

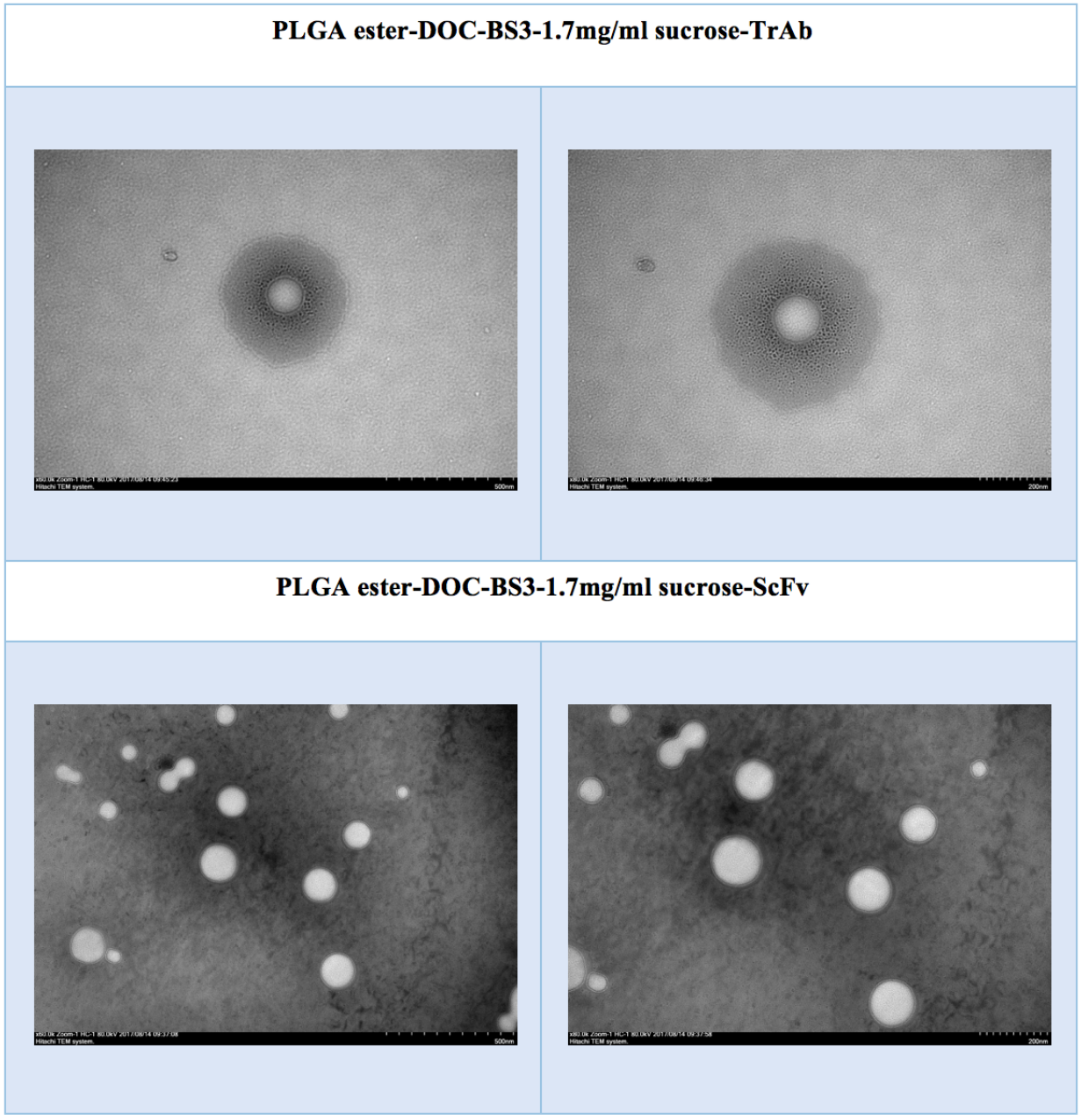

PLGA COOH-DOC-NHS/EDC-1.7mg/ml sucrose-TrAb

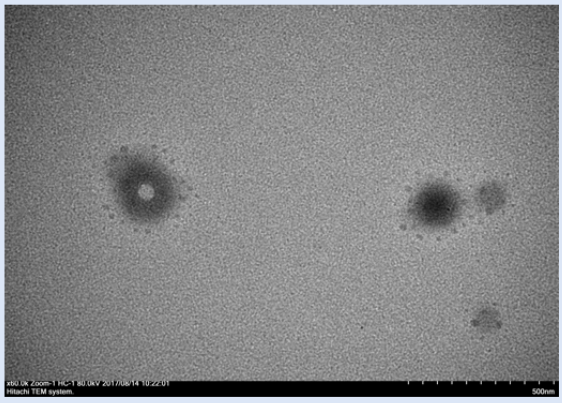

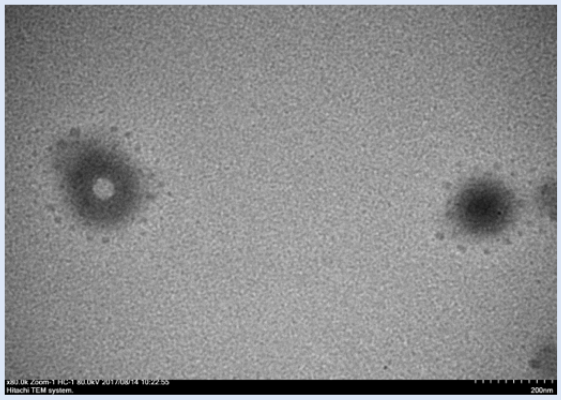

PLGA COOH-DOC-NHS/EDC-1.7mg/ml sucrose-ScFv

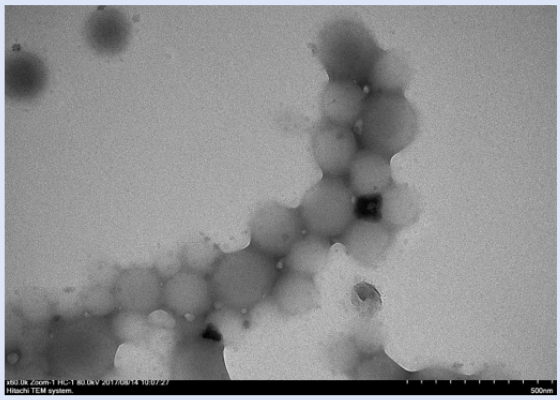

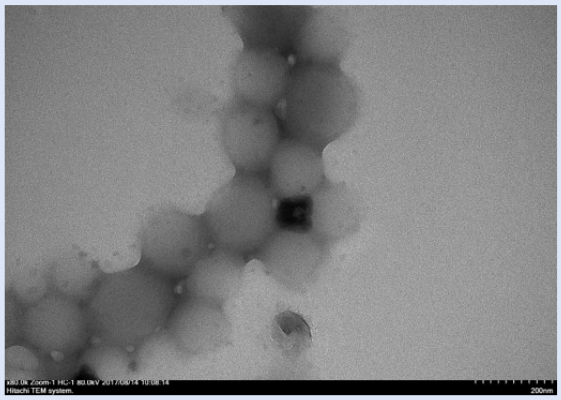

5.3.2.2. SEM

Scanning electron microscopy confirmed the size, shape, and PDI. Figures 10 and 11 demonstrate the images of different formulations obtained by using chromium and gold to coat NPs; this coating is necessary because direct beams melt the PLGA polymers. The NPs were chosen randomly. The pictures emphasized the uniformity of NPs, with near spherical in shape. SEM results, like the TEM results discussed above, differed with the Zetasizer measurements in terms of diameter.

Figure 10. Surface morphology of both ester and acid PLGA-encapsulated docetaxel conjugate by either trastuzumab (TrAb) as a whole IgG antibody or single-chain variable fragment (ScFv) coated with 5 nm chromium.

PLGA ester-DOC-BS3-1.7mg/ml sucrose

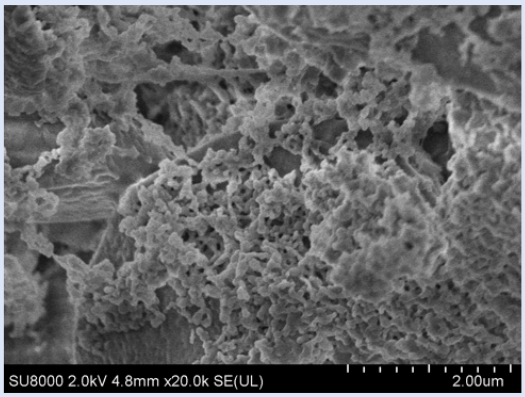

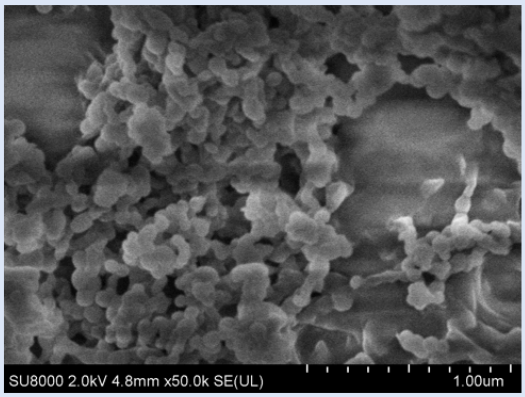

PLGA ester-DOC-BS3-1.7mg/ml sucrose-TrAb

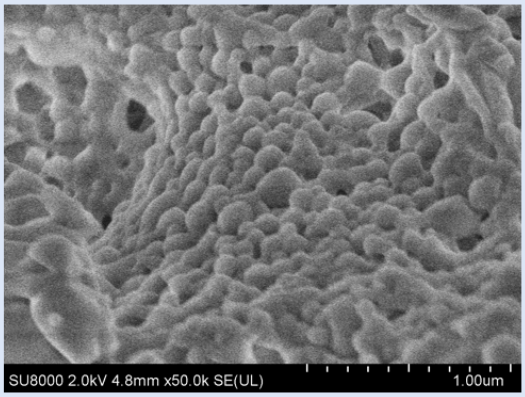

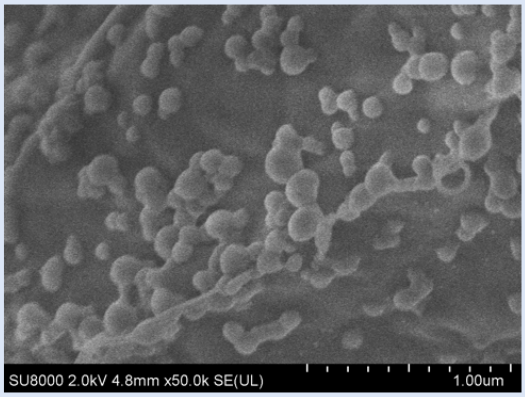

PLGA ester-DOC-BS3-1.7mg/ml sucrose-ScFv

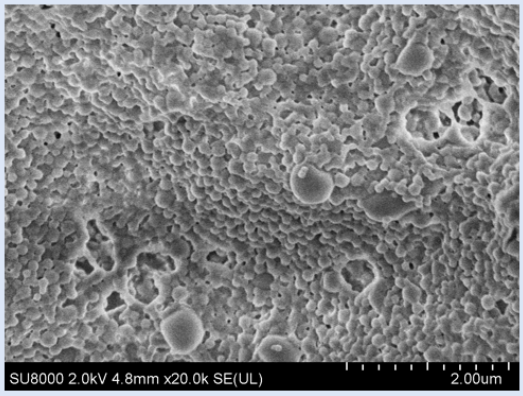

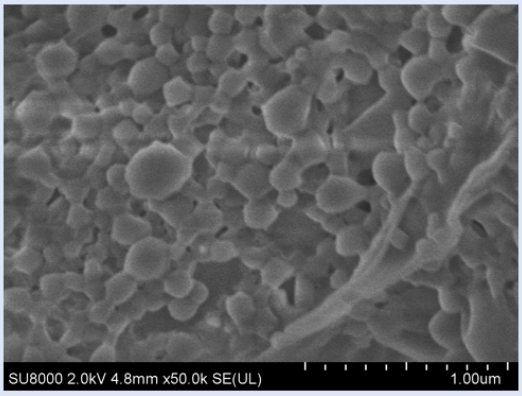

PLGA COOH-DOC-NHS/EDC-1.7mg/ml sucrose-TrAb

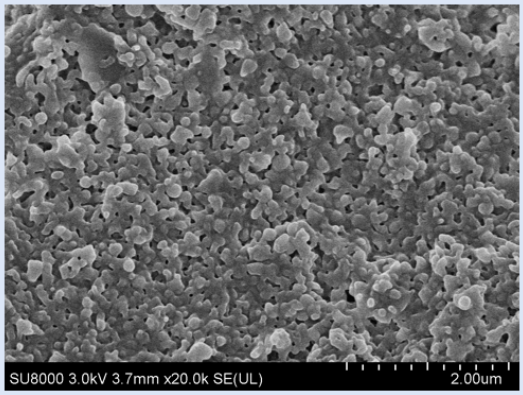

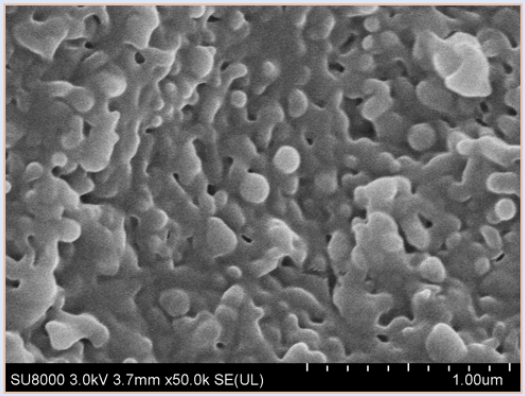

PLGA COOH-DOC-NHS/EDC-1.7mg/ml sucrose-ScFv	
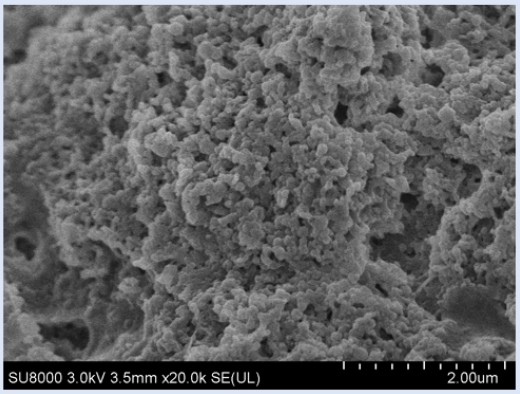	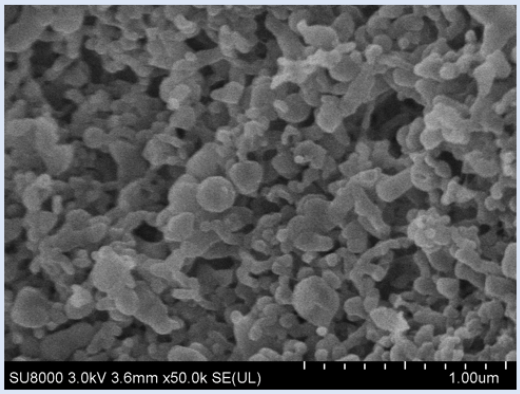

Figure 11. Surface morphology of both ester and acid PLGA-encapsulated docetaxel conjugate by either trastuzumab (TrAb) as a whole IgG antibody or single-chain variable fragment (ScFv) coated with 10 nm gold.

PLGA ester-DOC-BS3-1.7mg/ml sucrose

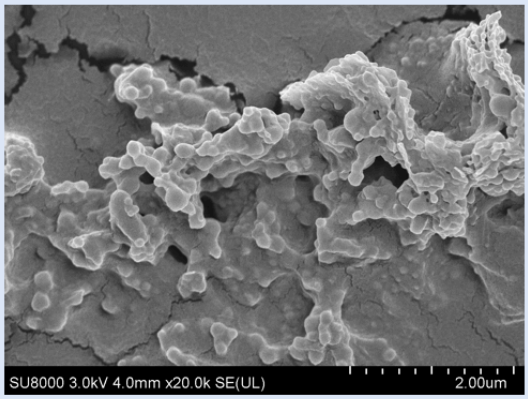

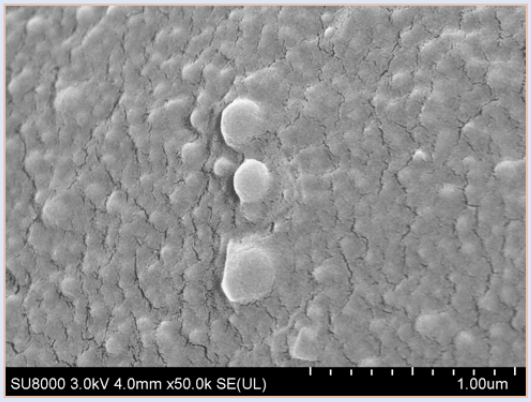

PLGA ester-DOC-BS3-1.7mg/ml sucrose-TrAb

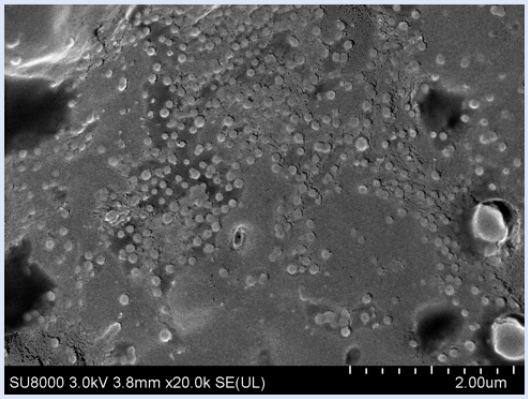

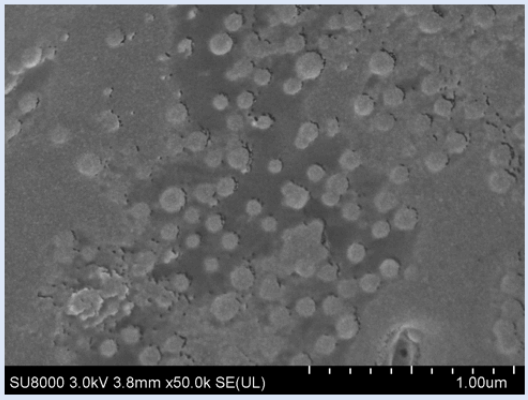

PLGA ester-DOC-BS3-1.7mg/ml sucrose-ScFv

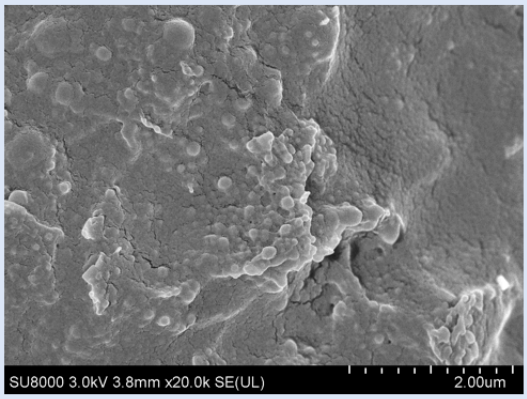

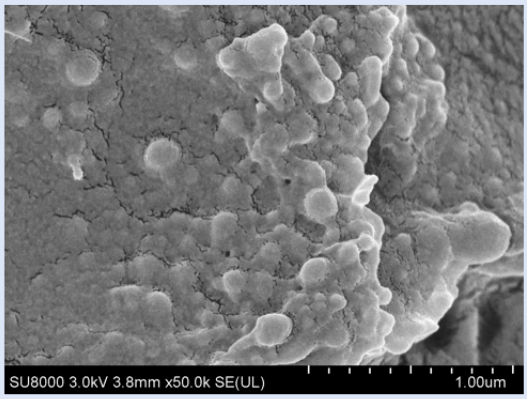

PLGA COOH-DOC-NHS/EDC-1.7mg/ml sucrose-TrAb

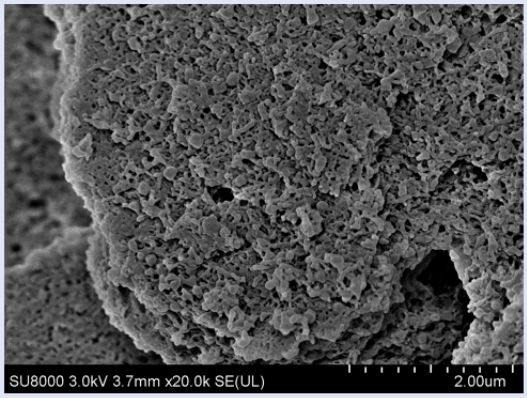

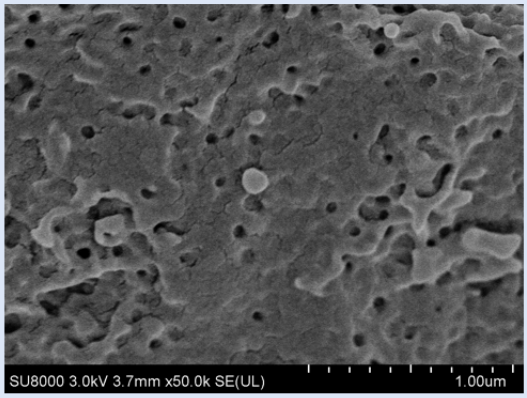

PLGA COOH-DOC-NHS/EDC-1.7mg/ml sucrose-ScFv	
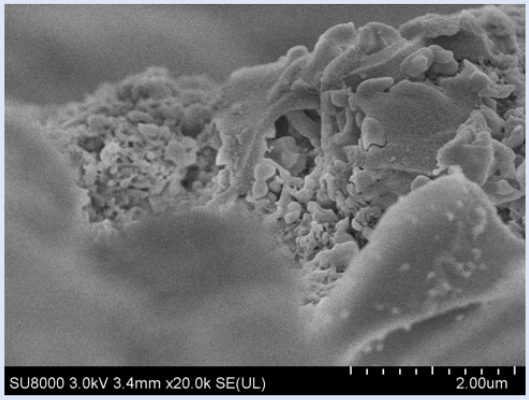	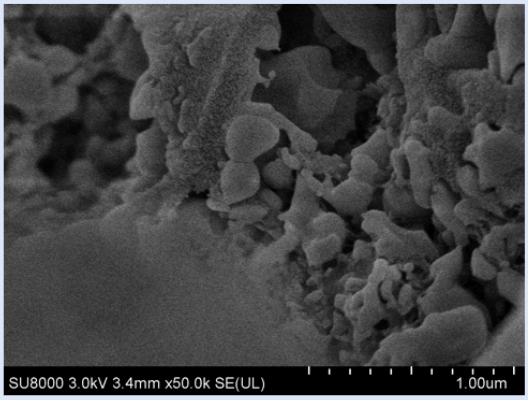

5.4. Docetaxel-Loading in NPs Formulations

The initial concentration of docetaxel used in all formulations is 3 mg/ml; this amount was chosen based on the previous project in our lab that indicated 3 mg is the most efficient quantity (Sadat, 2015). There was no statistical significance in DOC loading between ester or acidic PLGA for unmodified NPs formulations. There was a substantial difference in DOC loading for both ester and acid NPs when ScFv anti-HER2 was attached to the NPs surface. The tests for encapsulation efficiency showed that there were significant differences in the case of ester NPs and between modified NPs with TrAb and unmodified NPs (PLGA ester-DOC- versus PLGA ester-DOC-TrAb). Additionally, poor encapsulation of DOC appeared in modified acidic PLGA formulations when ScFv was attached; therefore, there was a statistical difference compared to the whole Ab attachment (TrAb).

Table 15. Docetaxel loaded in PLGA through mass spectrometry analysis and the percent of encapsulation efficiency (n=6).

NPs Formulation	Average loading ± SD µg/mg Of NPs	EE % ± SD
PLGA ester-DOC-BS3-1.7mg/ml sucrose	21.78 ± 3.33	49.8 % ± 6.1
PLGA ester-DOC-BS3-1.7mg/ml sucrose-300 μg TrAb	18.92 ± 3.86	70.8 % ± 12.4
PLGA ester-DOC-BS3-1.7mg/ml sucrose- 300 μg ScFv	14.88 ± 3.62	57.6 % ± 11.6
PLGA COOH-DOC-1.7mg/ml sucrose in chloroform	25.23 ± 2.32	68.5 % ± 5.4
PLGA COOH-DOC-NHS/EDC-1.7mg/ml sucrose in chloroform-300 μg TrAb	20.70 ± 6.61	85.6 % ± 19.6
PLGA COOH-DOC-NHS/EDC-1.7mg/ml sucrose in chloroform- 300 μg ScFv	13.68 ± 0.97	53.4 % ± 3.1

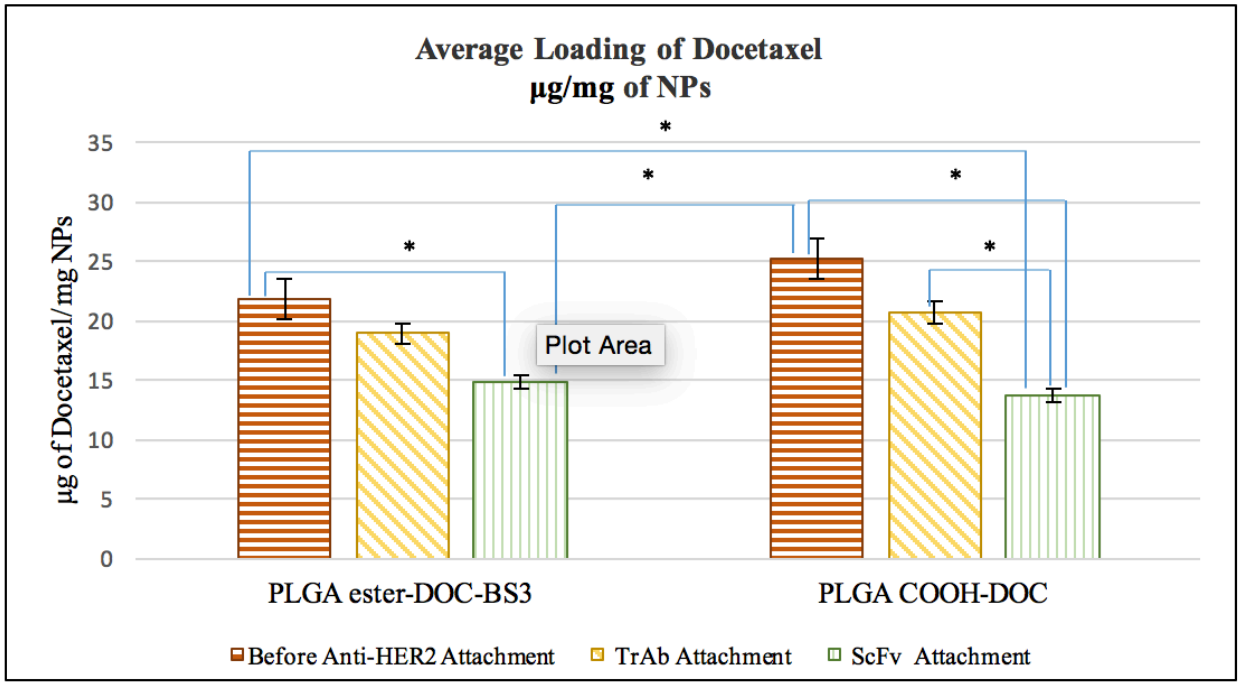

Figure 12. The differences between DOC loading in ester- and COOH- terminal PLGA. The same quantity of cryoprotectant (1.7 mg/ml) was used in all formulations. The statistical significance between and within the groups were represented by encompassing lines marked with sign (*). Horizontal column represent PLGA NPs before anti-HER2 attachment, diagonal column represent PLGA NPs attached to TrAb, and vertical column represent PLGA NPs attached to ScFv. The level of significance was set to $p < 0.05$ (ANOVA followed by Tukey's multiple comparison test method). Each bar represents the mean ± SD (n=6).

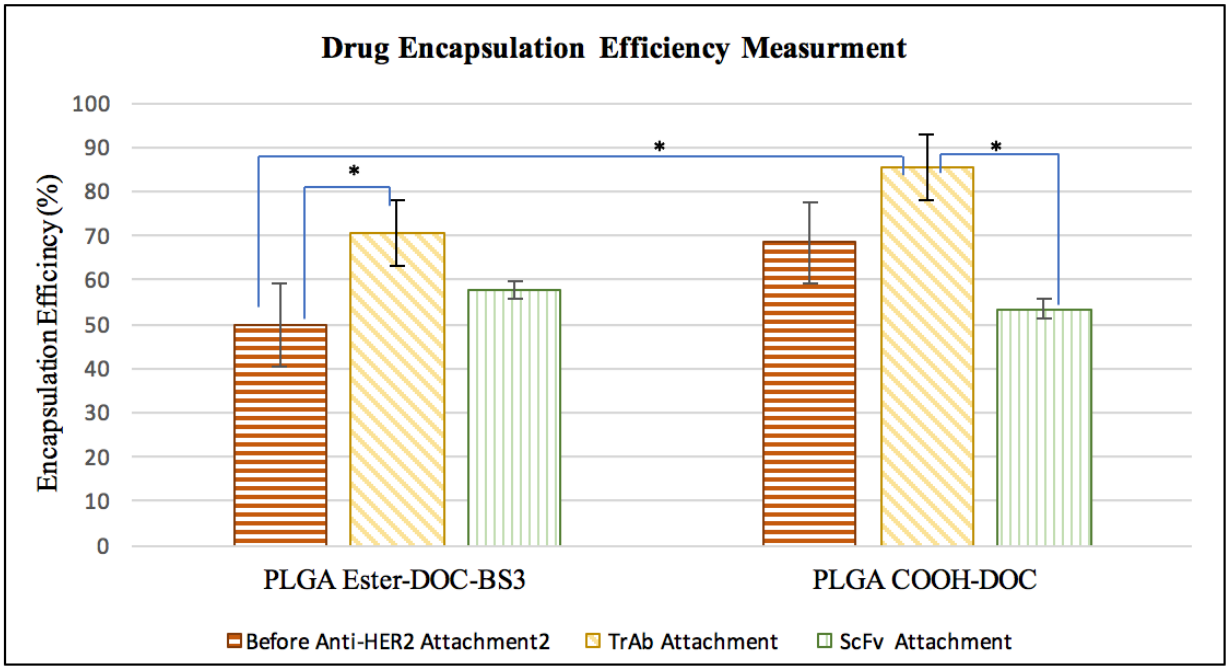

Figure 13. The differences between DOC encapsulation efficiency for both ester- and COOH- terminal PLGA formulations. The same quantity of cryoprotectant (1.7 mg/ml) was used in all formulations. The statistical significance between groups are represented by encompassing lines marked with the sign (*). Horizontal column represent PLGA NPs before anti-HER2 attachment, diagonal column representative PLGA NPs attached to TrAb, and vertical column represent PLGA NPs attached to ScFv. The level of significance was set to $p < 0.05$ (ANOVA followed by Tukey's multiple comparison test method). Each bar represents the mean percentage ± SD (n=6).

5.5. Anti-HER2 Attachment Quantification

5.5.1. Indirect Measurement of Ab Conjugation

The amount of anti-HER2 attached to PLGA-DOC NPs was determined by indirect calculation, in which the unbound Ab present in the collected supernatant during washing steps was subtracted from the original amount.

5.5.1.1. BS3 linker

After testing, we found that 1.5 mg BS3 is the most efficient amount to use for Ab attachment, and increasing the quantity of BS3 produces no significant increase in the Ab attachment (Sadat, 2015). Using 300 μg of anti-HER2 Ab resulted in a considerable quantity of Ab conjugation, reaching about 22.8 μg per mg of PLGA ester-DOC-BS3 NPs.

Table 16. Amount of whole Ab (trastuzumab) attached to ester PLGA-DOC NPs and the percentage of the attachment efficiency by indirect quantification (n=6).

NPs Formulation	Trastuzumab attachment (μg)/NPs mg $\pm$ SD	Trastuzumab attachment efficiency % $\pm$ SD
PLGA ester-DOC-BS3-1.7mg/ml sucrose-300μg TrAb	22.8 $\pm$ 3.78	45.8 $\pm$ 6.9
PLGA ester-DOC-BS3-1.7mg/ml sucrose-150μg TrAb	10.11 $\pm$ 2.5	40 $\pm$ 9.5
PLGA ester-DOC-BS3-1.7mg/ml sucrose-75μg TrAb	0.86 $\pm$ 5.31	6.9 $\pm$ 18.4
PLGA ester-DOC-BS3-1.7mg/ml sucrose-37.5μg TrAb	~100 %	~100 %

Table 17. Amount of ScFv anti-HER2 attached to ester PLGA-DOC NPs and the percentage of the attachment efficiency by indirect quantification (n=6).

NPs Formulation	Trastuzumab Attachment (μg)/NPs mg ± SD	Trastuzumab Attachment efficiency % ± SD
PLGA ester-DOC-BS3-1.7mg/ml sucrose-300µg-ScFv	~100 %	~100 %
PLGA ester-DOC-BS3-1.7mg/ml sucrose-150µg ScFv	~100 %	~100 %
PLGA ester-DOC-BS3-1.7mg/ml sucrose 75µg ScFv	~100 %	~100 %
PLGA ester-DOC-BS3-1.7mg/ml sucrose 37.5µg ScFv	~100 %	~100 %

5.5.1.2. NHS/EDC linker:

As the above result for BS3 suberate showed, NHS/EDC provided better Ab attachment when 300 µg was used for PLGA COOH-DOC. Around 23.3 µg of whole Anti-HER2 Ab was attached to 1 mg of NPs (Table 18); while, 100% of the ScFv, got attached to PLGA COOH-DOC (Table 19).

Table 18. Amount of whole Ab (trastuzumab) attached DOC-COOH PLGA NPs and the percentage of the attachment efficiency by indirect quantification (n=6).

NPs Formulation	Trastuzumab attachment (μg)/NPs mg ± SD	Trastuzumab attachment efficiency % ± SD
PLGA COOH-DOC-NHS/EDC-1.7mg/ml sucrose-300μg TrAb	23.31 ± 2.62	56.7 ± 6.3
PLGA COOH-DOC-NHS/EDC-1.7mg/ml sucrose-150μg TrAb	15.21 ± 1.31	73.9 ± 6.3
PLGA COOH-DOC-NHS/EDC-1.7mg/ml sucrose-75μg TrAb	~100 %	~100 %
PLGA COOH-DOC-NHS/EDC-1.7mg/ml sucrose-37.5μg TrAb	~100 %	~100 %

Table 19. Amount of ScFv anti-HER2 attached to DOC-COOH PLGA and the percentage of the attachment efficiency by indirect quantification (n=6).

NPs Formulation	Trastuzumab attachment (μg)/NPs mg ± SD	Trastuzumab attachment efficiency % ± SD
PLGA COOH-DOC-NHS/EDC-1.7mg/ml sucrose-300µg) ScFv	~100 %	~100 %
PLGA COOH-DOC- NHS/EDC-1.7mg/ml sucrose-150µg ScFv	~100 %	~100 %
PLGA COOH-DOC- NHS/EDC-1.7mg/ml sucrose-75µg ScFv	~100 %	~100 %
PLGA COOH-DOC-NHS/EDC-1.7mg/ml sucrose-37.5µg ScFv	~100 %	~100 %

5.5.2. Direct Measurement of Ab Conjugation

In this case, the amount of Ab attached to the NPs surfaces after FD was measured as a direct way by conducting the BCA assay (Table 20). TrAb attachment was up to 16.33 ± 2.69 μg/mg of acidic PLGA-DOC-NHS/EDC NPs which was higher than ester-PLGA-DOC-BS3 (14.1 ± 2.51 μg/mg of NPs). However, the PLGA ester-DOC-BS3 had high quantity of ScFv conjugation (12.75 ± 2.03 μg/mg).

Table 20. Direct quantification of anti-HER2 attached to DOC PLGA NPs (n=6).

NPs Formulation	**Trastuzumab attachment (μg)/NPs mg $\pm$ SD**
PLGA ester-DOC-BS3-1.7mg/ml sucrose-300μg TrAb	14.1 ± 2.51
PLGA ester-DOC-BS3-1.7mg/ml sucrose-300µg-ScFv	12.75 ± 2.03
PLGA COOH-DOC-NHS/EDC-1.7mg/ml sucrose-300μg TrAb	16.33 ± 2.69
PLGA COOH-DOC-NHS/EDC-1.7mg/ml sucrose-300µg) ScFv	10.6 ± 3.16

5.6. Evaluation of *In Vitro* Release of Docetaxel from Modified NPs

The *in vitro* drug release profile for modified ester-PLGA NPs was analyzed at neutral (pH 7.4) and acidic (pH 5.0) PBS for 120 hours. The results are presented in Figure 14. A calibration curve was developed in a range from 125-64,000 ng/ml (R^2 =0.998), and the accuracy and precision of data were determined by the validated MS method to identify the DOC concentration and evaluate the drug release. An early burst release was detected in the first 24 hours. After that, a control release occurred as a result of diffusion of DOC through the PLGA polymeric matrix.

5.6.1. Ester PLGA formulation

The release of the drug (DOC) from ester PLGA conjugated with whole IgG (TrAb) was found to be faster in acidic conditions; more than 50% of DOC was released within the first day at pH 5.0, whereas it took 72 hours to attain a comparable level of DOC release at pH 7.4.

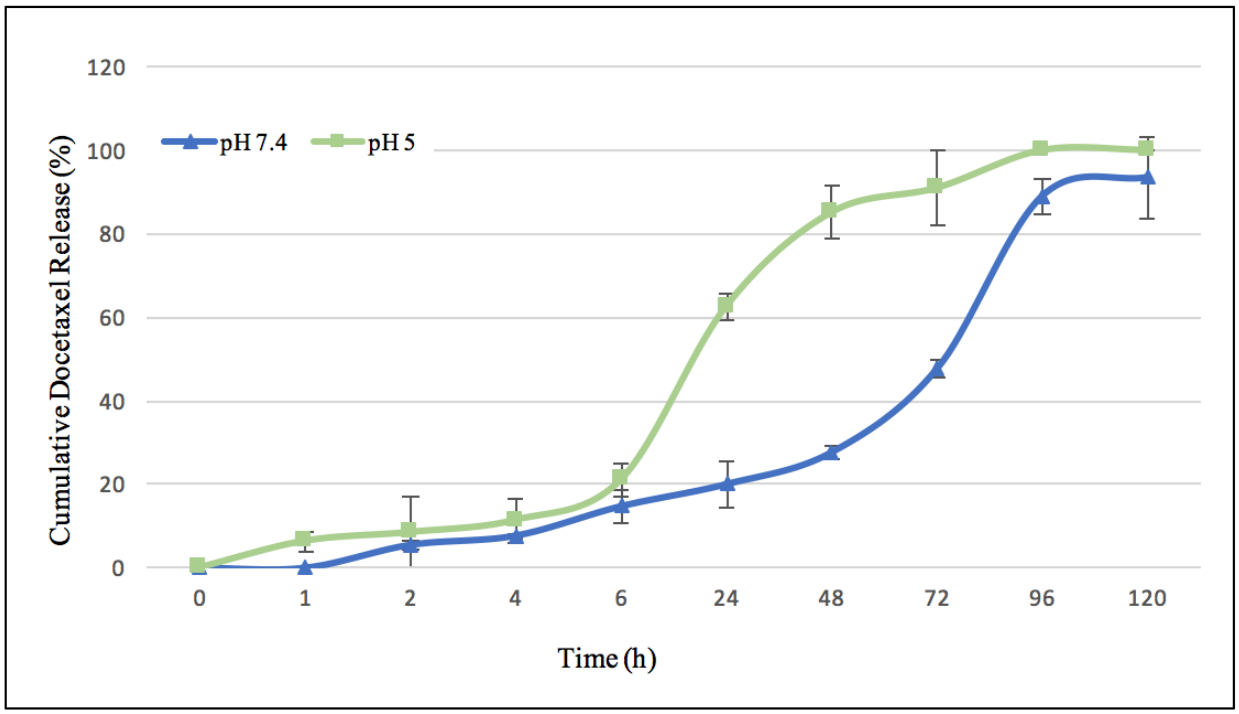

Figure 14. The *in vitro* release profiles of docetaxel from ester-PLGA NPs conjugated with whole anti-HER2 (TrAb) at pH 5.0 and 7.4 in PBS buffer under 100 rpm and 37°C. The level of significance was set to $p < 0.05$ (ANOVA). Each line represents the mean percentage of different pH ± SD (n=3).

- ✓ ***Third Objective:*** **To evaluate cell viability and IC_{50} in SK-BR-3 cell line**

5.7. Cell Cytotoxicity

In vitro cytotoxicity assay was conducted with all NPs formulations (modified and unmodified NPs). Then, the results were compared to the conventional DOC and Herceptin which are available in the market. The percentage of cell viability as well as the 50% inhibitory concentration (IC_{50}) were calculated to evaluate the difference in the efficacy of docetaxel in modified NPs formulations (conjugated with targeting moiety) in treating SK-BR-3 (HER2-positive) cell line. All experiments were conducted four times.

5.7.1. Cell Viability Percentage

The following formulations were tested on SK-BR-3 cells to determine the cell viability using the MTS assay (conventional DOC, conventional Herceptin, conventional combination DOC and Herceptin, plain PLGA ester NPs, plain PLGA COOH NPs, PLGA ester-DOC NPs, PLGA COOH-DOC NPs, PLGA ester-DOC-TrAb, PLGA ester-DOC-ScFv, PLGA COOH-DOC-TrAb, and PLGA COOH-DOC-ScFv). Statistical analysis showed that plain NPs for both ester- and acidic-terminated did not influence the cell viability significantly as shown in Figure 15.

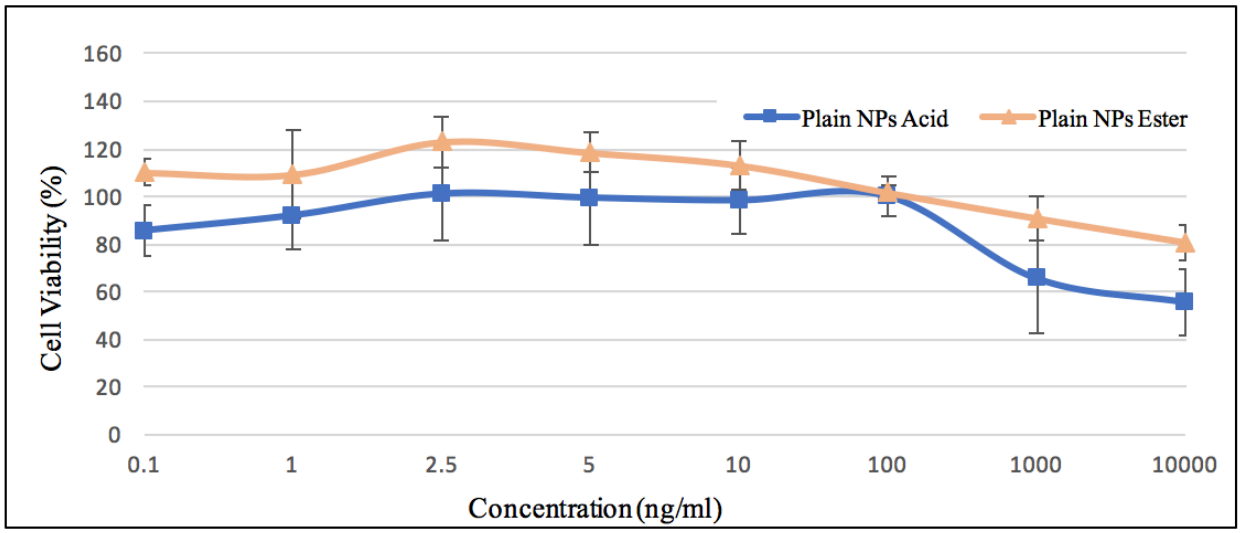

Figure 15. *In vitro* cytotoxicity of plain PLGA ester NPs, and plain acidic PLGA NPs in SK-BR-3 cells at 48 hours. Cell viability was evaluated by MTS assay. Data are represented as mean percentage ± SD (n=4).

Almost all DOC-loaded NPs formulations showed a significant advanced toxicity to cancer cell compared to conventional DOC and the combination of DOC and Herceptin. Modified NPs showed more significant cytotoxicity than unmodified NPs (PLGA encapsulated DOC without Ab conjugation). In general, the viability of SK-BR-3 breast cells decreased with increases in drug concentration. The results of cells viability percentage for ester PLGA loaded with DOC and the modified form of ester NPs with both TrAb and ScFv were compared to conventional DOC and the combination of conventional DOC and Herceptin in Figure 16. The percentage of cell viability was around 62% for the cells treated with ester-PLGA-DOC-TrAb and 78% for ester-PLGA-DOC-ScFv (0.1 ηg/ml of DOC). The percentage of cell viability for acidic PLGA DOC NPs was provided in Figure 17 to define the differences when both

modified and unmodified formulations of acidic NPs were compared to what is being used now in the market (DOC and Herceptin).

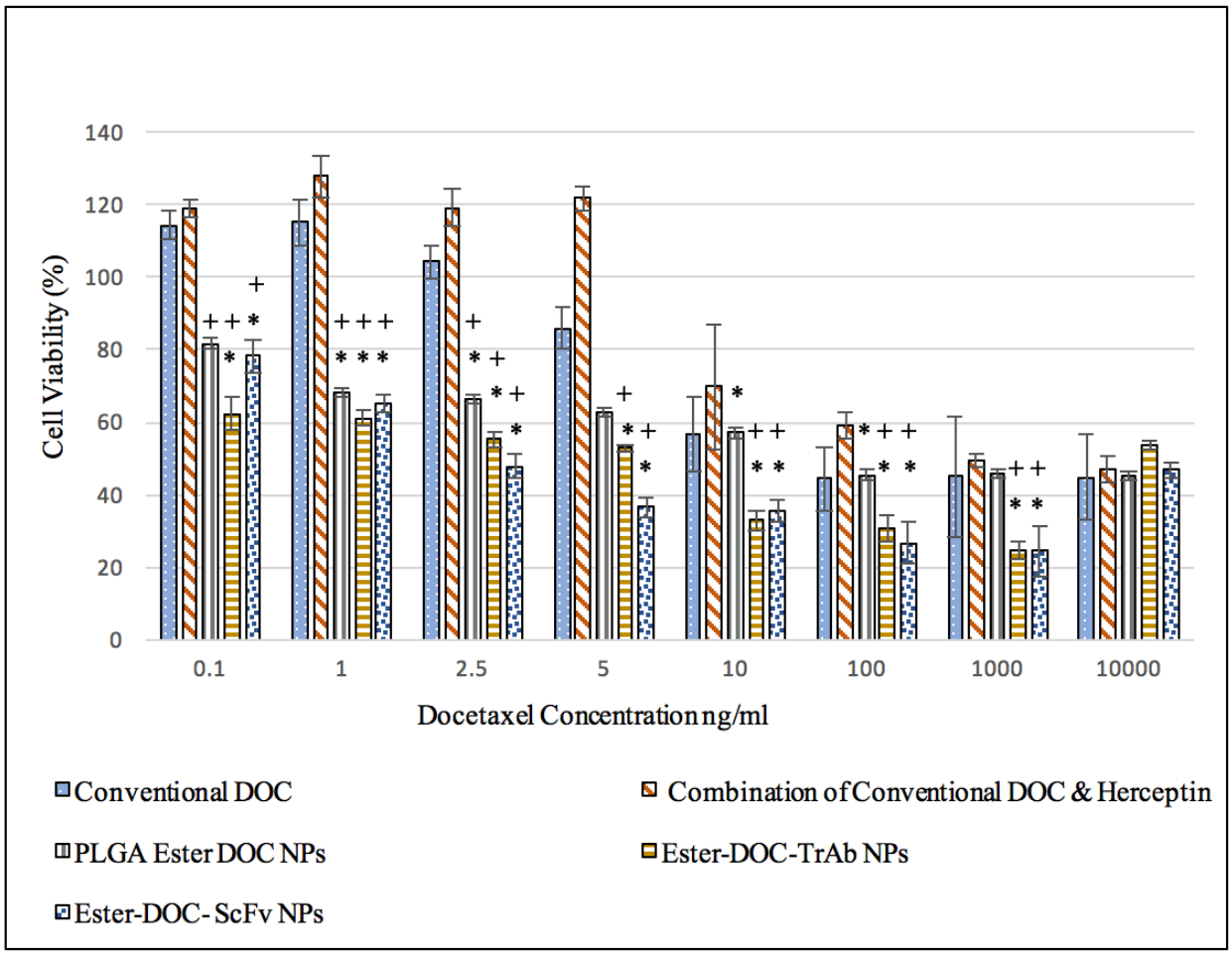

Figure 16. The percentage of *in vitro* cell viability for conventional docetaxel, combination of conventional docetaxel and Herceptin, PLGA ester-DOC, PLGA ester-DOC-TrAb, PLGA ester-DOC-ScFv in SK-BR-3 cells at 48 hours. Cell viability was evaluated by MTS assay. The statistical significance between NPs formulations and the conventional DOC were represented by the sign of (*); the significance of NPs formulations in comparison with the combination of conventional DOC and Herceptin are represented by the sign (+). The level of significance was set to $p < 0.05$. Data are represented as mean percentage ± SD (n=4).

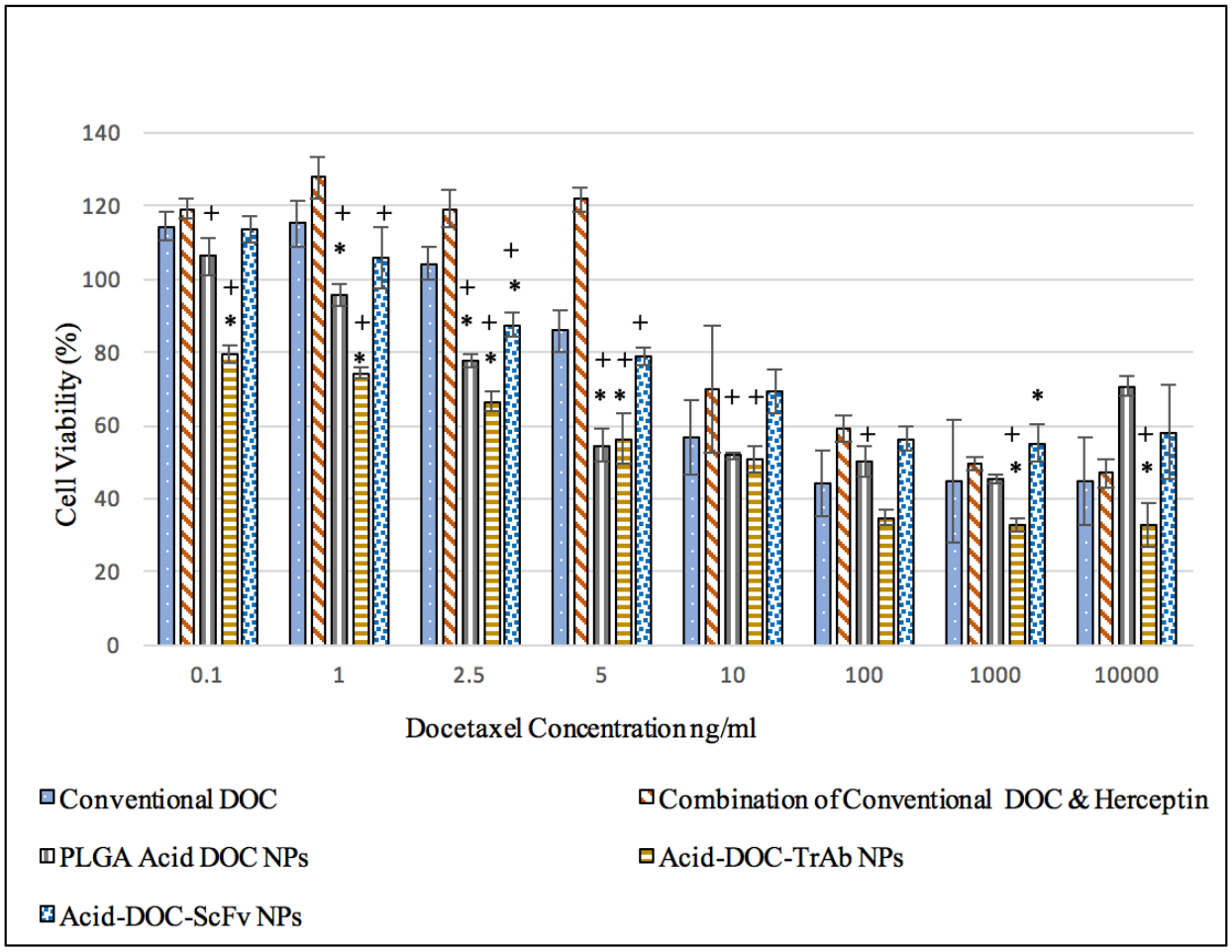

Figure 17. The percentage of *in vitro* cell viability for conventional docetaxel, combination of conventional docetaxel and Herceptin, PLGA acidic-DOC, PLGA acidic-DOC-TrAb, and PLGA acidic-DOC-ScFv. The statistical significance between NPs formulations and the conventional DOC were represented by the sign (*); the significance of NP formulations in comparison with the combination of conventional DOC and Herceptin are represented by the sign (+). The level of significance was set to $p < 0.05$. Data are represented as mean percentage ± SD (n=4).

We compared all modified NPs to conventional medications as presented in Figure 18 to determine whether it confirmed the effectiveness of modified NPs formulations in delivering DOC to the HER2 breast cancer cell line and in improving the toxicity to the cancers cells. Both ester modified NPs (with TrAb or ScFv) showed more potent cytotoxic, followed by acidic modified NPs. Moreover, Figure 19 highlights the significance of whole IgG anti-HER2 in ester- and acidic-terminated PLGA NPs as well as ScFv anti-HER2 in both ester- and acidic-terminated PLGA NPs. PLGA ester-DOC-TrAb showed more cytotoxicity than PLGA COOH-DOC-TrAb. The percentage of cell viability was around 35% for ester modified formulations in DOC concentration of 10 ηg/ml; whereas, acidic modified NPs had cell viability percentage above 50%. The destructive effects of ester PLGA modified with ScFv also were more significant than PLGA COOH NPs ligand with ScFv.

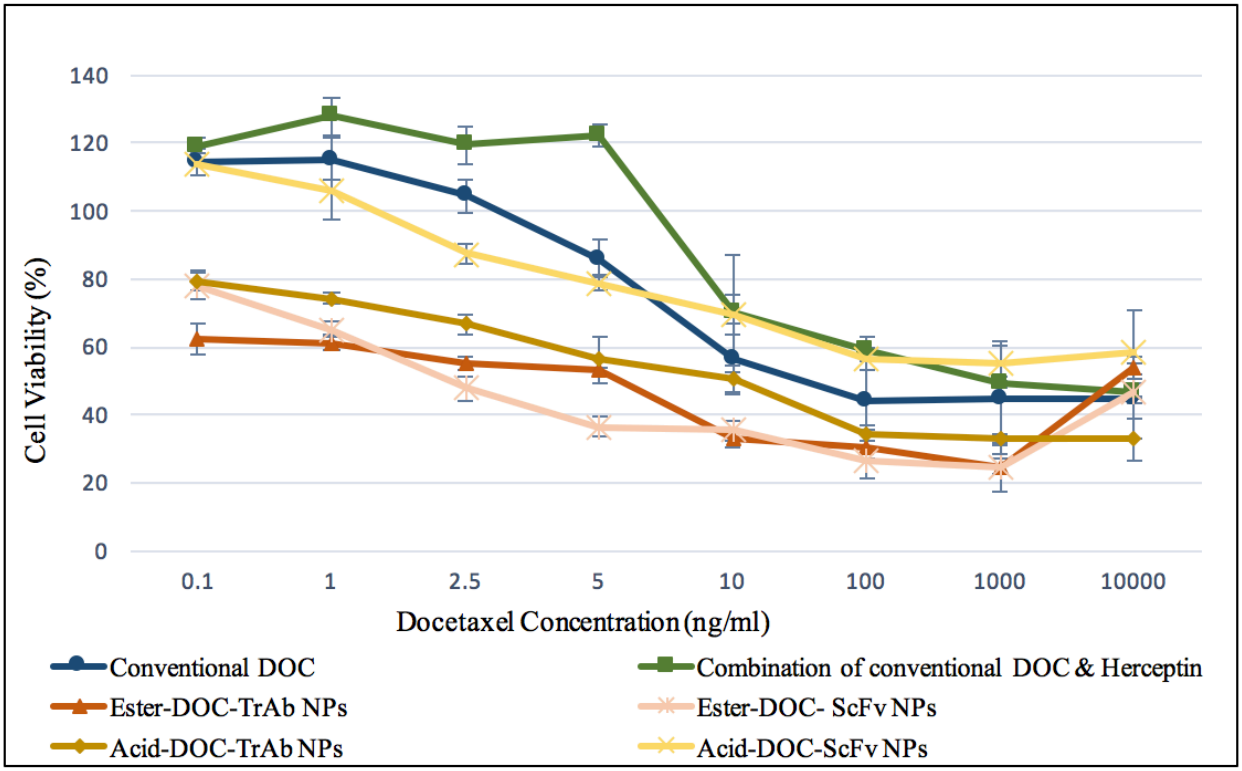

Figure 18. The percentage of *in vitro* cell viability for all modified PLGA NPs formulations, conventional docetaxel, combination of conventional docetaxel and Herceptin, PLGA ester-DOC-TrAb, PLGA ester-DOC-ScFv, PLGA acid-DOC-TrAb, and PLGA acid-DOC-ScFv in SK-BR-3 cells at 48 hours. Cell viability was evaluated by MTS assay. The level of significance was set to $p < 0.05$. Data are represented as mean percentage ± SD (n=4).

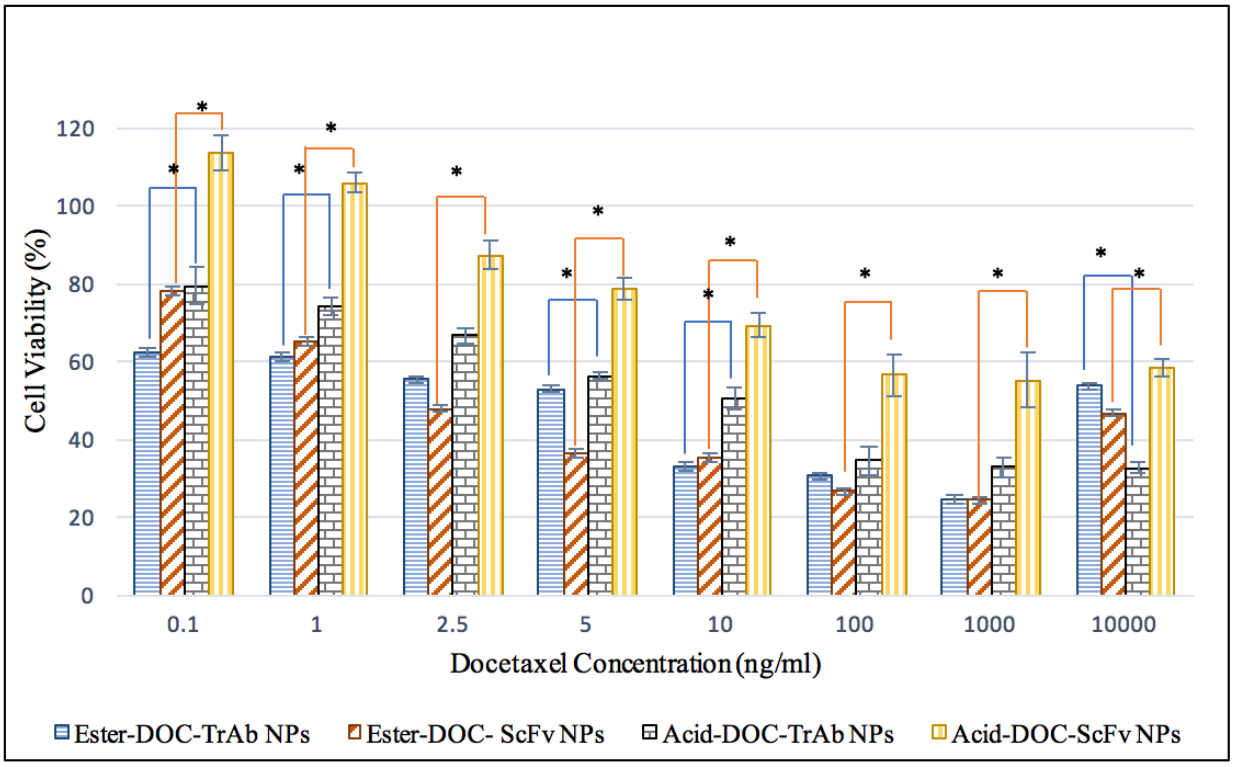

Figure 19. The percentage of *in vitro* cell viability for all modified PLGA NPs formulations, in comparison to each other; ester-DOC-TrAb, PLGA ester-DOC-ScFv, PLGA acidic-DOC-TrAb, and PLGA acidic-DOC-ScFv. The statistical significance between NPs formulations are represented by the sign of (*). The level of significance was set to $p < 0.05$. Data are represented as mean percentage ± SD (n=4).

Lastly, the modified PLGA showed a powerful cytotoxic ability compared with conventional DOC and Herceptin in the market. As a result, examining ester-PLGA formulations (PLGA ester-DOC, PLGA ester-DOC-TrAb, and PLGA ester-DOC-ScFv) alongside conventional DOC alone or the combination of conventional DOC and Herceptin revealed the significant targeted delivery system with whole Ab or with the ScFv (Figure 16). In addition, Figure 17 compares the percentage of cell viability for PLGA acid-DOC, PLGA acid-DOC-TrAb, PLGA acid-DOC-ScFv and conventional

medications; the above bar chart demonstrates the significance of modified formulations in lowering cell viability.

5.7.2. The Half Maximal Inhibitory Concentration (IC_{50})

The cytotoxicity quantitatively resulting in 50% growth inhibition (IC_{50}) was calculated by the formula of logarithmic concentration effect curves, in which the optical density of the control well was taken as 100%. Table 21 gives IC_{50} for SK-BR-3 cell line after 48 hours incubated with different formulations. Modified PLGA ester-DOC conjugated with ScFv exhibited the highest cytotoxicity (the lowest viability) followed by modified PLGA ester-DOC-TrAb in comparison with all cases of conventional DOC. Interestingly, modified acid PLGA showed less viability compared to modified ester PLGA, whereas the IC_{50} for PLGA acidic-DOC-ScFv was 2.11 ng/ml and 3.72 for the PLGA Acid-DOC-TrAb. The differences in IC_{50} for all formulations presented in Figure 20.

Table 21. Mean IC_{50} ± SD (cytotoxicity) of different docetaxel formulations on SK-BR-3 human breast cancer cells by MTS assay after 48 hours. Data are represented as mean.

NPs Formulations	**IC_{50} (ng/ml) ± SD**
Conventional DOC	8.23 ± 0.21
PLGA ester DOC NPs	8.34 ± 0.25
PLGA acid DOC NPs	6.06 ± 0.31
PLGA ester-DOC-TrAb NPs	1.28 ± 0.22
PLGA ester-DOC-ScFv NPs	0.842 ± 0.29
PLGA acid-DOC-TrAb NPs	3.72 ± 0.14
PLGA acid-DOC-ScFv NPs	2.11 ± 0.22

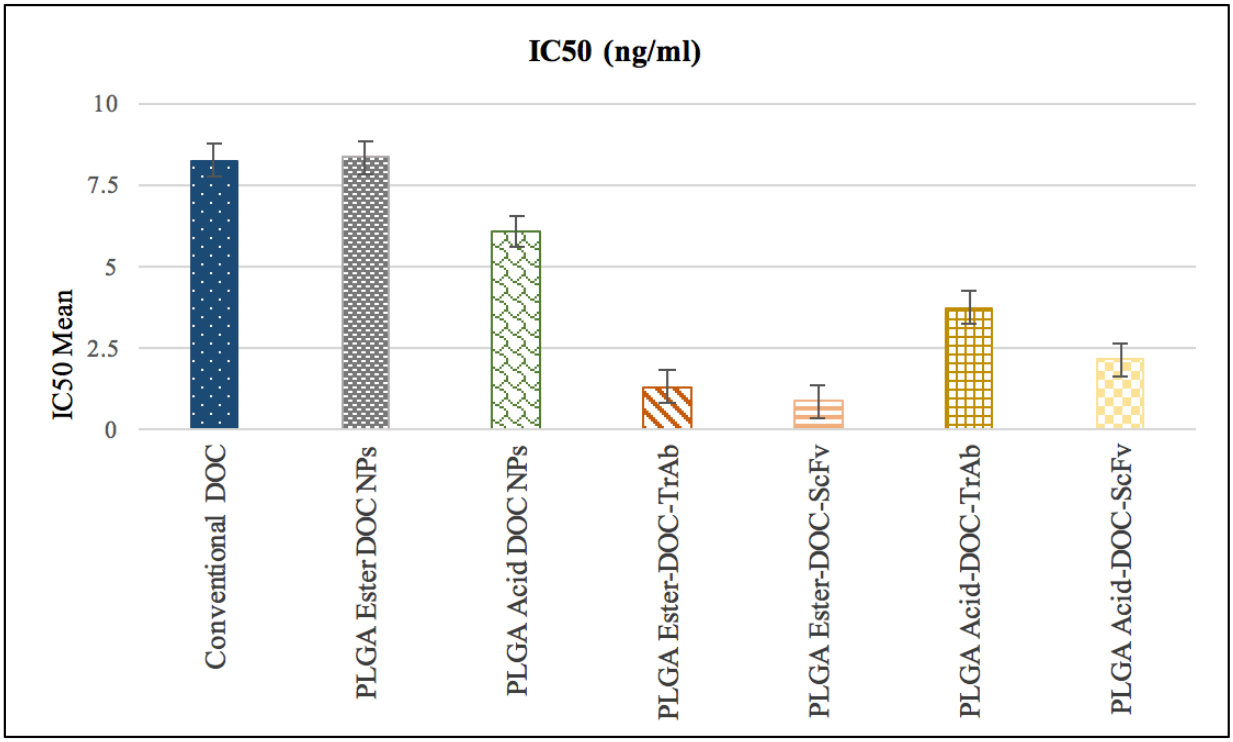

Figure 20. Mean *in vitro* IC_{50} for conventional docetaxel, PLGA ester-DOC, PLGA acid-DOC, PLGA ester-DOC-TrAb, PLGA ester-DOC-ScFv, PLGA acid-DOC-TrAb, and PLGA acid-DOC-ScFv in SK-BR-3 cells at 48 hours. Cell viability was evaluated by MTS assay. Data are represented as mean.

- ✓ ***Fourth Objective:*** **To investigate the *in vitro* tumor cell targeting by evaluation of HER2 receptor expression in MCF-7 (moderately expressed HER 2 receptor) and SK-BR-3 (overexpressed HER2)**

5.8. Measuring HER-2 Expression

Measuring HER2 receptor expression on the surface of breast cancer cells would be useful to confirm the ability of modified NPs formulations in targeting HER2 receptors. The fluorescent anti-HER-2 Ab was used to identify the HER-2 receptors on the cells treated with modified NPs by flow cytometry. Untreated cells, cells treated with conventional Herceptin, plain NPs were utilized as control groups. The similar groups were tested by western blotting analysis to confirm the results from flow cytometry.

5.8.1. Flow Cytometry

Different formulations were used to treat both MCF-7 and SK-BR-3 cell lines for 48 hours to measure the amount of HER2 expression on the cell line after treatment. Dot plots and forward side scattering histograms were employed to measure the effects of treatment with different formulations. Less than 5% of the gated population was considered for autofluorescence of untreated, isotype Ab and unstained cells.

5.8.1.1. HER2 expression in SK-BR-3 cell line

The difference between MCF-7 and SK-BR-3 is that SK-BR-3 overexpresses HER2 receptors. SK-BR-3 was treated with different formulations to show the differences in HER2 expressions which indicate the targeting ability of modified NPs formulations. Data are presented by depending on the type of polymer. The cells treated with conventional DOC, conventional Herceptin or conventional ScFv showed the relatively high parent fluorescence percentage (PF%) for HER2 expression (92.94%, 95.37, and 95.92% respectively). DOC-loaded NPs modified with both TrAb, or ScFv showed a significant reduction in the PF% for HER2 expression (around 86%). Nevertheless, modified acidic terminated NPs proved better at decreasing the PF% for HER2 expression in contrast to conventional medications (conventional DOC, conventional Herceptin, conventional ScFv or conventional combination of Herceptin and DOC), as shown in Figures 21 and 22.

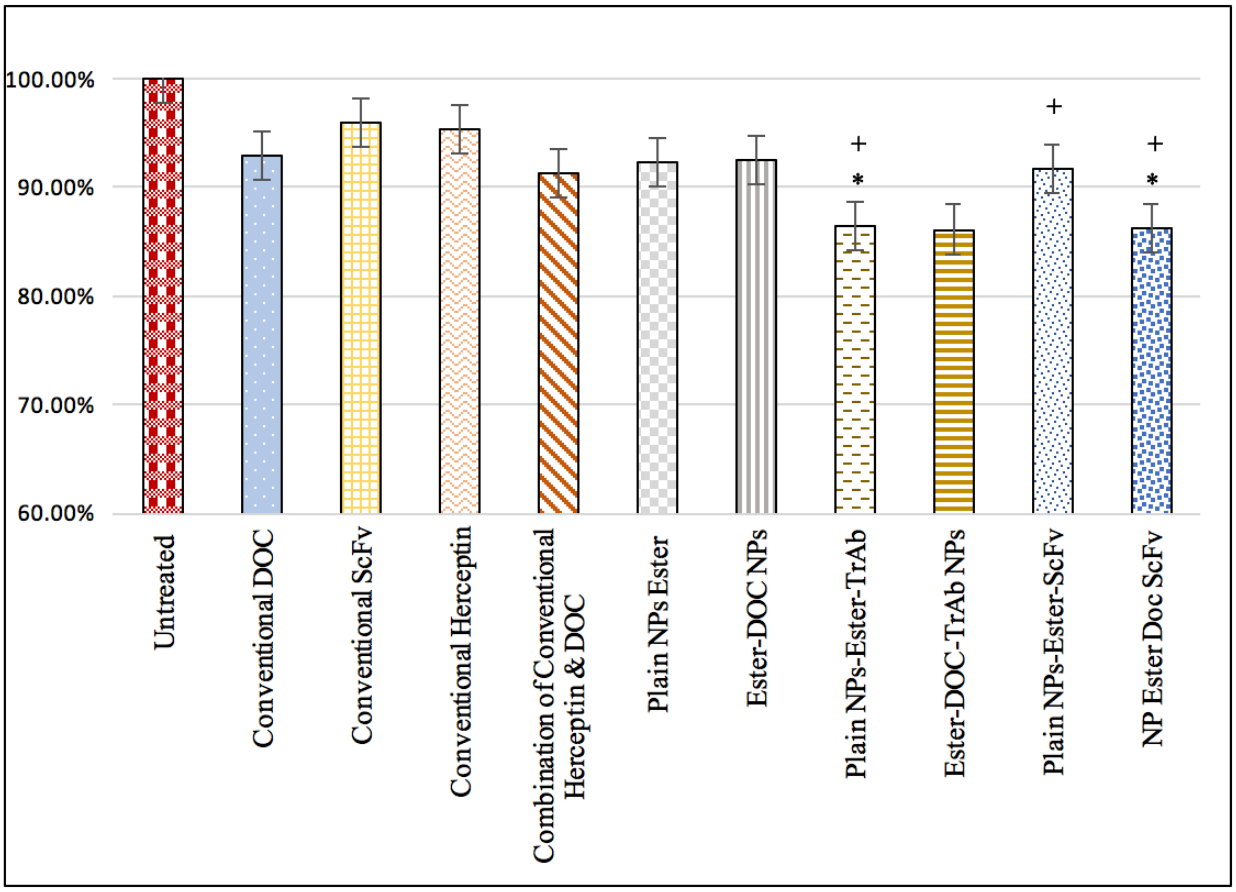

Figure 21. The parent fluorescence percentage of positive cells expressing HER2 after treating SK-BR-3 cells with ester PLGA NPs (plain PLGA ester, PLGA ester-DOC, PLGA ester plain-TrAb, PLGA ester-DOC-TrAb, PLGA ester plain-ScFv, PLGA ester-DOC-ScFv) compared to untreated, conventional DOC, conventional ScFv, conventional Herceptin, combination of conventional DOC & Herceptin, after 48 hours. The statistical significance between NPs formulations and conventional DOC is represented by the sign (*); the significance of NPs formulations in comparison with conventional anti-HER2 is presented by the sign (+). The level of significance was set to $p < 0.05$ (ANOVA followed by Pairwise multiple comparison test method). Data are represented as mean percentage ± SD (n=3).

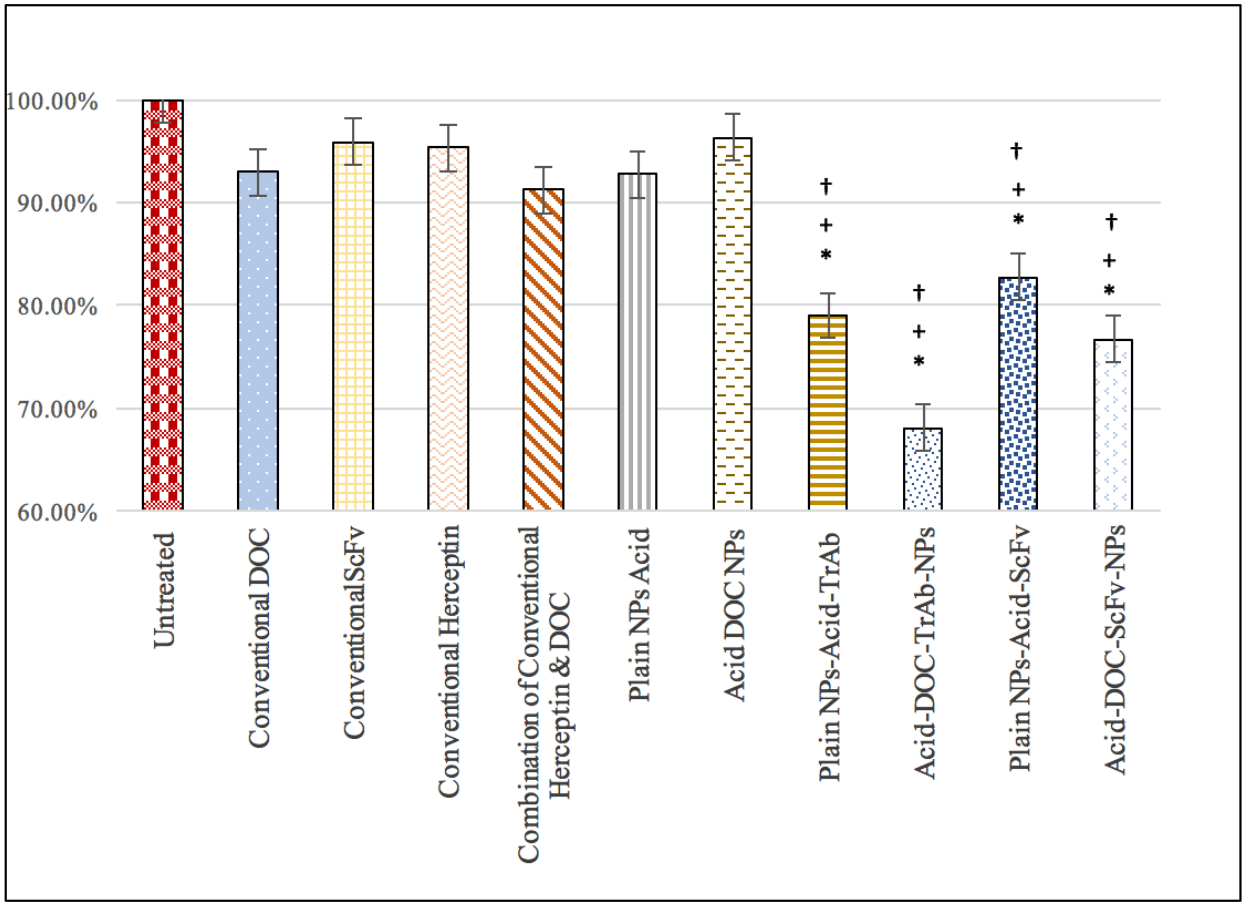

Figure 22. The parent fluorescence percentage of positive cells expressing HER2 after treating SK-BR-3 cells with COOH PLGA NPs (plain PLGA COOH, PLGA COOH-DOC, PLGA COOH plain-TrAb, PLGA COOH-DOD-TrAb, PLGA COOH plain-ScFv, PLGA COOH-DOC-ScFv) compared to untreated, conventional DOC, conventional ScFv, conventional Herceptin, combination of conventional DOC & Herceptin after 48 hours. The statistical significance between COOH modified NPs formulations and conventional DOC are represented by the sign (*); the significance of NPs formulation combating to conventional anti-HER2 is represented by the sign (+), and the significance of modified NPs in comparison to the combination of conventional DOC & Herceptin is represented by the sign (†). The level of significance was set to $p < 0.05$ (ANOVA followed by Pairwise multiple comparison test method). Data are represented as mean percentage ± SD (n=3).

The lowest percentage of HER2 expression appeared when the cells were treated with PLGA COOH-DOC-TrAb (68.06%), followed by PLGA COOH-DOC-ScFv, where the PF% was 76.75%. Modified PLGA COOH-DOC verified a powerful decline in the percentage of fluorescence intensity for HER2 expression compared to ester-modified NPs as Figure 23 shows.

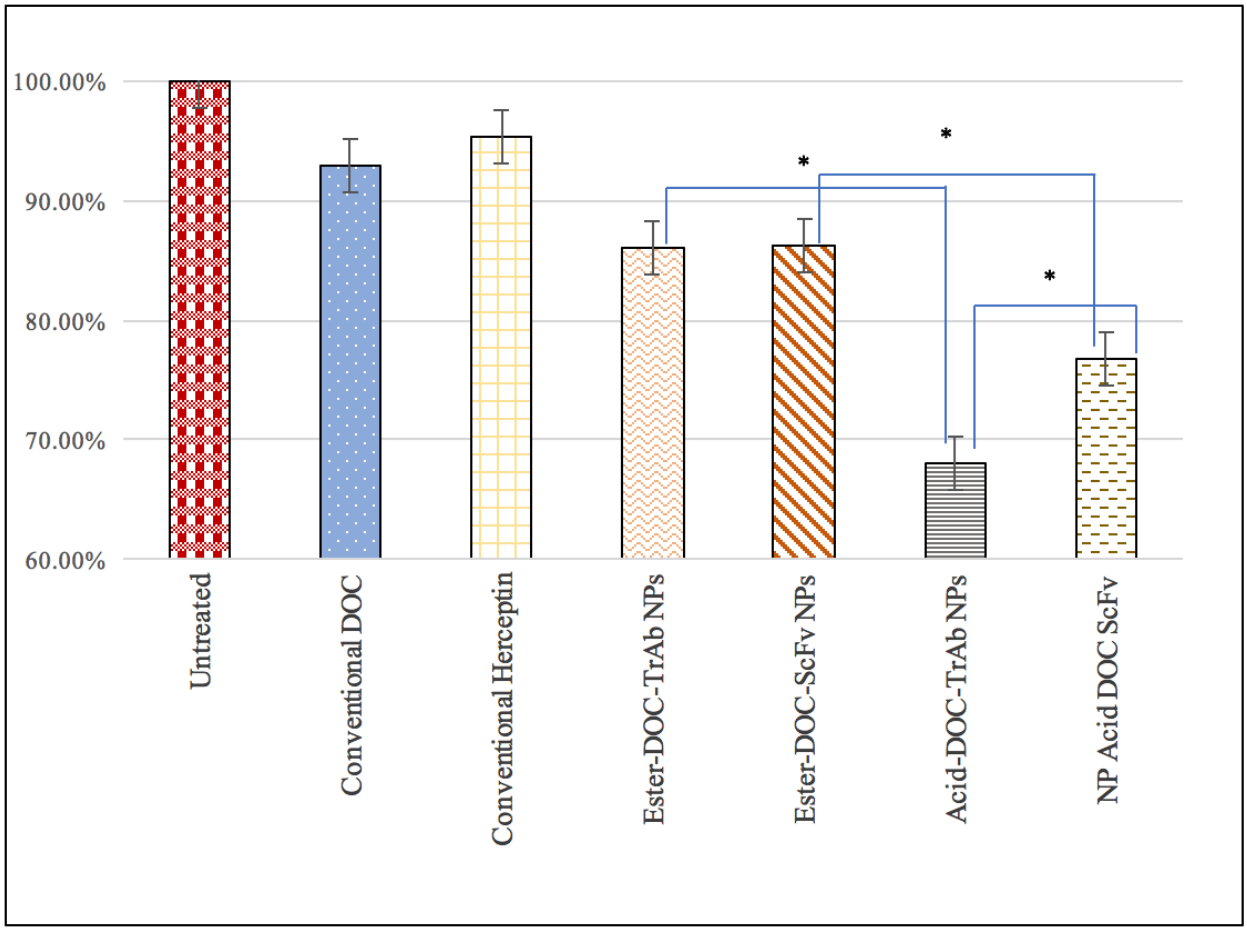

Figure 23. The parent fluorescence percentage of positive cells expressing HER2 after treating SK-BR-3 cells with both ester- and acidic-modified PLGA encapsulated DOC and conjugated with whole IgG and ScFv anti-HER2 NPs (PLGA ester-DOC-TrAb, PLGA ester-DOC-ScFv, PLGA COOH-DOC-TrAb, PLGA COOH-DOC-ScFv) after 48 hours. The statistical significance between modified NPs formulations are represented by the sign (*). Data are represented as mean percentage ± SD (n=3).

The percentage of median fluorescence intensity (%MFI) for HER2 expression was about 66% for both plain and loaded PLGA ester-TrAb, a percentage that showed a statistically significant difference in comparison to the combination of conventional DOC and Herceptin, conventional Herceptin, conventional ScFv, and conventional DOC (Figure 24). However, PLGA ester-DOC-ScFv did not show significant differences in %MFI for HER2 expression for SK-BR-3 cell line, in contrast with the combination of conventional DOC and Herceptin. Acidic terminated PLGA NPs showed the same results, whereas COOH NPs modified with whole Ab showed a significant reduction in %MFI for HER2 receptors, unlike the COOH NPs modified with ScFv as Figure 25 presents. The comparison of the %MFI for all modified NPs showed that ester PLGA-modified NPs had a serious decline in HER2 expressions (see Figure 26).

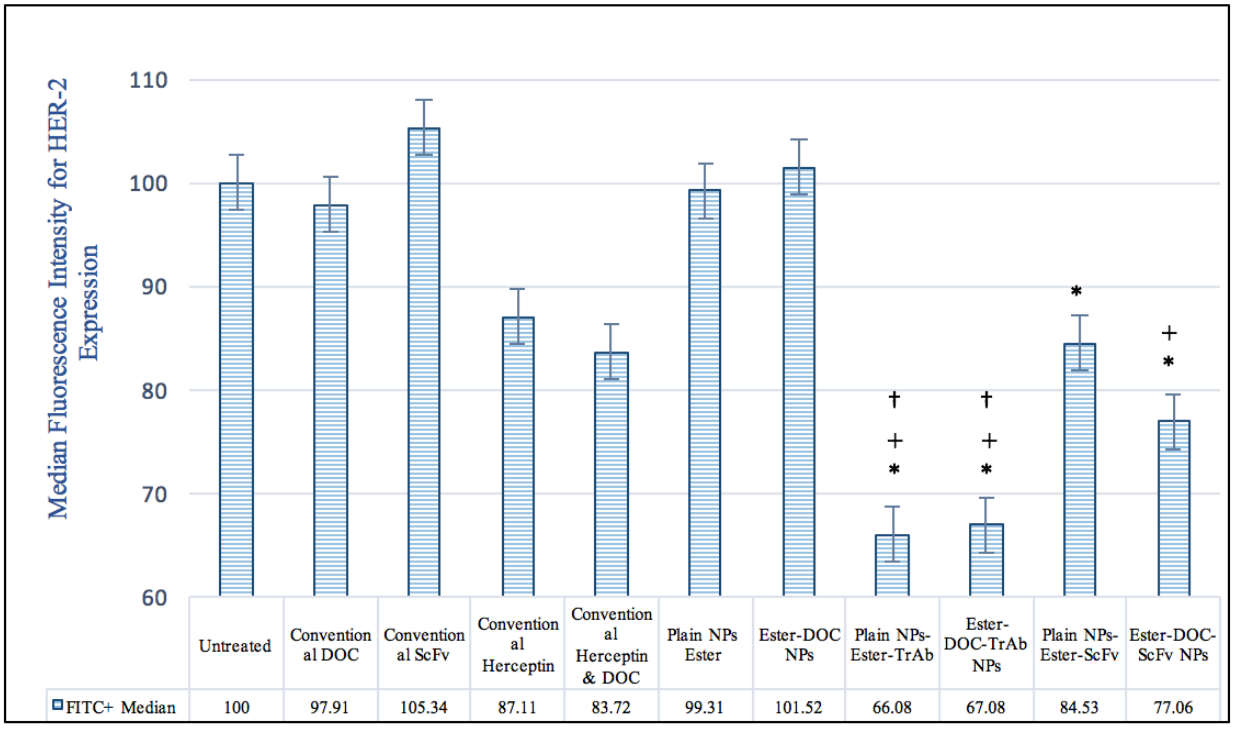

Figure 24. Relative percentage of median fluorescence intensity expressing HER2 after treating SK-BR-3 cells with ester-PLGA NPs (plain PLGA ester, PLGA ester-DOC, PLGA ester plain-TrAb, PLGA ester-DOC-TrAb, PLGA ester plain-ScFv, PLGA ester-DOC-ScFv) versus untreated, conventional DOC, conventional ScFv, conventional Herceptin, combination of conventional DOC & Herceptin, after 48 hours. The statistical significance between NPs formulations and conventional DOC and conventional ScFv are represented by the sign (*); the significant of modified NPs comparing to conventional Herceptin is presented by the sign (+), and the significance in comparison to the combination of conventional DOC & Herceptin is indicated the sign (†). Data are represented as mean percentage ± SD (n=3).

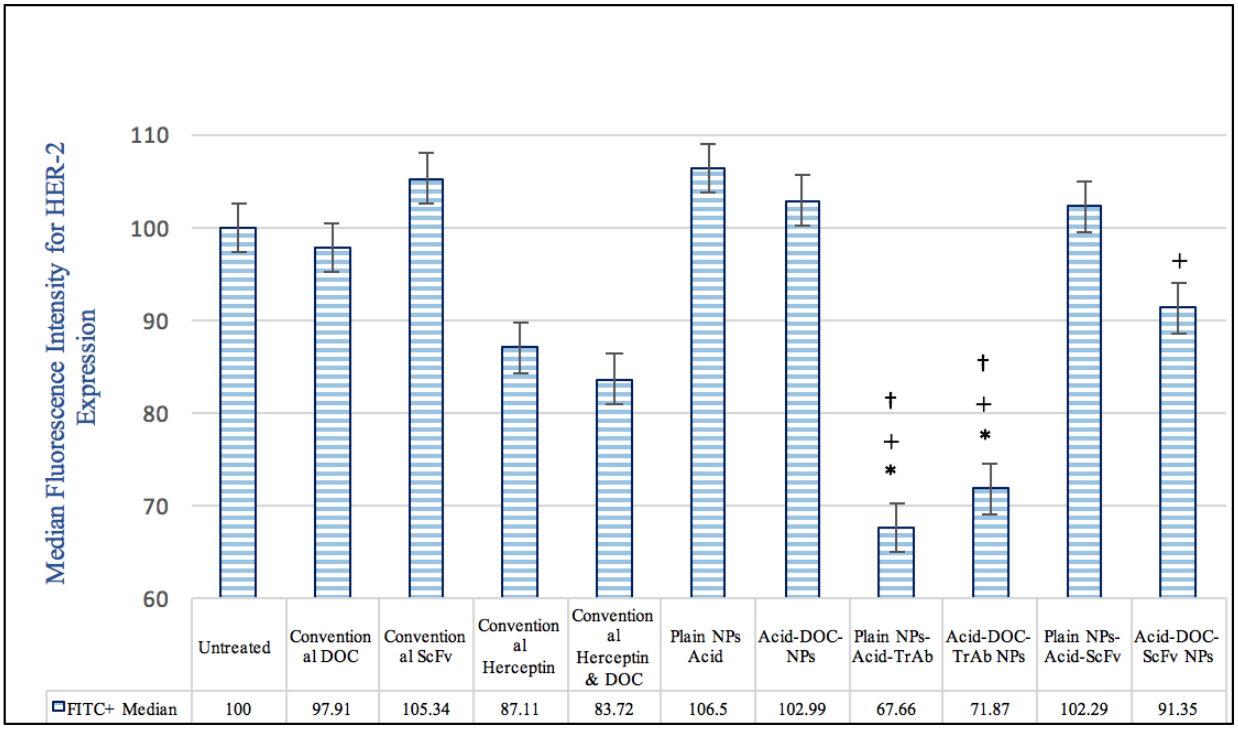

Figure 25. Relative percentage of positive median fluorescence intensity expressing HER2 after treating SK-BR-3 cells with acidic PLGA NPs (plain PLGA COOH, PLGA COOH-DOC, PLGA COOH plain-TrAb, PLGA COOH-DOC-TrAb, PLGA COOH plain-ScFv, PLGA COOH-DOC-ScFv) versus untreated, conventional DOC, conventional ScFv, conventional Herceptin, combination of conventional DOC & Herceptin, after 48 hours. The statistical significance between NPs formulations comparing to conventional DOC are represented by the sign (*); the significance of modified NPs formulation and conventional ScFv is represented by the sign (+), and the significance of modified NPs formulation comparing to the combination of conventional DOC & Herceptin and conventional Herceptin is indicated by the sign (†). Data are represented as mean percentage ± SD (n=3).

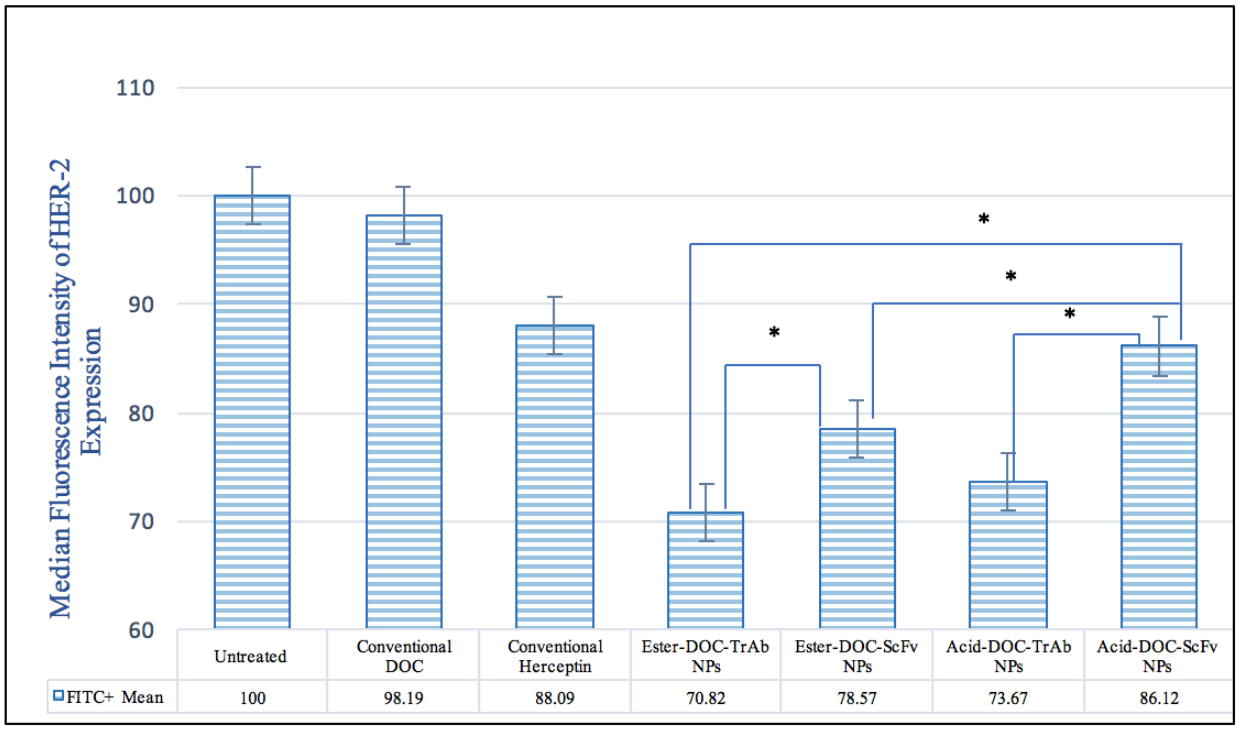

Figure 26. Relative percentage of positive median fluorescence intensity expressing HER2 after treating SK-BR-3 cells with both ester- and acidic-modified PLGA encapsulated DOC and conjugated with whole IgG and ScFv anti-HER2 NPs (PLGA ester-DOC-TrAb, PLGA ester-DOC-ScFv, PLGA COOH-DOC-TrAb, PLGA COOH-DOC-ScFv) after 48 hours. The statistical significance between modified NPs are represented by the encompassing line marked with the sign (*). The level of significance was set to $p < 0.05$ (ANOVA followed by multiple comparison test method). Data are represented as mean percentage ± SD (n=3).

5.8.1.2.HER2 expression in MCF-7 cell line

Following the same steps conducted with SK-BR-3, MCF-7 (moderately expresses HER2) was treated with different formulations to show the differences in median fluorescence intensity (MFI) of MCF-7 after staining with anti-HER2 FITC Ab as well as the percentage of positive cells for HER2 expression as Figure 27 represents.

Also, Figure 28, shows the differences in the percentage of mean fluorescence for HER2 expression after treating the cells for 48 hours.

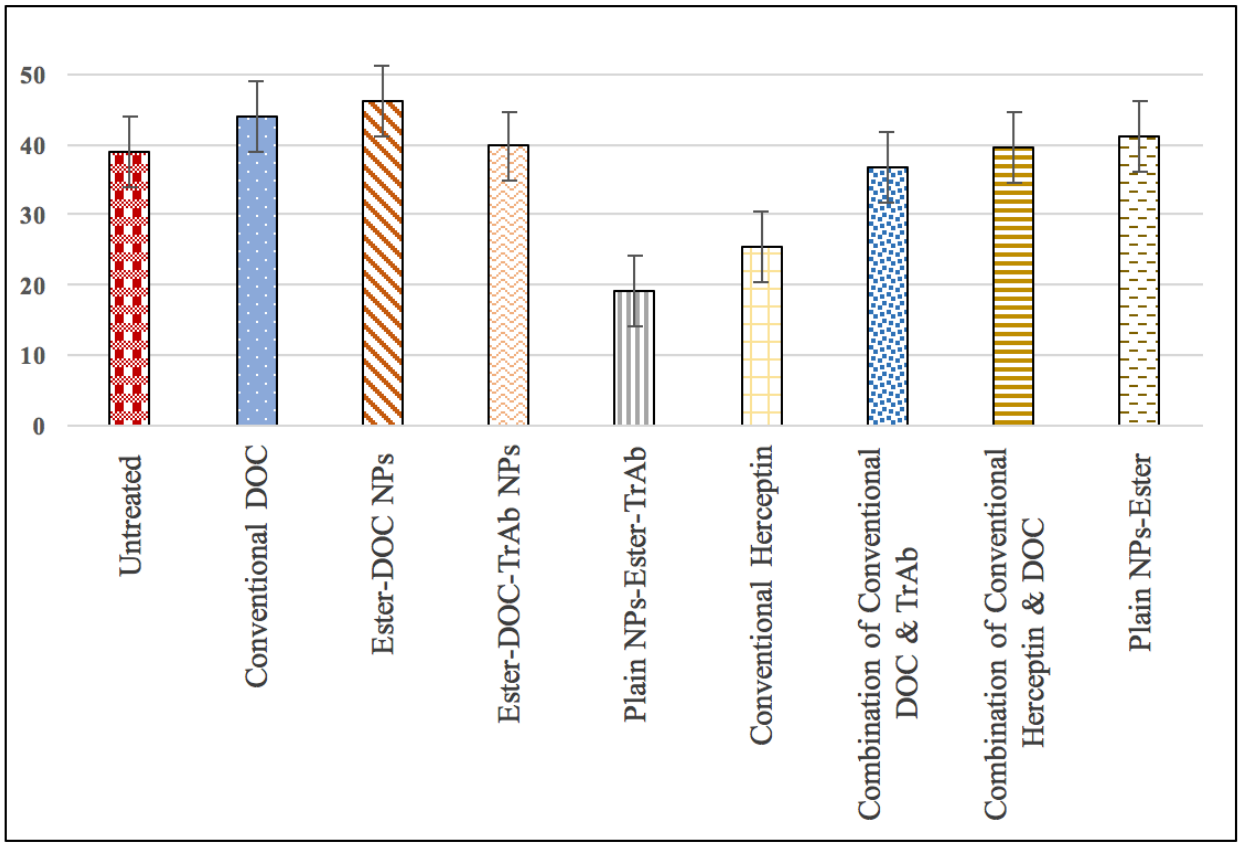

Figure 27. The parent fluorescence percentage of positive cells expressing HER2 after treating MCF-7 cells with plain PLGA ester, PLGA ester-DOC, PLGA ester plain-TrAb, and PLGA ester-DOC-TrAb compared to untreated, conventional DOC, conventional Herceptin, combination of conventional DOC & Herceptin, after 48 hours. Data are represented as mean percentage ± SD (n=2).

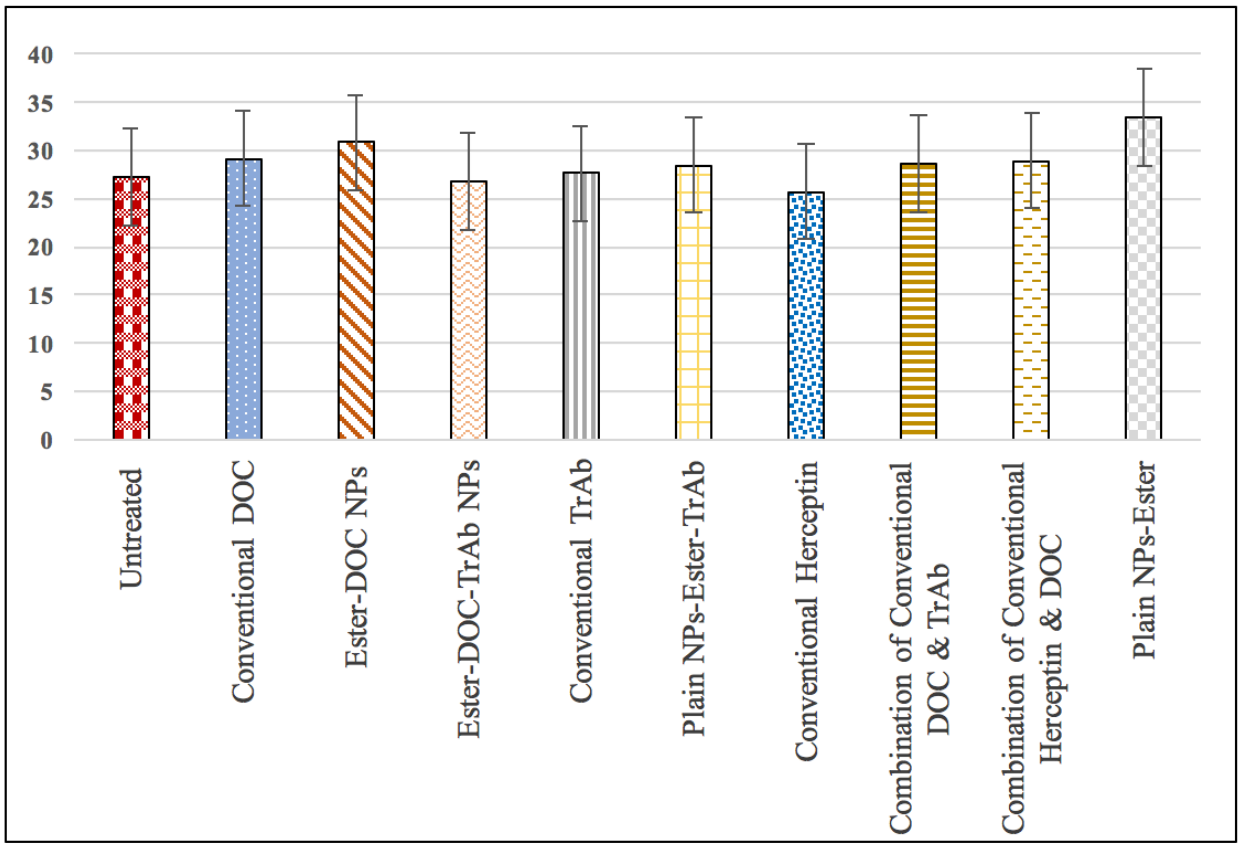

Figure 28. Relative percentage of positive median fluorescence intensity expressing HER2 after treating MCF-7 cells with plain PLGA ester, PLGA ester-DOC, PLGA ester plain-TrAb, and PLGA ester-DOC-TrAb versus untreated, conventional DOC, conventional Herceptin, combination of conventional DOC & Herceptin, after 48 hours. Data are represented as mean percentage ± SD (n=2).

5.8.2. Western Blot

To verify the results from flow cytometry studies, the western blot experiment was carried out to measure the relative HER2 protein expression levels after treating the SK-BR-3 cell with modified NPs formulations for both ester- and acidic-terminated PLGA and conventional Herceptin, conventional DOC and the conventional combination of DOC and Herceptin while maintaining similar conditions. Blotting membranes were incubated with the respective Ab against HER2 and GAPDH. Figure

29, shows the protein blotting bands and the relative HER2 protein expression percentage for both timelines presented in Figure 30.

Conventional DOC and plain NPs showed a high level of HER2 expression for both timelines which was almost similar to the level of HER2 for untreated cells. This result was expected because there was no targeting ligand available to conjugate to the HER2 receptors. The data for modified NPs showed the same pattern that was observed by flow cytometry. There was a remarkable reduction of HER2 expression, especially after 48 hours of the treatment. NPs ester-DOC-ScFv had the highest suppression of HER2 receptors (6.2%) and NPs ester-DOC-TrAb showed about 11.02% of HER2 expression. NPs COOH-DOC-TrAb suppressed the HER2 expression to 14.3%. The least reduction in HER2 expression occurred with NPs COOH-DOC-ScFv to 18.6 %.

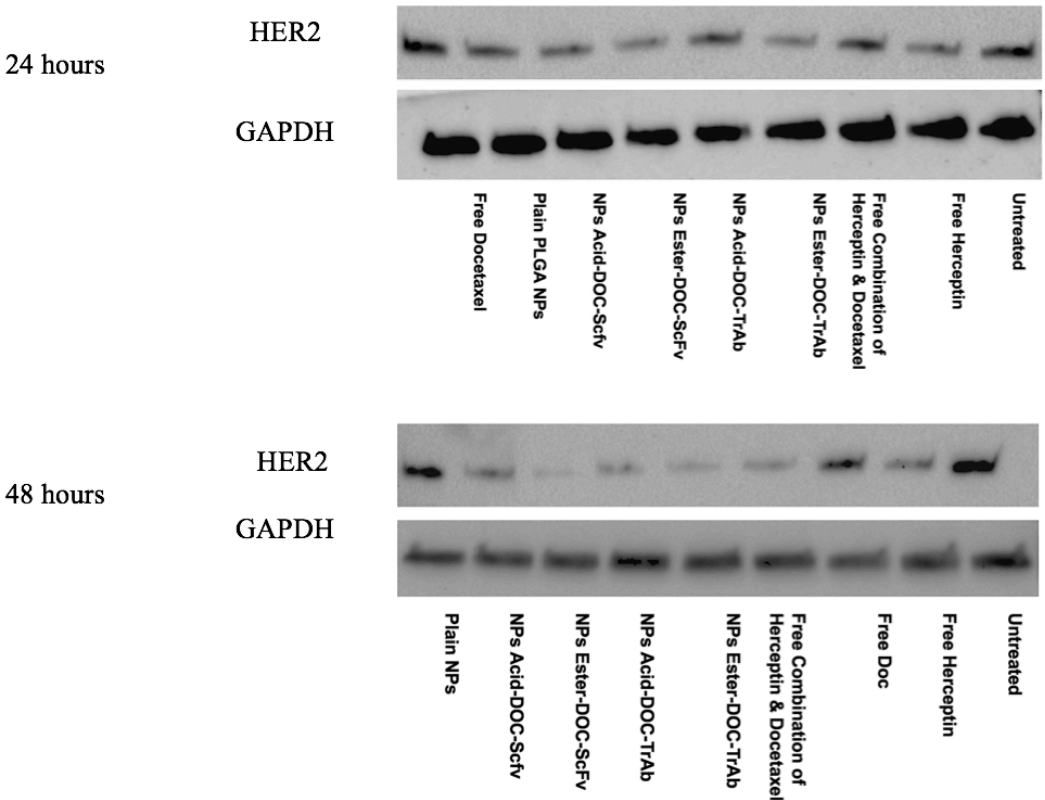

Figure 29. Protein expression profile (15 μg) for HER2 in SK-BR-3 cells which was treated by the conventional Herceptin, conventional DOC, combination of conventional DOC & Herceptin, PLGA ester-DOC-TrAb, PLGA ester-DOC-ScFv, PLGA COOH-DOC-TrAb, and PLGA COOH-DOC-ScFv for two different time points (24, 48 hours)

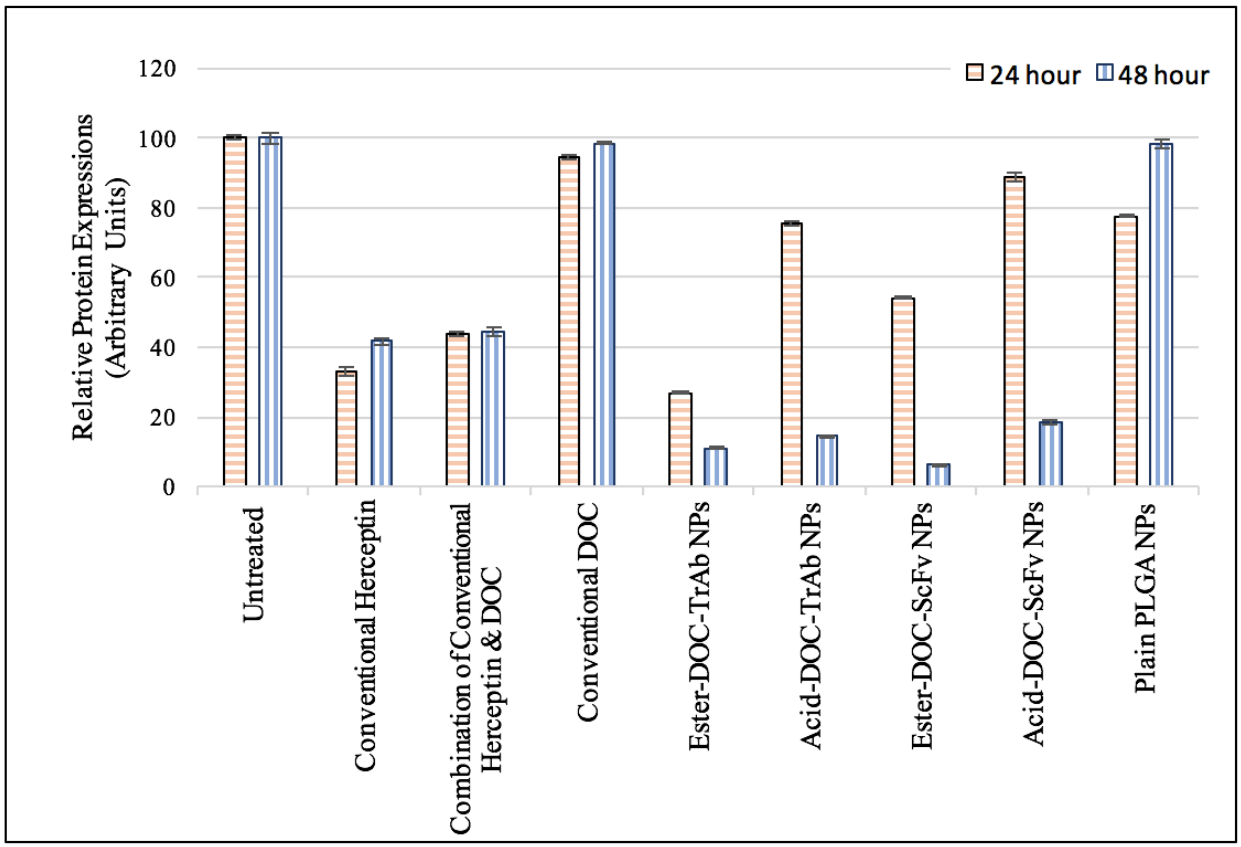

Figure 30. The percentage of protein expression profile for HER2 in SK-BR-3 cells which was treated by the conventional Herceptin, conventional DOC, combination of conventional DOC & Herceptin, PLGA ester-DOC-TrAb, PLGA ester-DOC-ScFv, PLGA COOH-DOC-TrAb, and PLGA COOH-DOC-ScFv for two different time points (24, 48 hours). The bands were analyzed by using BioRad Quantity Image Lab software

6. DISCUSSION

6.1. Yield Percentage

Several methods are available for preparation of polymeric PLGA formulations. Comparing the precipitation technique and the solvent evaporation method as two commonly used methods for NP development; the precipitation techniques resulted in a low yield percentage (recovery rate). The reason for this is the low encapsulation efficiency of the NPs formulations prepared by the precipitation method due to the insufficient emulsification between the hydrophilic and hydrophobic phases (Agnihotri, Mallikarjuna, & Aminabhavi, 2004; Bilati, Allemann, & Doelker, 2005). Besides, COOH PLGA NPs formulations had a higher yield percentage than ester NPs formulations that had been prepared by the solvent evaporation method. Using ethyl acetate as the organic solvent in the formulations with COOH-terminated PLGA polymer gave low yield; therefore, it was critical to use chloroform as an alternate since, it has been commonly used in NPs preparation. When ethyl acetate was used with COOH-terminated PLGA, the particle size was very small, as shown in Table 12, which means the drug encapsulation was low, and this also explains the low yield (Sahana, Mittal, Bhardwaj, & Kumar, 2008; Soppimath & Aminabhavi, 2002). The results confirmed the superiority of the solvent evaporation technique in polymeric PLGA NPs preparation, because of the high encapsulation efficiency of DOC (recovery rate).

6.2. Antibody Conjugation to NPs Surface

Many researchers endeavor different techniques to conjugating Ab to nanoparticles for targeting drug delivery formulation by trying different linkers because there is no established method yet (Arruebo et al., 2009; Montenegro et al., 2013; Yang et al., 2009; Yezhelyev et al., 2006). The Ab can be attached directly to the surface of NPs, depending on the physical adsorption. However, physical adsorption attachment is not entirely stable, and it might cover the binding site of the Ab. Thus, the idea of using linkers to conjugate the ligand is a common approach in drug targeting formulation research, but many factors must be considered in choosing the spacer (Veiseh, Gunn, & Zhang, 2010). One of the main factors is the length of the spacer arm, which helps to reduce the steric hindrance and improve the accessibility of the Ab to receptor binding sites (Khandare & Minko, 2006; Mehvar, 2000).

In this study, two different linkers were used (BS3 or NHS/EDC) to conjugate TrAb, or ScFv anti-HER2 in the surface of PLGA NPs encapsulated DOC. Bis(sulfosuccinimidyl) (BS3) was added in the first step of NPs preparation to be embedded in the surface of NPs. BS3 has a reactive group (N-hydroxysulfosccinimid (NHS) at both ends, and it is conjugated to the ligand in a one-step reaction (homobifunctional) by releasing Sulpho-NHS (Figure 31). The covalent amide bond between the BS3 and the ligand is more stable than the physical adsorption and conjugation occurs at neutral pH to avoid Ab denaturation.

Conjugation of NHS/EDC (N-hydroxysuccinimide)/ (1-ethyl-3- [3 dimethylaminopropyl]-carbodiimide) to the PLGA NPs surface involves a heterobifunctional process (Figure 32). In fact, the NHS/EDC linker was the reason

behind using COOH-terminated PLGA because carboxylic acid was needed to conjugate to EDC. The COOH forms an unstable reactive acylisourea ester with EDC and subsequent addition of NHS results in a semi-stable amine that conjugates to the Ab directly by forming the amide bond. FTIR confirmed the formation of amide bond between linkers (BS3 or NHS/EDC) and antibodies (TrAb or ScFv). However, because the amide bond is distinctive character to the compound-containing protein, the FTIR spectrum of modified and unmodified NPs needed to be compared to emphasize the difference. The presence of the amide bond between BS3 linker and NPs showed in Figure 7, and Figure 8 for the NHS/EDC linker. The central peak for PLGA appeared in 1750 cm^{-1}, and the amide bond vibrates in ~1640 cm^{-1} confirming the attachment of the Ab (Fu, Griebenow, Hsieh, Klibanov, & Langer, 1999; Ya-Ping Li, 2001).

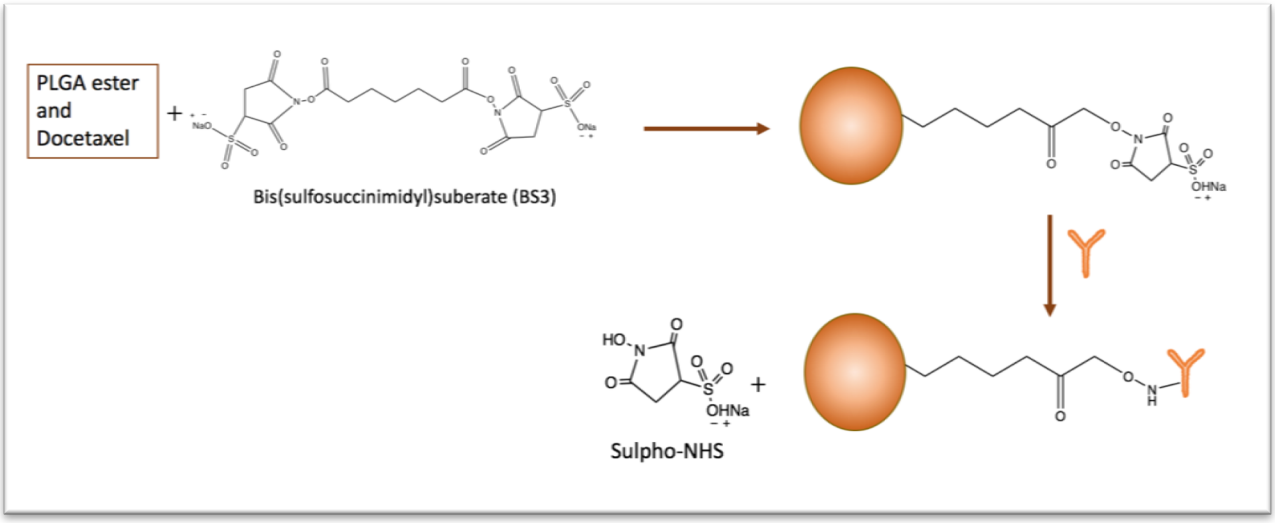

Figure 31. Schematic reaction to show the conjugation between the spacer (BS3) and the ligand in ester PLGA polymeric nanoparticles. The BS3 linker embeds on the NPs surface to form a covalent bond between the BS3 and ligand. This method can be applicable for both ester-and acidic-terminated PLGA nanoparticles

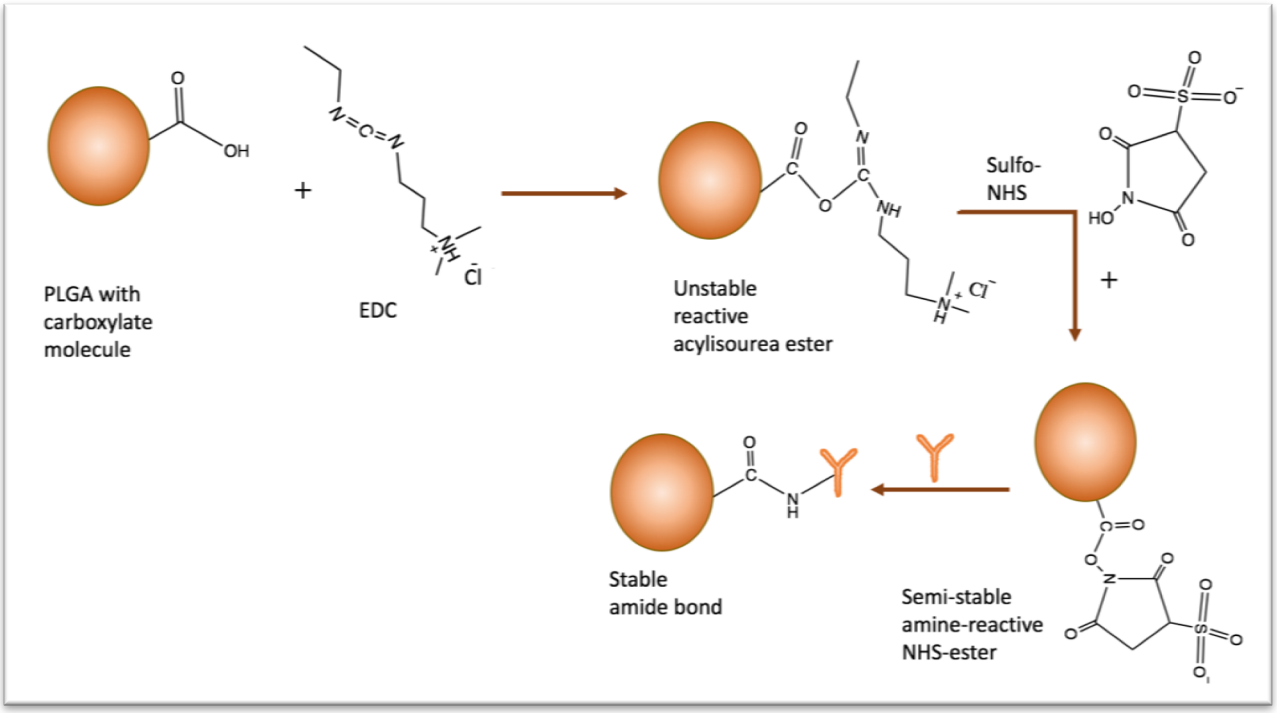

Figure 32. Schematic reaction to show the conjugation between the spacer (N-hydroxysuccinimide)/ (1-ethyl-3- [3 dimethylaminopropyl]-carbodiimide) and the ligand in COOH-terminated PLGA polymeric nanoparticles, using a EDC/NHS spacer with COOH-terminated PLGA only. The ligand attaches to the nanoparticle by forming a covalent amide bond after confirming the intermediate compounds (acylisourea ester and amine-reactive NHS-ester).

6.3. Physicochemical Properties (Size, ZP, and PDI)

One of the most critical factors in targeting drug delivery formulations is internalizing the therapeutic agent into the specific cells. The size, ZP, shape, and the surface chemistry of the NPs significantly impact cellular uptake as well as biodistribution and pharmacokinetics of the formulations (De Jong & Borm, 2008; Veiseh et al., 2010). However, the aggregation and agglomeration, chemical composition, and NPs protein interaction play an essential role in the cellular uptake mechanism (Oh & Park, 2014; C. Sun, Lee, & Zhang, 2008). There are different pattern endocytosis cellular uptake (pinocytosis or phagocytosis) depending on the size of the particles (J. Wang, Byrne, Napier, & DeSimone, 2011; Zhao et al., 2011).

During nanoparticle development, our initial focus was NPs size because large NPs would be filtered via the reticuloendothelial system specifically by phagocytosis, which would result in unfavorable biodistribution and pharmacokinetic characteristics of the formulation (Albanese, Tang, & Chan, 2012; Jiang, Kim, Rutka, & Chan, 2008). Solid tumors have vascular pores around 400–600 nm and high interstitial pressure at the center of the tumor site, which can increase retention time because of reduction in blood flow. Therefore, NPs formulations in this size range (400–600 nm) could take advantage of the permeability and retention effect (Adiseshaiah, Hall, & McNeil, 2010). Also, an anti-HER2 Ab attached on the surface of NPs would actively target the NPs to the tumor tissue (Cho, Wang, Nie, Chen, & Shin, 2008; Danhier, Feron, & Preat, 2010). NPs around 500 nm would be internalized through receptor-mediated endocytosis (Ding & Ma, 2012; Vacha, Martinez-Veracoechea, & Frenkel, 2011).

Another important factor is the surface charge of the NPs (ZP). Low ZP prolongs the formulation's circulating time in blood to reach and accumulate in the tumor. On the other hand, having a positive charge on the surface helps electrostatic interaction with the negative charge on the cell surface; however, the formulation would end up with nonspecific internalization (Frohlich, 2012; He, Hu, Yin, Tang, & Yin, 2010). Also, freeze-drying (FD) is one of the challenges in this research; all NPs formulations sizes and PDI increased after FD, which could be due to the aggregation stress on the particles during FD or to the disruption of electrostatic repulsion between particles (Holzer et al., 2009). The high aggregation tendency led to a large PDI, so the highest value of the PDI is 1, which means that the formulation has a wide range of size distribution. Moreover, the ZP showed a trend toward more negative values after FD. Therefore, different amounts of cryoprotectant (sucrose) (0.1%, 0.16%, 0.33%, 0.5%, 0.66%, 0.83%, 1%, and 1.16%) were added as a steric stabilizer to avoid the attraction between NPs to prevent the aggregation and coagulation. The effect of cryoprotectant decreased the particle size and PDI for NPs, when 1.7 mg/ml of sucrose used, the mean size of PLGA ester-DOC-BS3 was 257.2 ± 15.77 nm and 329.8 ± 9.39 nm for PLGA COOH-DOC (Table 10 and 12). The ZP rate was also found to be less negative after using sucrose.

DOC addition also led to lowering the particle size; during NPs preparation, there was would be an interaction between the polymer and the drug that could condense the droplet in the emulsion, leading to smaller particle sizes. After the Ab attachment, there was an increase in NPs size, and ZP shifted towards more positive or neutral; however, no change was noted in the PDI. Interestingly, there was no

significant difference in the size when the whole anti-HER2 (TrAb) was attached to the surface in comparison to the fragment Ab (ScFv) (Table 13). Finally, four NPs formulations were chosen for further analysis because its potential of targeting and delivering DOC depending on their physicochemical characterizations; PLGA ester-terminated polymer encapsulate DOC with 1.7 mg/ml sucrose decorated with 300 μg of TrAb or Scfv by BS3 spacer, and PLGA COOH-terminated polymer encapsulated DOC with 1.7 mg/ml sucrose decorated with 300 μg of TrAb or Scfv.

6.4. Surface Morphology

The shape of the particles affects the cellular uptake; therefore, both transmission electron microscopy (TEM) and scanning electron microscope (SEM) were used to study the morphology of NPs formulations. SEM and TEM images confirmed the uniform spherical shape for all formulations. Spherical particles have better uptake than other shapes because of the small angle (acute ~ 45^{o}) between the surface of the cells and the NPs (Arkan, Saber, Karimi, & Shamsipur, 2015; Florez et al., 2012). The large angle on top of the cells means particles would be spread on the surface, negatively affecting internalization. Chromium and gold are used to coat the formulations in SEM imaging to prevent the direct contact between the beam and NPs. Conjugating the Ab on the surface of polymeric NPs did not change the morphology of NP. Both microscopes gave smaller diameters of NPs in comparison to the Zetasizer size because of the differences in the measuring techniques. In the microscope, the samples are present in dry form; besides, it usually images a single particle. In contrast, in the Zetasizer, the samples are dispersed in the aqueous phase, and DLS gives the average size (Bootz, Vogel, Schubert, & Kreuter, 2004; Chattopadhyay et al., 2012; Ito, Sun, Bevan, & Crooks, 2004).

6.5. Drug-Loading Quantification for Docetaxel

Compared to previous work in our lab, the amount of DOC loaded per mg of NPs improved significantly (about 3-fold) for PLGA ester-BS3-TrAb NPs formulation (from 7.13 ± 0.89 μg per mg of NPs to 21.78 ± 3.34 μg per mg of NPs). This may be due to enhanced sonication time, amplitude and temperature which encourages uniform mixing with higher drug loading. One of the important factors in NP preparation is maintaining the cold temperature in all steps of NPs preparation to keep the particle from denaturing, especially because both sonication and centrifugation produce heat. Unmodified acidic-terminated PLGA NPs had higher loading compared to ester-formulations, but the differences in the amount of DOC loading was not statistically significant. However, with modified NPs with TrAb for COOH NP, the loading of DOC was found to be higher than ester-modified NPs, which could be attributed to the presence of BS3 (hydrophilic) in the surface of NPs that caused more drug loss in the Ab attachment step.

The DOC encapsulation efficiency depends directly on the initial amount of DOC, PLGA, and sucrose added in the first step of NPs preparation. Another difference in the formulations compared to previous work is that the amount of sucrose significantly decreased from 10% to 0.5%, which gave us 15 % and 45 % entrapment of DOC, respectively. Overall, there was a significant improvement in DOC loading compared to similar preparation techniques were done by Musumeci et al., 2006 and Youm et al., 2011 lab.

6.6. Antibody Loading Quantification

As discussed before, there is no well-established method to attach the ligand with polymeric NPs efficiently while maintaining the efficiency of the medications. Therefore, in this research, both BS3 or NHS/EDC were used to examine the capability. Hence, quantitation of protein by the BCA assay supported the notion that conjugation was successful. Based on previous work in our lab, there is no significant increase in the amount of Ab conjugation when increasing the amount of the linker (Sadat, 2015). However, after using different amounts of trastuzumab to attach to NPs, we found that the higher amount of Ab initially used provided a higher amount of attached Ab; 300 μg of Ab gave the highest amount of Ab attachment as well as a higher attachment efficiency percentage.

Initially, indirect quantification was obtained by measuring the remainder of the unconjugated Ab in the washing solvent. There was a significant improvement in the amount of Ab attached to the ester-terminated nanoparticles compared to prior work in our lab, from around 12.05 ± 1.39 μg/mg to 22.8 ± 3.78 μg/mg for modified ester-terminated PLGA NPs with TrAb. The detection of the fragment ScFv and low quantity TrAb was zero, which meant 100% attachment, as presented in Tables 16 to 23, which was a big concern for the efficiency of indirect quantification. Consequently, Ab conjugation was determined by measuring how much Ab attached to the surface of NPs after FD directly (Table 20). The modified COOH-terminated PLGA with TrAb had the highest amount of Ab incorporated at 16.33 ± 2.69 μg/mg of NPs, which could be attributed to the smaller size and larger surface area. Conversely, there was no

significant difference in the amount of ScFv anti-HER2 attached to both ester- and COOH-modified NPs.

In conclusion, having the Ab on the surface of NPs increases the hydrophilicity, and positive charge of NPs. Also, the modified NPs would improve the specific targeting and, the uptake of the tumor overexpresses HER2 receptors. The conjugation of TrAb was higher in comparison with the fragment anti-HER2 (ScFv), though the modified COOH PLGA NPs had the highest amount of TrAb attachment (16.33 ± 2.69 μg/mg).

6.7. Evaluation of *In Vitro* Release Pattern of Docetaxel from Modified NPs

Ester-modified PLGA NPs with TrAb was conducted in both pH 7.4 and pH 5 for 120 hours. Early burst release phenomena showed a higher release in the presence of acidic pH. This could be attributed to the presence of DOC on the surface or close to the surface of NPs, which would release faster. Also, the faster release at the lower pH value could be due to the re-protonation of the amino group of DOC. Although, having the TrAb conjugating on the surface of NPs increased the hydrophilicity, which enhanced the rate of erosion and/or diffusion of the polymer. Then, DOC continued diffusion through the polymeric matrix, which is referred to as control release. This concept of burst release could help to suppress the growth of a tumor as an immediate action, whereas the maintaining effect comes from the control release of chemotherapy (Avgoustakis et al., 2002; Mittal, Sahana, Bhardwaj, & Ravi Kumar, 2007; Z. Zhang & Feng, 2006).

Another remarkable phenomenon is having a higher release of DOC in acidic media compared to neutral pH. A tumor has an acidic environment, so the release of DOC would be more specific in the tumor area compared to other organs or in the circulation, where the pH is neutral. That would help in minimizing the side effects of DOC (Sepehri et al., 2014; Xu et al., 2012).

6.8. Cell Cytotoxicity

Modified and unmodified formulations were tested in SK-BR-3 cell line to measure the cancer cell viability (or cancer cell mortality) against the recently used medications (DOC and Herceptin). Because the new formulations have ester- and acidic- terminated PLGA as a carrier, a cytotoxicity study is needed to confirm that there was no toxicity influence for PLGA in general except in when a high concentration was used. This toxicity could be caused by to having a high quantity of NPs, which would change the pH and the viscosity of the media, leading to cell death as shown in Figure 15.

The same concentration of DOC was used to compare the cell viability for the modified formulations with each other and with conventional DOC, Herceptin, and the combination of DOC and Herceptin. Overall, a more significant cytotoxicity (cancers toxicity) effect was observed when the DOC concentration was increased. In the case of ester PLGA formulations, the NPs conjugated with TrAb, showed an excellent result (cancers toxicity) in at low concentrations, when compared with NP ester-DOC-ScFv. However, by increasing the concentration of both NPs formulations (ester-DOC-TrAb and ester-DOC-ScFv) the cytotoxicity effect was almost equal. Both TrAb and ScFv anti-HER2 modified ester NPs formulations showed significant synergistic anticancer activity compared to the current clinical dosage form. This enhancement in cytotoxicity can be attributed to the effect of Ab in targeting and enhancing the cellular uptake via HER2 receptor-mediated endocytosis.

For acidic-terminated PLGA formulations, NPs conjugated to TrAb showed higher tumor cell cytotoxicity than ScFv. COOH PLGA-DOC-TrAb had a higher and

significant cytotoxic effect than a combination of conventional DOC and Herceptin treatment. TrAb might be more bioactive, so NPs had a higher level of interaction with the cell. However, the cell viability for COOH PLGA-DOC-ScFv formulations was not low. These data suggested that the targeting and uptake were not that effective, which could be attributed to performing the attachment in acidic pH (5 pH). The acidic environment might denature the fragment Ab (Calmettes, 1991; Vermeer & Norde, 2000; Welfle, Misselwitz, Hausdorf, Hohne, & Welfle, 1999). Also, the TrAb might have had a better effect than the fragment anti-HER2 because, according to the literature, the density of the Ab is more critical in drug targeting and uptake (Holliger & Hudson, 2005). In addition, the fragment Ab has only one binding site, whereas the TrAb can conjugate to the receptors by two binding epitopes.

By comparing the modified formulations to each other, it can be concluded that both ester-modified PLGA formulations (TrAb or ScFv) were able to induce cell death more than COOH PLGA-modified formulations. Thus, the Ab in the ester formulation was more biologically effective for directing the HER2 receptor and probably internalizing the cell via receptor-mediated endocytosis. Another reason could be that the BS3 gave a more accessible spacer arm, which improves the targeting and the delivery as well as the cytotoxicity. Also, to perform the attachment via NHS/EDC requires acidic pH, which might denature or inactivate the Ab, reducing the targeting and the toxicity.

For quantitative analysis for the formulations, IC_{50} was performed to result in the drug concentration that killed 50% of the cells at the designated time. The IC_{50} can be ranked according to the killing efficiency as follows: ester PLGA-DOC-ScFv > ester

PLGA-DOC-TrAb > COOH PLGA-DOC-ScFv > COOH PLGA-DOC-TrAb. Fragment Ab showed better IC_{50} values versus TrAb, which could be because the penetration of the fragment Ab takes only 16 hours. However, the penetration of the entire IgG Ab takes 54 hours (Hudson & Souriau, 2003). Therefore, the recycling of the HER2 receptor would be faster in the cells treated with fragment formulations, which made the cytotoxicity higher in low concentrations.

6.9. Measuring HER2 Expression

All the cell lines were used to evaluate the expression of HER2 receptor on the surface of the cells. The incubation time for the treatments was 48 hours based on prior work in our lab. The data presented by focusing on the %PF, which refers to the fluorescence percentage of the receptors that stained all cells, and similarly the percentage of median fluorescence (%MFI) demonstrates the percent of the receptors stained per one cell. For the MCF-7 cell line, there was no significant difference in either the %PF or %MFI while treating the cells with different formulations. This was expected because the expression of HER2 receptors is low to moderate in the MCF-7 cell line.

For SK-BR-3 cells, all modified ester formulations showed a significant reduction in the %PF compared to the cells treated with conventional Herceptin and untreated as well, and there was no significant difference between the fragment and whole Ab in ester-modified NPs. Also, acidic-modified PLGA NPs with ScFv had a significant reduction of %PF; however, the COOH PLGA-DOC-TrAb yielded the highest reduction in %PF (68%). Additionally, all formulations showed a significant reduction in the %MFI, except for COOH PLGA-DOC-ScFv NPs whereas the %MFI was 86.1%. Remarkably, the %MFI was higher in untreated cells than in the cells treated with conventional ScFv and plain NPs, which could be because more HER2 receptors were produced in surviving cells. Overall, all NPs formulations showed an ability to deliver chemotherapy to targeted tumor cells that overexpress HER2 receptors.

HER2 expression in SK-BR-3 cell line after different treatments was evaluated by Western blot analysis. Overall there was an obvious reduction in HER2 expression for the cells treated with modified NPs which confirmed the capability of delivering and targeting HER2 receptors. There was limited reduction in HER2 expressions when the cells were treated with plain NPs, that could be attributed to the electrostatic interaction between the plain NPs that had negative ZP and HER2 receptors which is carries a positive charge.

7. CONCLUSION

Chemotherapeutics are currently the most effective treatments for cancer patients; however, most chemotherapy has many side effects that can adversely affect other organs due to its inability to target tumor cells. Therefore, this study is focused on preparing modified PLGA nanoparticles with a chemotherapeutic agent (DOC) and attaching TrAb or the fragment ScFv anti-HER2 to the surface of the NPs as a ligand to target HER2 expressing breast tumor cells. This process would enhance the targeting properties of the treatment and improve chemotherapeutic residence time and distribution to tumor. Nanoparticles are used in novel drug delivery systems to control and target therapeutic agents to the disease site.

One of the vital factors in the NPs' preparation is size. Taking into consideration the advantages of the tumor microvasculature with a pore size between 400 nm and 600 nm, NPs of similar size may accumulate in the tumor site (Ding & Ma, 2012). Many studies have confirmed the ability for intracellular uptake with NPs that have a diameter of less than 500 nm (Vacha et al., 2011). Because FD is an essential step in NPs preparation and there is a significant increase in NPs' size after FD, a different quantity of cryoprotectant was used to decrease stress and aggregation during FD. Technically, a cryoprotectant, or sucrose specifically, minimizes the hyperosmotic effect and stabilizes both the steric and electrostatic hindrance, which prevents aggregation as well as crystallization.

The second focus was on the ZP of NPs, where the FD induced a more negative surface charge. DOC and PVA residues also demonstrated a negative charge. PVA was essential for maintaining the interfacial tension between the particles and to uniformly

distribute small NPs. The presence of sucrose helped decrease the negative ZP. Almost all the modified formulations in this study had neutral ZP, which helped reduce the phagocytic rate and increased the NPs' circulation time so it could reach the tumor site. Besides, neutral ZP prevents nonspecific electrostatic binding. In addition, having high negative ZP made the formulation pharmaceutically unstable as well as decreased cellular uptake because of phagocytosis. Both TrAb and ScFv modified the NPs' required size (>400 nm) with uniform PDI and neutral ZP, which was achieved for all formulations.

A surface morphology analysis assured the spherical shape of NPs and affirmed that an Ab conjugation did not change the NPs shape. Having spherical NPs helped the NPs' uptake due to the small, acute angle between the cell surface and the particles.

The DOC loading efficiency improved significantly and reached 85% for the TrAb-modified COOH-PLGA NPs and around 70% for TrAb-modified ester-PLGA NPs. BS3 and NHS/EDC cross-linking agents were used to conjugate Ab to the surface of the NPs by covalent conjugation. There was no prominent or significant difference in the amount of Ab attached to the NPs surface.

NPs loaded with DOC and modified with TrAb had burst release at first where 50% of the DOC was released in the first 24 hours in acidic pH, which could instantly help suppress a tumor's growth. Then DOC had a controlled release to continue the effect. The release was affected by the pH; therefore, in an acidic medium, the rate of release would be higher than in a neutral pH. This pH-dependent phenomenon would be beneficial in tumor-targeting the drug delivery because tumors have an acidic

environment where the DOC can be released in the tumor site, thus minimizing systemic toxicity.

The percentage of cell viability and the cytotoxicity that quantitatively resulted in 50% growth inhibition (IC_{50}) were analyzed to evaluate the chemotherapeutic response for conventional drug and all modified PLGA NPs. Cell viability was higher with cells treated with conventional DOC and with a combination of conventional DOC and Herceptin compared to ester NPs modified with either TrAb or ScFv. In addition, the acidic modified NPs showed high cytotoxicity. Modified PLGA ester exhibited the lowest IC_{50} (the highest cytotoxicity) followed by modified PLGA acidic-DOC-ScFv when compared to the PLGA acidic-DOC-TrAb. This result suggests the enhancement of cytotoxicity that might be related to the active cellular uptake mediated by targeting HER2 receptors, which then increased the intracellular concentration of DOC.

All the modified NPs formulations confirmed their ability to target HER2 receptors and deliver chemotherapy (DOC) by measuring the level of HER2 expression. The results from flow cytometry showed the reduction in HER2 expression for all the cells treated with modified NPs. Remarkably, both ester- and acidic- PLGA encapsulated with DOC and modified with TrAb were found to be more prominent in targeting HER2 receptors when compared to fragment-modified NPs. A western blot analysis affirmed that all modified NPs formulations had the ability to target HER2 receptors, which therefore decreased HER2 expression.

To conclude, there is the potential that all anti-HER2-modified PLGA NPs formulations can target drug delivery to HER2 overexpressing breast cancer. Thus,

ligand-modified, structurally concealed PLGA NPs could be a promising delivery tool for targeting HER2 breast tumors *in vivo* to improve the therapeutic effects of chemotherapy while reducing its systemic side effects.

8. FUTURE DIRECTION

The present work was an attempt to improve the drug loading of PLGA NPs encapsulated DOC that was modified with anti-HER2 ligands to target and deliver the DOC to HER2 overexpressing breast cancer. This research can be advanced by further investigating different objectives. The following recommendations and future directions should be considered:

1. Acidic terminated PLGA could be used with the BS3 cross-linker to conjugate the anti-HER2 on the surface of NPs were the NPs could better load the chemotherapy as well as the ligand, which would improve the physiochemical properties and the efficacy of the NPs.
2. A smaller recombined Ab like Fab or Fab_2 could work better than ScFv. First, the spacer arm could be longer due to the attachment of the Fab to the variable region and this might help the accessibility of Ab in conjugating the epitope of the antigen (receptors). Second, there would be two antigens' bonding sites instead of one, as is the case of ScFv.
3. The MDA-MB-453 and BT-474 cell lines could be used to confirm the targeted drug delivery of all formulations by measuring the HER2 expressions. Furthermore, this test would help in animal modeling for future in-vivo experiments.
4. Subcellular localization could examine the location of the protein in a cell, which would assist in investigating the intracellular Ab pathway.
5. Cell cycle and apoptosis assays could also help investigate the antitumor mechanism of DOC loaded in PLGA NPs.

6. Investigate the down regulation pathways for further direction of anti-HER-2 mechanism of action.
7. *In vivo* studies such as the following could evaluate the effects of the targeted delivery systems for breast cancer, overexposing HER2 receptors:
    A. A pharmacokinetics study to measure the DOC concentration in the plasma.
    B. Tumor-targeting assays, modified PLGA NPs formulations could encapsulate infrared dye (DiR) instead of DOC; then, injecting the florescent formulations into a xenograft animal model so its organs that could be imaged to investigate the targeting ability of modified NPs formulations.
    C. Antitumor assays with all modified NPs formulations injected into a xenograft animal model and the weight and volume of the tumor calculated to investigate whether the tumor had shrunk after treatment with modified NPs formulations.
8. Optimization of modified NPs formulations could be useful after conducting the in-vivo studies.

9. REFERENCES

Adams, G. P., Shaller, C. C., Dadachova, E., Simmons, H. H., Horak, E. M., Tesfaye, A., ... & Weiner, L. M. . (2004). Single treatment of yttrium-90-labeled CHX-A ″–C6. 5 diabody inhibits the growth of established human tumor xenografts in immunodeficient mice. *Cancer Research*, 64(17), 6200-6206.

Adiseshaiah, P. P., Hall, J. B., & McNeil, S. E. (2010). Nanomaterial standards for efficacy and toxicity assessment. *Wiley Interdisciplinary Reviews: Nanomedicine and Nanobiotechnology*, 2(1), 99-112.

Agnihotri, S. A., Mallikarjuna, N. N., & Aminabhavi, T. M. (2004). Recent advances on chitosan-based micro-and nanoparticles in drug delivery. *Journal of Controlled Release*, 100(1), 5-28.

Ahmad, Z. A., Yeap, S. K., Ali, A. M., Ho, W. Y., Alitheen, N. B., & Hamid, M. (2012). scFv antibody: principles and clinical application. *Clinical and Developmental Immunology*, 2012.

Albanese, A., Tang, P. S., & Chan, W. C. (2012). The effect of nanoparticle size, shape, and surface chemistry on biological systems. *Annual Review Biomedical Engineering*, 14, 1-16.

Anhorn, M. G., Wagner, S., Kreuter, J., Langer, K., & von Briesen, H. (2008). Specific targeting of HER2 overexpressing breast cancer cells with doxorubicin-loaded trastuzumab-modified human serum albumin nanoparticles. *Bioconjugate chemistry*, 19(12), 2321-2331.

Arkan, E., Saber, R., Karimi, Z., & Shamsipur, M. (2015). A novel antibody–antigen based impedimetric immunosensor for low level detection of HER2 in serum samples of breast

cancer patients via modification of a gold nanoparticles decorated multiwall carbon nanotube-ionic liquid electrode. *Analytica Chimica Acta,* 874, 66-74.

Arruebo, M., Valladares, M., & González-Fernández, Á. (2009). Antibody-conjugated nanoparticles for biomedical applications. *Journal of Nanomaterials*, 2009, 37.

Avgoustakis, K., Beletsi, A., Panagi, Z., Klepetsanis, P., Karydas, A. G., & Ithakissios, D. S. (2002). PLGA-mPEG nanoparticles of cisplatin: in vitro nanoparticle degradation, in vitro drug release and in vivo drug residence in blood properties. *Journal of Controlled Release*, 79(1-3), 123-135.

Bang, Y. J., Van Cutsem, E., Feyereislova, A., Chung, H. C., Shen, L., Sawaki, A., ... & Aprile, G. (2010). Trastuzumab in combination with chemotherapy versus chemotherapy alone for treatment of HER2-positive advanced gastric or gastro-oesophageal junction cancer (ToGA): a phase 3, open-label, randomised controlled trial. *The Lancet*, 376(9742), 687-697.

Banu, H., Sethi, D. K., Edgar, A., Sheriff, A., Rayees, N., Renuka, N., . . . Vasanthakumar, G. (2015). Doxorubicin loaded polymeric gold nanoparticles targeted to human folate receptor upon laser photothermal therapy potentiates chemotherapy in breast cancer cell lines. *Journal of Photochemistry and Photobiology B: Biology*, 149, 116–128.

Barnato, S. E., & Gradishar, W. J. (2015). Biological subtypes of breast cancer. *In Breast Cancer Biology for the Radiation Oncologist* (pp. 1-6). Springer, Berlin, Heidelberg

Bilati, U., Allémann, E., & Doelker, E. (2005). Poly (D, L-lactide-co-glycolide) protein-loaded nanoparticles prepared by the double emulsion method—processing and formulation issues for enhanced entrapment efficiency. *Journal of Microencapsulation*, 22(2), 205-214.

Boekhout, A. H., Beijnen, J. H., & Schellens, J. H. (2011). Trastuzumab. *The oncologist*, 16(6), 800–810.

Bootz, A., Vogel, V., Schubert, D., & Kreuter, J. (2004). Comparison of scanning electron microscopy, dynamic light scattering and analytical ultracentrifugation for the sizing of poly (butyl cyanoacrylate) nanoparticles. *European Journal of Pharmaceutics and Biopharmaceutics,* 57(2), 369-375.

Brannon-Peppas, L., & Blanchette, J. O. (2004). Nanoparticle and targeted systems for cancer therapy. *Advanced Drug Delivery Review*, 56(11), 1649–1659.

Brufsky, A. (2010). Trastuzumab-based therapy for patients with HER2-positive breast cancer: from early scientific development to foundation of care. *American Journal of Clinical Oncology*, 33(2), 186-195.

Byrne, J. D., Betancourt, T., & Brannon-Peppas, L. (2008). Active targeting schemes for nanoparticle systems in cancer therapeutics. *Advanced Drug Delivery Review*, 60(15), 1615–1626.

Calmettes, P., Cser, L., & Rajnavölgyi, E. (1991). Temperature and pH dependence of immunoglobulin G conformation. *Archives of Biochemistry and Biophysics*, 291(2), 277-283.

Canadian Cancer Statistics 2017. Toronto, ON: Canadian Cancer Society; 2017. Available at: http://www.cancer.ca/~/media/cancer.ca/CW/publications/Canadian%20Cancer%20Statistics/Canadian-Cancer-Statistics-2017-EN.pdf

Chattopadhyay, S., Chakraborty, S. P., Laha, D., Baral, R., Pramanik, P., & Roy, S. (2012). Surface-modified cobalt oxide nanoparticles: new opportunities for anti-cancer drug development. *Cancer Nanotechnology*, 3(1–6), 13–23.

Cho, K., Wang, X. U., Nie, S., & Shin, D. M. (2008). Therapeutic nanoparticles for drug delivery in cancer. *Clinical Cancer Research*, 14(5), 1310-1316.

Choi, W. I., Lee, J. H., Kim, J. Y., Heo, S. U., Jeong, Y. Y., Kim, Y. H., & Tae, G. (2015). Targeted antitumor efficacy and imaging via multifunctional nano-carrier conjugated with anti-HER2 trastuzumab. *Nanomedicine: Nanotechnology, Biology and Medicine,* 11(2), 359-368.

Cirstoiu-Hapca, A., Buchegger, F., Lange, N., Bossy, L., Gurny, R., & Delie, F. (2010). Benefit of anti-HER2-coated paclitaxel-loaded immuno-nanoparticles in the treatment of disseminated ovarian cancer: Therapeutic efficacy and biodistribution in mice. *Journal of Controlled Release,* 144(3), 324–331.

Citri, A., & Yarden, Y. (2006). EGF-ERBB signaling: Towards the systems level. *Nature Reviews Molecular Cell Biology*, 7(7), 505–516.

Danhier, F., Feron, O., & Préat, V. (2010). To exploit the tumor microenvironment: passive and active tumor targeting of nanocarriers for anti-cancer drug delivery. *Journal of controlled release,* 148(2), 135-146.

Davis, M. E., & Shin, D. M. (2008). Nanoparticle therapeutics: an emerging treatment modality for cancer. *Nature Reviews Drug Discovery,* 7(9), 771-82.

De Jong, W. H., & Borm, P. J. (2008). Drug delivery and nanoparticles: applications and hazards. *International Journal of Nanomedicine*, 3(2), 133-49.

Ding, H. M., & Ma, Y. Q. (2012). Role of physicochemical properties of coating ligands in receptor-mediated endocytosis of nanoparticles. *Biomaterials,* 33(23), 5798-802.

Farokhzad, O. C., Cheng, J., Teply, B. A., Sherifi, I., Jon, S., Kantoff, P. W., . . . Langer, R. (2006). Targeted nanoparticle-aptamer bioconjugates for cancer chemotherapy in vivo. *Proceedings of the National Academy of Sciences*, 103(16), 6315-6320.

Fauzee, N. J. S., Wang, Y. L., Dong, Z., Li, Q. G., Wang, T., Mandarry, M. T., ... & Pan, J. (2012). Novel hydrophilic docetaxel (CQMU-0519) analogue inhibits proliferation and induces apoptosis in human A549 lung, SKVO3 ovarian and MCF7 breast carcinoma cell lines. *Cell Proliferation,* 45(4), 352-364.

Ferlay, J., Soerjomataram, I., Dikshit, R., Eser, S., Mathers, C., Rebelo, M., ... & Bray, F. (2015). Cancer incidence and mortality worldwide: sources, methods and major patterns in GLOBOCAN 2012. *International Journal of Cancer*, 136(5), E359-386.

Florez, L., Herrmann, C., Cramer, J. M., Hauser, C. P., Koynov, K., Landfester, K., ... & Mailänder, V. (2012). How shape influences uptake: interactions of anisotropic polymer nanoparticles and human mesenchymal stem cells. *Small*, 8(14), 2222-2230.

Frasco, M. F., Almeida, G. M., Santos-Silva, F., Pereira Mdo, C., & Coelho, M. A. (2015). Transferrin surface-modified PLGA nanoparticles-mediated delivery of a proteasome inhibitor to human pancreatic cancer cells. *Journal of Biomedical Materials Research Part A*, 103(4), 1476-1484.

Fröhlich, E. (2012). The role of surface charge in cellular uptake and cytotoxicity of medical nanoparticles. *International Journal of Nanomedicine*, 7, 5577-91.

Fu, K., Griebenow, K., Hsieh, L., Klibanov, A. M., & Langera, R. (1999). FTIR characterization of the secondary structure of proteins encapsulated within PLGA microspheres1. *Journal of Controlled Release,* 58(3), 357-366.

Fumoleau, P., Seidman, A. D., Trudeau, M. E., Chevallier, B., & Huinink, W. T. B. (1997). Docetaxel: a new active agent in the therapy of metastatic breast cancer. *Expert Opinion on Investigational Drugs,* 6(12), 1853-1865.

Gaspar, V. M., Costa, E. C., Queiroz, J. A., Pichon, C., Sousa, F., & Correia, I. J. (2015). Folate-targeted multifunctional amino acid-chitosan nanoparticles for improved cancer therapy. *Pharmaceutical Research*, 32(2), 562-577.

Gillet, J. P., & Gottesman, M. M. (2010). Mechanisms of multidrug resistance in cancer. *In Multi-Drug Resistance in Cancer* (pp. 47-76). Humana Press.

Grislain, L., Couvreur, P., Lenaerts, V., Roland, M., Deprez-Decampeneere, D., & Speiser, P. (1983). Pharmacokinetics and distribution of a biodegradable drug-carrier. *International Journal of Pharmaceutics,* 15(3), 335-345.

Hamdy, S., Haddadi, A., Hung, R. W., & Lavasanifar, A. (2011). Targeting dendritic cells with nano-particulate PLGA cancer vaccine formulations. *Advanced Drug Delivery Reviews,* 63(10-11), 943-955.

He, C., Hu, Y., Yin, L., Tang, C., & Yin, C. (2010). Effects of particle size and surface charge on cellular uptake and biodistribution of polymeric nanoparticles. *Biomaterials,* 31(13), 3657-3666.

He, Y., Zhang, L., Zhu, D., & Song, C. (2014). Design of multifunctional magnetic iron oxide nanoparticles/mitoxantrone-loaded liposomes for both magnetic resonance imaging and targeted cancer therapy. *International Journal of Nanomedicine,* 9, 4055-4066.

Holliger, P., & Hudson, P. J. (2005). Engineered antibody fragments and the rise of single domains. *Nature Biotechnology*, 23(9), 1126-36.

Holzer, M., Vogel, V., Mäntele, W., Schwartz, D., Haase, W., & Langer, K. (2009). Physico-chemical characterisation of PLGA nanoparticles after freeze-drying and storage. *European Journal of Pharmaceutics and Biopharmaceutics,* 72(2), 428-437.

Huang, J., Zhang, H., Yu, Y., Chen, Y., Wang, D., Zhang, G., . . . Zhong, Y. (2014). Biodegradable self-assembled nanoparticles of poly (D,L-lactide-co-glycolide)/hyaluronic acid block copolymers for target delivery of docetaxel to breast cancer. *Biomaterials,* 35(1), 550–566.

Huang, Y., He, L., Liu, W., Fan, C., Zheng, W., Wong, Y. S., & Chen, T. (2013). Selective cellular uptake and induction of apoptosis of cancer-targeted selenium nanoparticles. *Biomaterials,* 34(29), 7106–7116.

Hu, C. M. J., & Zhang, L. (2009). Therapeutic nanoparticles to combat cancer drug resistance. *Current Drug Metabolism,* 10(8), 836-841.

Hudson, P. J., & Souriau, C. (2003). Engineered antibodies. *Nature Medicine,* 9(1), 129-34.

Irache, J. M., Esparza, I., Gamazo, C., Agüeros, M., & Espuelas, S. (2011). Nanomedicine: novel approaches in human and veterinary therapeutics. *Veterinary Parasitology,* 180(1-2), 47-71.

Ito, T., Sun, L., Bevan, M. A., & Crooks, R. M. (2004). Comparison of nanoparticle size and electrophoretic mobility measurements using a carbon-nanotube-based coulter counter, dynamic light scattering, transmission electron microscopy, and phase analysis light scattering. *Langmuir*, 20(16), 6940-6945.

Jahan, S. T., & Haddadi, A. (2015). Investigation and optimization of formulation parameters on preparation of targeted anti-CD205 tailored PLGA nanoparticles. *International journal of nanomedicine,* 10, 7371-84.

Jemal, A., Bray, F., Center, M. M., Ferlay, J., Ward, E., & Forman, D. (2011). Global cancer statistics. *CA: a Cancer Journal for Clinicians,* 61(2), 69-90.

Jiang, W., Kim, B. Y., Rutka, J. T., & Chan, W. C. (2008). Nanoparticle-mediated cellular response is size-dependent. *Nature Nanotechnology*, 3(3), 145-50.

Jo, H., Her, J., & Ban, C. (2015). Dual aptamer-functionalized silica nanoparticles for the highly sensitive detection of breast cancer. *Biosensors and Bioelectronics,* 71, 129-136.

Kamaly, N., Xiao, Z., Valencia, P. M., Radovic-Moreno, A. F., & Farokhzad, O. C. (2012). Targeted polymeric therapeutic nanoparticles: design, development and clinical translation. *Chemical Society Reviews,* 41(7), 2971-3010.

Kanazaki, K., Sano, K., Makino, A., Shimizu, Y., Yamauchi, F., Ogawa, S., ... & Saji, H. (2015). Development of anti-HER2 fragment antibody conjugated to iron oxide nanoparticles for in vivo HER2-targeted photoacoustic tumor imaging. *Nanomedicine: Nanotechnology, Biology and Medicine,* 11(8), 2051-2060.

Keizer, H. G., Pinedo, H. M., Schuurhuis, G. J., & Joenje, H. (1990). Doxorubicin (adriamycin): a critical review of free radical-dependent mechanisms of cytotoxicity. *Pharmacology and Therapeutics*, 47(2), 219-231.

Khandare, J., & Minko, T. (2006). Polymer–drug conjugates: progress in polymeric prodrugs. *Progress in Polymer Science,* 31(4), 359-397.

Koopaei, M. N., Dinarvand, R., Amini, M., Rabbani, H., Emami, S., Ostad, S. N., & Atyabi, F. (2011). Docetaxel immunonanocarriers as targeted delivery systems for HER 2-positive tumor cells: preparation, characterization, and cytotoxicity studies. *International Journal of Nanomedicine,* 6, 1903-1912.

Koutras, A. K., & Evans, T. J. (2008). The epidermal growth factor receptor family in breast cancer. *OncoTargets and therapy*, 1, 5.

Li, S. Y., Sun, R., Wang, H. X., Shen, S., Liu, Y., Du, X. J., . . . Jun, W. (2015). Combination therapy with epigenetic-targeted and chemotherapeutic drugs delivered by nanoparticles to enhance the chemotherapy response and overcome resistance by breast cancer stem cells. *Journal of Controlled Release*, 205, 7–14.

Li, Y. P., Pei, Y. Y., Zhang, X. Y., Gu, Z. H., Zhou, Z. H., Yuan, W. F., ... & Gao, X. J. (2001). PEGylated PLGA nanoparticles as protein carriers: synthesis, preparation and biodistribution in rats. *Journal of Controlled Release,* 71(2), 203-211.

Liu, Y., Zhu, Y. H., Mao, C. Q., Dou, S., Shen, S., Tan, Z. B., & Wang, J. (2014). Triple negative breast cancer therapy with CDK1 siRNA delivered by cationic lipid assisted PEG-PLA nanoparticles. *Journal of Controlled Release,* 192, 114–121.

Longley, D. B., Harkin, D. P., & Johnston, P. G. (2003). 5-fluorouracil: mechanisms of action and clinical strategies. *Nature Reviews Cancer*, 3(5), 330-338

Ma, P., Zhang, X., Ni, L., Li, J., Zhang, F., Wang, Z., . . . Sun, K. (2015). Targeted delivery of polyamidoamine-paclitaxel conjugate functionalized with anti-human epidermal growth factor receptor 2 trastuzumab. *International Journal of Nanomedicine,* 10, 2173–2190.

Makadia, H. K., & Siegel, S. J. (2011). Poly lactic-co-glycolic acid (PLGA) as biodegradable controlled drug delivery carrier. *Polymers (Basel),* 3(3), 1377–1397.

Manchanda, R., Fernandez-Fernandez, A., Nagesetti, A., & McGoron, A. J. (2010). Preparation and characterization of a polymeric (PLGA) nanoparticulate drug delivery system with simultaneous incorporation of chemotherapeutic and thermo-optical agents. *Colloids Surface B Biointerfaces,* 75(1), 260–267.

Mansour, H. M., Sohn, M., Al-Ghananeem, A., & DeLuca, P. P. (2010). Materials for pharmaceutical dosage forms: molecular pharmaceutics and controlled release drug delivery aspects. *International Journal of Molecular Sciences,* 11(9), 3298-3322.

McGuire, S. (2016). World cancer report 2014. Geneva, Switzerland: World Health Organization, international agency for research on cancer, WHO Press, 2015. *Advances in Nutrition: An International Review Journal,* 7(2), 418-419.

Mehvar, R. (2000). Dextrans for targeted and sustained delivery of therapeutic and imaging agents. *Journal of Controlled Release,* 69(1), 1-25.

Misra, R., Acharya, S., & Sahoo, S. K. (2010). Cancer nanotechnology: Application of nanotechnology in cancer therapy. *Drug Discovery Today,* 15(19–20), 842-850.

Mitri, Z., Constantine, T., & O'Regan, R. (2012). The HER2 receptor in breast cancer: pathophysiology, clinical use, and new advances in therapy. *Chemotherapy Research and Practice,* 2012.

Mittal, G., Sahana, D. K., Bhardwaj, V., & Kumar, M. R. (2007). Estradiol loaded PLGA nanoparticles for oral administration: effect of polymer molecular weight and copolymer composition on release behavior in vitro and in vivo. *Journal of Controlled Release,* 119(1), 77-85.

Montenegro, J. M., Grazu, V., Sukhanova, A., Agarwal, S., Jesus, M., Nabiev, I., ... & Parak, W. J. (2013). Controlled antibody/(bio-) conjugation of inorganic nanoparticles for targeted delivery. *Advanced Drug Delivery Reviews*, 65(5), 677-688.

Nishioka, Y., & Yoshino, H. (2001). Lymphatic targeting with nanoparticulate system. *Advanced Drug Delivery Reviews*, *47*(1), 55–64.

Nobs, L., Buchegger, F., Gurny, R., & Allémann, E. (2004). Current methods for attaching targeting ligands to liposomes and nanoparticles. *Journal of Pharmaceutical Sciences,* 93(8), 1980-1992.

Oh, N., & Park, J. H. (2014). Endocytosis and exocytosis of nanoparticles in mammalian cells. *International Journal of Nanomedicine*, 9(Suppl 1), 51.

Park, J., Kim, S., Saw, P. E., Lee, I. H., Yu, M. K., Kim, M., . . . Jon, S. (2012). Fibronectin extra domain B-specific aptide conjugated nanoparticles for targeted cancer imaging. *Journal of Controlled Release, 163*(2), 111–118.

Rafiei, P., Michel, D., & Haddadi, A. (2015). Application of a rapid ESI-MS/MS method for quantitative analysis of docetaxel in polymeric matrices of PLGA and PLGA-PEG nanoparticles through direct injection to mass spectrometer. *American Journal of Analytical Chemistry, 6*(2), 164–175.

Rejman, J., Oberle, V., Zuhorn, I. S., & Hoekstra, D. (2004). Size-dependent internalization of particles via the pathways of clathrin-and caveolae-mediated endocytosis. *Biochemical Journal,* 377(Pt 1), 159-169.

Sadat, S. M. A. (2015). Targeted Chemotherapy:Trastuzumab Tailored Docetaxel Loaded PLGA Nanoparticles For HER2 Positive Breast Cancer. *Thesis*.

Sahana, D. K., Mittal, G., Bhardwaj, V., & Kumar, M. N. V. (2008). PLGA nanoparticles for oral delivery of hydrophobic drugs: influence of organic solvent on nanoparticle formation and release behavior in vitro and in vivo using estradiol as a model drug. *Journal of Pharmaceutical Sciences,* 97(4), 1530-1542.

Salomon, D. S., Brandt, R., Ciardiello, F., & Normanno, N. (1995). Epidermal growth factor-related peptides and their receptors in human malignancies. *Critical Reviews in Oncology/Hematology,* 19(3), 183-232.

Scheuer, W., Friess, T., Burtscher, H., Bossenmaier, B., Endl, J., & Hasmann, M. (2009). Strongly enhanced antitumor activity of trastuzumab and pertuzumab combination treatment on HER2-positive human xenograft tumor models. *Cancer Research,* 69(24), 9330-9336.

Sepehri, N., Rouhani, H., Tavassolian, F., Montazeri, H., Khoshayand, M. R., Ghahremani, M. H., ... & Dinarvand, R. (2014). SN38 polymeric nanoparticles: in vitro cytotoxicity and in vivo antitumor efficacy in xenograft balb/c model with breast cancer versus irinotecan. *International Journal of Pharmaceutics,* 471(1-2), 485-497.

Shapira, A., Livney, Y. D., Broxterman, H. J., & Assaraf, Y. G. (2011). Nanomedicine for targeted cancer therapy: Towards the overcoming of drug resistance. *Drug Resist Updates, 14*(3), 150–163.

Sharma, B., Peetla, C., Adjei, I. M., & Labhasetwar, V. (2013). Selective biophysical interactions of surface modified nanoparticles with cancer cell lipids improve tumor targeting and gene therapy. *Cancer Letters, 334*(2), 228–236.

Smith, I., Procter, M., Gelber, R. D., Guillaume, S., Feyereislova, A., Dowsett, M., ... & Kaufmann, M. (2007). 2-year follow-up of trastuzumab after adjuvant chemotherapy in HER2-positive breast cancer: a randomised controlled trial. *The lancet,* 369(9555), 29-36.

Soppimath, K. S., & Aminabhavi, T. M. (2002). Ethyl acetate as a dispersing solvent in the production of poly (DL-lactide-co-glycolide) microspheres: effect of process parameters and polymer type. *Journal of Microencapsulation*, 19(3), 281-292.

Spector, N. L., & Blackwell, K. L. (2009). Understanding the mechanisms behind trastuzumab therapy for human epidermal growth factor receptor 2-positive breast cancer. *Journal of Clinical Oncology*, 27(34), 5838–5847.

Steinhauser, I., Spankuch, B., Strebhardt, K., & Langer, K. (2006). Trastuzumab-modified nanoparticles: Optimisation of preparation and uptake in cancer cells. *Biomaterials,* 27(28), 4975–4983.

Sun, B., Ranganathan, B., & Feng, SS. (2008). Multifunctional poly(D,L-lactide-co-glycolide)/montmorillonite (PLGA/MMT) nanoparticles decorated by trastuzumab for targeted chemotherapy of breast cancer. *Biomaterials,* 29(4), 475–486.

Sun, C., Lee, J. S., & Zhang, M. (2008). Magnetic nanoparticles in MR imaging and drug delivery. *Advanced Drug Delivery Reviews*, 60(11), 1252-1265.

Tai, W., Mahato, R., & Cheng, K. (2010). The role of HER2 in cancer therapy and targeted drug delivery. *Journal of Controlled Release*, 146(3), 264–275.

Talaei, F., Azizi, E., Dinarvand, R., & Atyabi, F. (2011). Thiolated chitosan nanoparticles as a delivery system for antisense therapy: Evaluation against EGFR in T47D breast cancer cells. *International Journal of Nanomedicine*, 6, 1963–1975.

Tarver, T. (2012). Cancer facts & figures 2012. American Cancer Society (ACS). *Journal of Consumer Health on the Internet,* 16(3), 366–367

Tavassolian, F., Kamalinia, G., Rouhani, H., Amini, M., Ostad, S. N., Khoshayand, M. R., . . . Dinarvand, R. (2014). Targeted poly (L-gamma-glutamyl glutamine) nanoparticles of docetaxel against folate over-expressed breast cancer cells. *International Journal of Pharmaceutics,* 467(1–2), 123–138.

Thamake, S. I., Raut, S. L., Ranjan, A. P., Gryczynski, Z., & Vishwanatha, J. K. (2011). Surface functionalization of PLGA nanoparticles by non-covalent insertion of a homo-bifunctional spacer for active targeting in cancer therapy. *Nanotechnology*, 22(3), 035101.

Toraya-Brown, S., Sheen, M. R., Baird, J. R., Barry, S., Demidenko, E., Turk, M. J., ... & Fiering, S. (2013). Phagocytes mediate targeting of iron oxide nanoparticles to tumors for cancer therapy. *Integrative Biology*, 5(1), 159-171.

Torre, L. A., Bray, F., Siegel, R. L., Ferlay, J., Lortet-Tieulent, J., & Jemal, A. (2015). Global cancer statistics, 2012. *CA: a Cancer Journal for Clinicians,* 65(2), 87-108.

Tsai, T. H. (2001). Analytical approaches for traditional chinese medicines exhibiting antineoplastic activity. *Journal of Chromatography B: Biomedical Sciences and Applications*, 764(1-2), 27-48.

Ueda, M., Hisada, H., Temma, T., Shimizu, Y., Kimura, H., Ono, M., . . . Saji, H. (2015). Gallium-68-labeled anti-HER2 single-chain Fv fragment: Development and in vivo monitoring of HER2 expression. *Molecular Imaging and Biology, 17*(1), 102–110.

Vácha, R., Martinez-Veracoechea, F. J., & Frenkel, D. (2011). Receptor-mediated endocytosis of nanoparticles of various shapes. *Nano letters,* 11(12), 5391-5395.

Veiseh, O., Gunn, J. W., & Zhang, M. (2010). Design and fabrication of magnetic nanoparticles for targeted drug delivery and imaging. *Advanced Drug Delivery Reviews*, 62(3), 284-304.

Vermeer, A. W., & Norde, W. (2000). The thermal stability of immunoglobulin: unfolding and aggregation of a multi-domain protein. *Biophysical Journal*, 78(1), 394-404.

Vogel, C. L., Cobleigh, M. A., Tripathy, D., Gutheil, J. C., Harris, L. N., Fehrenbacher, L., ... & Shak, S. (2002). Efficacy and safety of trastuzumab as a single agent in first-line treatment of HER2-overexpressing metastatic breast cancer. *Journal of Clinical Oncology,* 20(3), 719-726.

Wang, H., Zhao, Y., Wang, H., Gong, J., He, H., Shin, M. C., . . . Huang, Y. (2014). Low-molecular-weight protamine-modified PLGA nanoparticles for overcoming drug-resistant breast cancer. *Journal of Controlled Release, 192*, 47–56

Wang, J., Byrne, J. D., Napier, M. E., & DeSimone, J. M. (2011). More effective nanomedicines through particle design. *Small, 7*(14), 1919–1931.

Wang, J. J., Zeng, Z. W., Xiao, R. Z., Xie, T., Zhou, G. L., Zhan, X. R., & Wang, S. L. (2011). Recent advances of chitosan nanoparticles as drug carriers. *International Journal of Nanomedicine, 6*, 765–774.

Wang, Y., Liu, P., Qiu, L., Sun, Y., Zhu, M., Gu, L., . . . Duan, Y. (2013). Toxicity and therapy of cisplatin-loaded EGF modified mPEG-PLGA-PLL nanoparticles for SKOV3 cancer in mice. *Biomaterials, 34*(16), 4068–4077.

Welfle, K., Misselwitz, R., Hausdorf, G., Höhne, W., & Welfle, H. (1999). Conformation, pH-induced conformational changes, and thermal unfolding of anti-p24 (HIV-1) monoclonal antibody CB4-1 and its Fab and Fc fragments. *Biochimica et Biophysica Acta (BBA)-Protein Structure and Molecular Enzymology,* 1431(1), 120-131.

Wolff, A. C., Hammond, M. E. H., Schwartz, J. N., Hagerty, K. L., Allred, D. C., Cote, R. J., ... & McShane, L. M. (2007). American Society of Clinical Oncology/College of American Pathologists guideline recommendations for human epidermal growth factor receptor 2 testing in breast cancer. *Archives of Pathology & Laboratory Medicine,* 131(1), 18-43.

Xu, Q., Liu, Y., Su, S., Li, W., Chen, C., & Wu, Y. (2012). Anti-tumor activity of paclitaxel through dual-targeting carrier of cyclic RGD and transferrin conjugated hyperbranched copolymer nanoparticles. *Biomaterials,* 33(5), 1627-1639.

Yang, L., Mao, H., Wang, Y. A., Cao, Z., Peng, X., Wang, X., ... & Smith, M. Q. (2009). Single chain epidermal growth factor receptor antibody conjugated nanoparticles for in vivo tumor targeting and imaging. *Small,* 5(2), 235-243.

Yezhelyev, M. V., Gao, X., Xing, Y., Al-Hajj, A., Nie, S., & O'Regan, R. M. (2006). Emerging use of nanoparticles in diagnosis and treatment of breast cancer. *The Lancet Oncology,* 7(8), 657-667.

Youm, I., Yang, X. Y., Murowchick, J. B., & Youan, B. B. (2011). Encapsulation of docetaxel in oily core polyester nanocapsules intended for breast cancer therapy. *Nanoscale Research Letters, 6*(1), 630-372.

Zhang, K. X., Kim, C., Chow, E., Chen, I. S., Jia, W., & Rennie, P. S. (2011). Targeting trastuzumab-resistant breast cancer cells with a lentivirus engineered to bind antibodies that recognize HER-2. *Breast Cancer Research and Treatment,* 125(1), 89-97.

Zhang, Z., & Feng, S. S. (2006). The drug encapsulation efficiency, in vitro drug release, cellular uptake and cytotoxicity of paclitaxel-loaded poly (lactide)–tocopheryl polyethylene glycol succinate nanoparticles. *Biomaterials,* 27(21), 4025-4033.

Zhao, F., Zhao, Y., Liu, Y., Chang, X., Chen, C., & Zhao, Y. (2011). Cellular uptake, intracellular trafficking, and cytotoxicity of nanomaterials. *Small, 7*(10), 1322–1337.